THE UNIVERSITY of ADELAIDE

Investigation of Stockpile-Voxel Profile and Material Reclaiming Optimization Using Bucket Wheel Reclaimer

Thirein Myo

Thesis submitted for the degree of Doctor of Philosophy

School of Mechanical Engineering
The University of Adelaide

August 2017

Declaration

Originality

I certify that this work contains no material which has been accepted for the award of any other degree or diploma in any university or other tertiary institution.To the best of my knowledge and belief, contains no material previously published or written by another person, except where due reference has been made in the text. In addition, I certify that no part of this work will, in the future, be used in a submission in my name, for any other degree or diploma in any university or other tertiary institution without the prior approval of the University of Adelaide and where applicable, any partner institution responsible for the joint-award of this degree.

Permissions

I give consent to this copy of my thesis when deposited in the University Library, being made available for loan and photocopying, subject to the provisions of the Copyright Act 1968. The author acknowledges that copyright of published works contained within this thesis resides with the copyright holder(s) of those works.

I also give permission for the digital version of my thesis to be made available on the web, via the University's digital research repository, the Library catalogue, the Australasian Digital Theses Program (ADTP) and also through web search engines, unless permission has been granted by the University to restrict access for a period of time.

Thirein Myo

Dated this ……21th ……day of …August...2017

Acknowledgment

I sincerely thank Allah, the Most Gracious, the Most Merciful for giving me the inspiration, patience, time, and the ability to complete my Ph.D. successfully. With His will and mercy, I have been guided to all those great people who helped me to complete this work. In completing my Ph.D. thesis I owe a great debt to many people. I wish to extend my deep thanks gratitude and appreciation to everyone contributed to the successful.

First and foremost, I would like to express my sincere thanks, gratitude and deep appreciation to my supervisor Dr. Tien-Fu Lu for his sincere effort, interest and time he has kindly spent to guide my research. Also, I would like to extend my appreciation to co-supervisor Dr. Lei Chen for his valuable contribution to my research.

Many colleages at the University of Adelaide have enriched my PhD experience by providing me with a good social environment, without which the 'world' would have been a lonelier place. I would like to give thanks to all members of the Robotics group, University of Adelaide for giving me friendly warm environment. Especially, I owe an gratitude to my colleague, Shi Zhao for much assisting works and providing necessary data for the research. My gratitude is also extended to Ben and Chris from Matrix group for giving input for the project and providing the field information.

I am grateful to Mr. Billy Constantine for his assistance on the IT support. I also would like to thank staff members of the office of the School of Mechanical Engineering for the kind support. Without the English support from Alison-jane Hunter, I am not able to complete my thesis. I would like to express my gratitude to her for the generous and prompt response whenever the help is requested. She is always ready to help.

Finally, I apologize to my family for all the sacrifices they have had to make during my candidature, and I cannot thank my wife, Thazin Naing enough for her moral support during my candidature. The inspiration received from my daughter, Khaira and my son, Zackaria plays a vital role in completing my study.

Last but not least, no words are ever sufficient to express my everlasting gratitude, appreciation and thanks to my beloved, wonderful mother and father for being the light in my life. Without their warm love, care, sincere prayers and support, it would have been impossible for me to be myself and to continue learning. My special thanks and gratitude also extend to my sister, parents-in–law and brother-in-law for their kind support and encouragement. I wish to extend my deep thanks gratitude and appreciation to everyone contributed to the successful completion of my thesis.

Publications

Journal papers

- Myo, M.T.R. and Lu, Tien-Fu, February, 2013. Investigation of the bucket wheel reclaimer's cutting trajectory to define optimal voxel shape. Transaction on Control and Mechanical Systems, 2(2): 54-60.
- Lu, Tien-Fu and Myo, M.T.R., 2010. Optimal stockpile voxel identification based on reclaimer minimum movement for target grade. International Journal of Mineral Processing, 98(1-2): 74-81.

Under review

- Myo, T. R and Lu, Tien-Fu, Voxelization of stockpile into sickle-shape voxels based on bucket wheel reclaimer's kinematics, International Journal of Mining Science and Technology.
- Myo, T. R and Lu, Tien-Fu, Energy consumption optimization in reclaiming sickle-shape voxels from multiple stockpiles using bucket wheel reclaimer, International Journal of Mining, Reclamation and Environment.

Conference papers

- Myo, M.T.R. and Lu, Tien-Fu, 2013. Investigation of the Volume Calculation of Sickle-shaped Voxel of a Stockpile, 11th International Conference on Bulk Materials, Storage, Handling & Transportation (ICBMH 2013), Newcastle, Australia.
- Myo, M.T.R. and Lu, Tien-Fu, 2013. Sickle-shaped voxel approach to enhance automatic reclaiming operation using bucket wheel reclaimer, The 8th IEEE Conference on Industrial Electronics and Applications (ICIEA 2013), Melbourne, Australia, pp. 1700-1705.
- Myo, M.T.R. and Lu, Tien-Fu, 2011. The Study of BWR Cutting Trajectory for Optimal Stockpile-Voxel Profile Design, 2011 IEEE International Conference on Robotics and Biomimetics, Phuket Island, Thailand pp. 1961-1966.
- Lu, Tien-Fu. and Myo, M.T.R., 2010. Optimization of reclaiming voxels for quality grade target with reclaimer minimum movement, 11th International Conference on Control Automation Robotics & Vision (ICARCV) Singapore, pp. 341-345.

Abstract

Ore producers aim to supply iron ore as close as possible to the requested specifications as blast furnaces are finely tuned to accept a particular mineral composition of ore. Besides a quality reputation, handling cost is the main concern for ore producers as iron ore is sold at a price lower than the cost of delivering garden sand. In addition, the growth in demand for iron ore and the depletion of high-grade ore resources over the years has drawn attention to improve in automation of operations. In order to fulfill the aforementioned objectives and challenges, robotics technology has been integrated into automatic mining operations over the last decade.

Generally, blending is used to compensate the short term fluctuations occurred in mining ore. However, the unavailability of assay at the blending stage has motivated researchers to focus on improving the reclaiming approach where accurate assay is available. In the literature, the cuboid voxel approach, in which stockpile is treated as a combination of virtual cuboid grids instead of being treated as a single entity, has been introduced. However, voxels are usually reclaimed using a bucket wheel reclaimer (BWR) in a circular slewing motion, which does not articulate with the cuboid shape. So the investigation is carried out on the accuracy of the reclaiming cuboid voxels by the BWR. The disparity between the cuboid voxel and the BWR reclaiming profile indicates a need to introduce an optimal voxel profile based on the BWR reclaiming profile. Hence, the sickle-shape voxel is introduced in this study, based on the BWR kinematics. Then, the stockpile is voxelized in a process through which the stockpile in Cartesian coordinate is transformed into sickle-shape voxels associated with the BWR joint parameters. The use of a single coordinate for the voxels and the BWR will reduce computational time for real time operation. A small-scaled stockpile is voxelized into sickle-shape voxels to demonstrate the process.

Besides, the quantity knowledge of the voxels is essential in voxel-based approach to identify the reclaiming voxels. So, the volume model of the sickle-shape voxel is derived in Spherical coordinate. Moreover, the volumes of voxels in the small-scaled stockpile are computed and added together to compare with the whole stockpile volume to verify the proposed volume model. Instead of using manual selection of voxels carried out in the literature, automatic identification of the optimal voxels to reclaim in order to meet the demand specifications considering the movement of the BWR is introduced. In doing that, two approaches are proposed for the minimum movement of the BWR. In the first approach, the minimum travelled distance of the BWR is taken into account to reclaim cuboid voxels in Cartesian coordinate. The objective function is defined based on Euclidean distance between voxels' position and the BWR bucket wheel current position. The demand quality and quantity along with the reclaiming order are defined as constraints in the optimization problem. Secondly, the minimum movements of the BWR joints are considered to reclaim sickle-shape voxels. The weighting factors are assigned to each joint to prioritise the minimum movement of the high energy consumption joint. Case studies are conducted for both approaches, using Binary integer programming to solve the optimization problems. The introduction of the sickle-shape voxel approach and the automatic identification of the voxels considering the minimum movement of the BWR will improve the reclaiming accuracy required to meet the demand specifications and minimise the handling costs.

Table of Contents

LIST OF TABLES

LIST OF FIGURES

LIST OF ACRONYMS

BWR	Bucket wheel reclaimer
DOF	Degrees of freedom
2-D	Two dimension
3-D	Three dimension
D-H	Danevit-Hartennberg notation

CHAPTER 1: INTRODUCTORY BACKGROUND

The Australian mining industry generated $138 billion income through exporting minerals, which accounts for 54% of the total annual income, in the 2009-2010 financial year. In addition, the industry created 187,400 jobs directly, and a further 599,680 jobs in supporting industries for the national economy [1]. Among the range of mining products, iron ore is Australia's biggest export commodity, to rank the country at second place in the 2012 world ranking of ore producers [2]. However, Australian mining industry is in need of innovation similar with other world producers in handling and exploring of the ores to overcome shortcomings, which will be stated at the later part of the paragraph and to compete in the global market. Besides, the demand for iron ore is gradually increasing as the consumption of iron ore to make steel has increased from 850 million tons at the end of the twentieth century to more than 1.3 billion tons in the first quarter of the twenty-first century, at a rate of 10% every year [3]. However, the known world's resources of crude iron ores are estimated at barely 800 billion tonnes, comprising of 230 billion tons of iron [4]. So it is apparent that most of the known deposits contain low-grade ores with iron contents of less than 30%. Moreover, the known resources of iron ore will have run out within the next 64 years if the growth rate of iron ore consumption maintains [3]. Hence, it is a vital concern for the ore producers to discover new ore resources and to exploit the preserved ore efficiently in order to preserve the deposits for a prolonged future.

Ore producers export iron ore to steel producers all around the world. Steel producers feed iron ore into finely tuned blast furnaces to produce steel. As blast furnaces are finely tuned to accept the iron ore with specific mineral composition, steel producers demand iron ore with their required mineral compositions. Common minerals included in ore are iron as the core mineral and phosphorous, silica and alumina as contaminants. The existence of contaminants in iron ore produces better quality steel, however exceeding the required percentage would affect the steel quality [5]. The requirement of supplying iron

ore closest to the demand specification makes quality reputation a significant factor [6]. On the other hand, the supply of ore with additional iron contents than the requested percentage will burden an opportunity cost for ore producers. The improvement in meeting quality grade requirements as closely as possible will reduce opportunity costs, leading to the preservation of available ore efficiently in the long term.

Despite the export of iron ore generates a significant income for national economy, the price of iron ore is sold at a price per tonne less than the cost of delivering garden sand [7]. Moreover, a large portion of the cost derives from the storing, handling and transporting of bulk materials in most of the cases [8]. Thus, the minimization of operating costs is one of the the major concerns for the ore producers. In summation, the three main objectives for the ore producers are to produce maximum output tonnage, to minimize material handling costs and to deliver quality grade targets with minimum tolerance [7].

In the last century, the innovation is mainly carried out on on-site human operated mining machines. Then, the focus of innovation is shifted to remotely operate and autonomous mining equipments in the last decade [9]. Nowadays, ore producers realized that automation is the only solution for the mining industry to meet the demand and to overcome the following challenges. The concerns of the ore producers are the continuous increase of resource demand, global competition, the declining of ore grade, health and safety issues of workers, shortage of skilled workers and the environment and possible carbon constraints imposed by the respective governments [9].

The success of using Robotics technology in other industries convinced the ore producers to introduce it in the mining industry over the past ten years [10]. For instance, giant autonomous and semi-autonomous robots have been deployed at mine site in Pilbara, Western Australia since 2002 [11]. Since then, the extent of automation in that mine site has been gradually increased by introducing new technologies over the time. However, the

main obstacle challenging in developing and installing new technology is the costs as the extent of the process stretching from research centers to multiple intermediate stages to the development of a full-scale commercial used product [9]. Though the cost is substantial, the benefits are potentially far outweighed by the benefits they can deliver. The benefits cover from productive rates to environmental benefits as well as safety and health of the workers involved in the operation [9]. This study is intended to assist in increasing the extent of automation whilst improving in meeting the industry requirement by treating the giant bucket wheel reclaimer as a robotic manipulator.

Mining industry covers activities such as exploring, processing, transportation (stacking, reclaiming and railing) and exporting of iron ore [12]. This study will focus on the reclaiming process of ore from the stockpile to load onto ships for overseas export. Stockpile is conventionally considered as a single entity, whether manual or automated reclaiming process is used. Mostly, the operator reclaims portions of the stockpile using either a pilgrim approach or the whole stockpile using a bench approach, based on operator's experience, to meet the demand specifications [13]. There is no substantial information available to illustrate the standing of the supply grade regards to the demanded grade. Moreover, the achievement of the target grade is only aimed at reclaiming without considering the reclaiming process carried out by the reclaimer. The commonly used reclaimer in the mining industry is a bucket wheel reclaimer (BWR) which is one of the heaviest machines on earth [14]. It is evident that a large machine requires much energy to move in order to carry out the operation. Hence, any small reduction of the BWR movement in reclaiming will considerably reduce the handling costs. In brief, there is no explicit knowledge about the stockpile in the existing studies till 2009 to guide the operator or automatic operation what to reclaim and what is expected to achieve after reclaiming.

In 2009, Simine introduced Simine^{CIS} MAQ, in which the stockpile is treated as a

combination of volume elements called voxels in order to achieve better accuracy in the quality grade contrary to the conventional single volume stockpile approach [15]. In that study, the cubic voxel profile is used with a manual selection of voxels to reclaim by the operator. As the reclaiming pattern of the BWR is in circular motion, cuboid voxels are not apparently suitable for BWR reclaiming to achieve optimal accuracy. The visual investigation is carried out in Section 3.1.2 to highlight the need for an optimal voxel profile. In order to obtain an optimal voxel profile, the new voxel shape is defined based on the kinematics of the BWR by treating it as a 4 DOF (degrees of freedom) robotic manipulator in this study. Moreover, automatic selection of voxels will be introduced, contrary to the manual selection of voxels in the previous study. In that, the minimum movement of the BWR is taken into account in selecting voxels to minimize energy consumption. Before the objectives are defined for this study, the blending operation used in stacking is discussed in the following section to highlight the need for a voxel-based approach.

1.1 Blending oriented material handling system

Ore producers plan mines production over a year, based on the forecast assay from drilling holes, which is carried out before excavation begins to meet the demand specification. However, an unavoidable short-term fluctuation of mineral composition is commonly occurred in mining industry, which can affect meeting demand specifications [6]. In order to compensate for that, a blending operation is commonly used while stockpiling is carried out at the port. Blending refers to the combination of ore from different blocks (pits, streams, etc.) onto a single stockpile to produce a consistent quality [16].

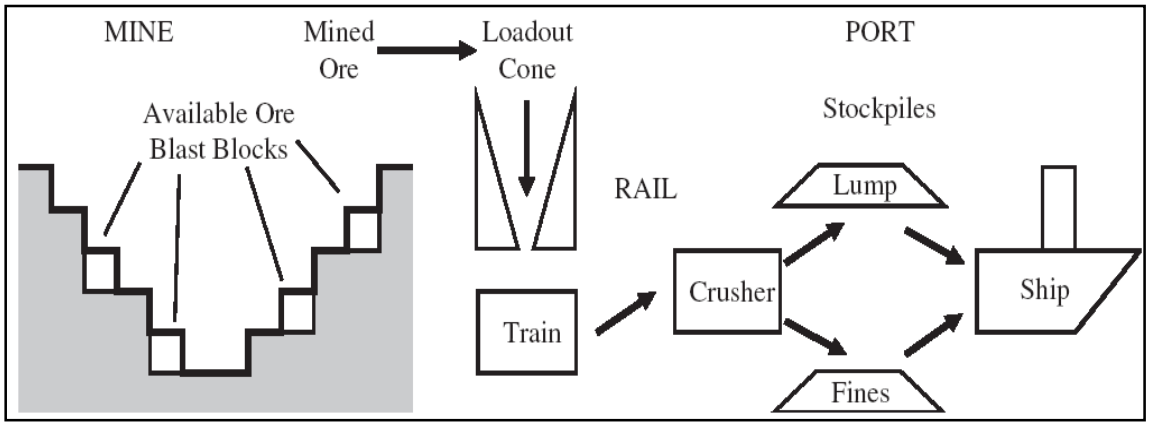

Figure 1.1: A typical iron ore production system

Generally, iron ore is excavated from open cut pits using large shovels and transported to the port by rail [16]. The flow of iron ore from the mine site to the port for shipping to overseas is shown in Figure 1.1 [7]. At the port, the ore is crushed and separated into lumps and fines. The reason for crushing at the port instead of doing at the mine site is to avoid valuable lumps degrading to fines in railing [17]. A sample of crushed lumps and fines are assayed in the laboratory before stacking onto stockpiles to obtain the accurate mineral composition. However, lumps and fines are required to stack at the port before obtaining the assay result from the laboratory as the process of assaying mineral composition generally takes few hours [6]. The material handling operation at the port is shown in Figure 1.2 [18]. In addition to stockpiles being used as buffers between 'before' processes and 'after' processes, they are also used in the blending process to reduce the variation in mineral composition to compensate for the short term fluctuations [19]. Conventionally, a stockpile is treated as a single volume with an average mineral composition. There are a limited number of studies in literature conducted to improve in meeting the demanded grade based on blending operations. A review of the literature is discussed in the following section.

Figure 1.2: Material handling at the port

1.1.1 Literature review on blending operation

With regard to the optimization of stockpile handling, Pavloudakis and Agioutantis developed a bulk solid blending simulator for longitudinal stockpiles to optimize blending in stockyards [20]. Stockpile blending simulation (SBS) was used to estimate blending efficiency for certain stacking and reclaiming techniques. The stockpile blending simulation (SBS) comprises two parts. In the first part, the input series of bulk solid property values are generated to use as input in the second part. Stockpile blending is simulated for Chevron and Windrow stacking with section and bench reclaiming. The study claimed to take into account the statistical parameters of the examined qualitative property in the stockyard input, the geometry of the stockpiles and the stockyard machinery movements. The proposed model was validated through a multi-parametric analysis and aimed to contribute to the reliable evaluation of different bulk solids handling in stockyards.

Cheng et al. looked at the issue from a different perspective in optimizing the handling of the material. They investigated the blending optimized algorithm of the

WSICO industrial port, considering the logistics equilibrium [21]. The blending model is optimized to select varieties of single-irons, adjusting supply and demand, constraining with quantity and composition requirements. The model was solved as a linear programming model of multi-variable and linear constraints. The proposed model was solved for a case study and claimed to be effective in the steel and iron industries.

Everett proposed decision support systems for daily ore selection to maintain the target composition [7]. A flow system was proposed, targeting an exponentially smoothed continuous stockpile to replace the batch system in which each stockpile is built to target. The Continuous Stockpile Management System (CSMS) was introduced as a decision support system for mining operators. The stress defined by (Grade-target)/tolerance is squared in the objective function, featuring as a continuous parabolic shape for a smoothly controlling process of mineral composition percentages. CSMS is claimed to give the opportunity for the operational decoupling between the mine and port operations, leading to great cost saving in rehandling.

Robinson discussed the amount of stockpile blending required to reduce grade variation [19]. Many types of predictive models for the variation amount are discussed in his study. Blending models are analyzed using mathematical and computer models for the geometry of a stockpile. Moreover, the input variation is described by the actual grade data and a variogram. Simulation was carried out for different reclaiming approaches with various stockpile types and suggested which approach is suitable for what type of stockpile. It was concluded that blending performance of stockpiles can be predicted and it is very useful for the industry.

The design model to plan iron ore handling procedures and to improve quality performance is described by Everett [5]. It is believed that composition variation can partly be reduced by the way the ore is stored in and reclaimed from stockpiles. The forecast ore

composition is used to guide the automatic sequence of feeding stockpiles for smooth composition. A simulation model was developed to investigate the assay variability achievable using automatic and intelligent sequencing methods for building stockpiles. The benefits of improved composition uniformity trade against the costs of handling and storage is considered in the objective function. Simulations were carried out for three case sets. The first set used automatic sequencing, with the destination changing in turn at each review. The second set used intelligent sequencing, with the forecast assays being used to choose the destination. The third set also used intelligent sequencing, with the accurate assays used to determine the destination stockpile. Intelligent sequencing gives noticeably higher stockpile quality, with less frequent review than automatic sequencing.

In reviewing the blending oriented studies, there are major shortfalls in terms of available mineral composition knowledge while blending is carried out. Firstly, the assay from the drill hole is not accurate as lighter and finer minerals tend to blow away, causing silica and alumina to be underestimated and iron content to be overestimated [22]. Moreover, the more accurate assay carried out after crushing is not available at the time of blending due to delays in processing [6]. As a result, blending has to be carried out using an inaccurate assay from blast hole drilling. Although the more accurate assay is not available at the stacking phase, it is accessible at the reclaiming stage. In taking advantage of the availability of the accurate assay at the reclaiming stage, Siemens introduced a material management system in which the reclaiming stage is focused on improving and meeting demand specifications [15].

1.2 Voxel based reclaiming system

In voxel based approach, the required groups of voxels from multiple stockpiles are identified and reclaimed to meet the demand specifications. The use of the voxel based approach in reclaiming will provide the capability to reduce the use of blending operation as group of voxels from multiple stockpiles are reclaimed similar to the blending operation, where ore from different pits are distributed among many stockpiles in stacking. Moreover, the accurate assay is accessible at the reclaiming stage, whereas it was not available at the stacking stage whilst blending was carried out. So the voxel based approach has the advantage of better accuracy in meeting demand specifications to eliminate the use of blending.

1.2.1 Literature review on voxel based reclaiming system

A first study using voxel based approach called Simine^{CIS} MAQ is found in literature which was introduced by Simines [15]. In Simine^{CIS} MAQ, the stockyard is divided into cubic meter virtual grids in regard to quantity and quality, as shown in Figure 1.3 [15], for straightforward quality planning and material blending. The quality data, quantity information and a timestamp are stored in the material-data record and updated each time the stockpile is changed. The updated 3-D and compressed 2-D model of the stockpiles is shown on a monitor for operator viewing. Based on the stockpile view on screen, the operator selects the relevant unit volume grids to meet the demand quantity and target grade. The calculated resulting total grade and quantity information is displayed before being physically reclaimed from the stockpile.

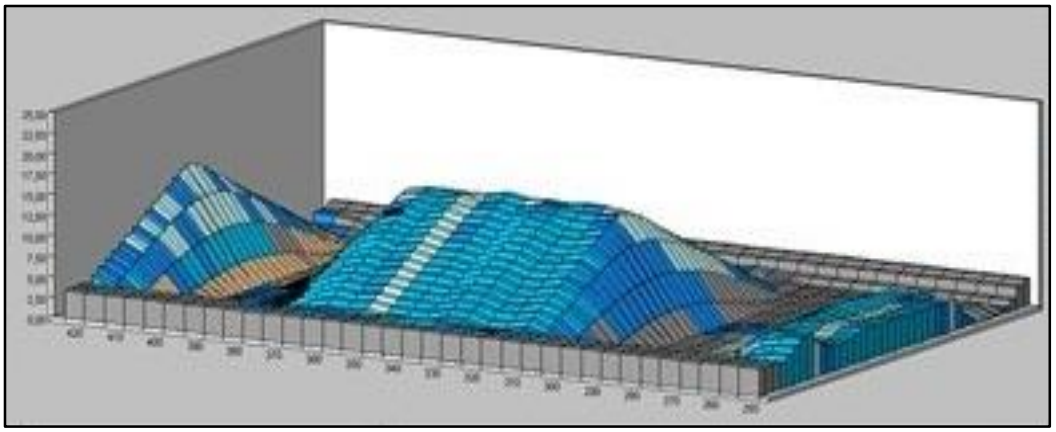

Figure 1.3: 3-D stockpile image

In reviewing the above literature, the system is found to be using manual selection of voxels by the operator to reclaim, based on an individual experience, without considering the movement of the BWR. In fact, the consideration of the BWR minimum movement in selecting voxels to reclaim will definitely reduce the handling costs as the giant machine consumes huge energy to operate. Moreover, cubic shaped profiles are used in dividing stockpiles into voxels. Thus, further investigation is required as to whether a cuboid shape is suitable for the reclaiming pattern of the bucket wheel reclaimer as BWR reclaims in a circular movement.

The other literature studies related to voxel based system are conducted by Zhao et al. mainly focusing on the modelling of 3D stockpile and the calculation of quality distribution within a stockpile and within voxels. In their first study, stockpile surface is measured in real time using 3 DOF laser scanner and the 3D stockpile is automatically modelled during stacking and reclaiming operations [23]. Point clouds are extracted from laboratory scaled stockpile contours and 3D stockpile was developed using Fourier series for wired frame model and Universal Fourier model for surface model.

The stockpile model developed in the previous study was used to calculate the quality of cuboid voxel grids in stockpile in the second paper [24]. The study also involved the calculation of stacked layers volume inscribed in cuboid voxels as stockpile are stacked

with different grade layers for blending purpose. Then the quality grade composition of cuboid voxels are estimated to assist in reclaiming operations. The small stockpile was experimented to verify the approach and it is claimed to improve in meeting quality and quantity demand specifications.

The final study was conducted by Zhao et. al to estimate the quality of the BWR reclaiming cut in advance as continuation of previous two studies [25]. The volume of the reclaiming cut was calculated using Quasi-Monte Carlo (QMC) technique. A quality embedded geometric stockpile model is associated with the BWR kinematics model to calculate the quality composition of the BWR reclaiming cut. The authors suggested to optimize the reclaiming pattern of the BWR based on the quality and quality information available to improve in meeting the target grade in an effective and efficient manner. Based on the review of these three literatures, the studies are focused on the geometric modelling of the 3D stockpile and calculation of quality distribution within a stockpile and voxels. The integration of stockpile model and BWR model is based on the geometrical approach. However, the developed studies of these literature can be integrated with the proposed approaches in this study to develop the fully automatic reclaiming system in the future.

1.3 Aims and hypothesis

The aim of this study is to improve outcomes in meeting ore producers' three previously stated objectives, using a voxel based approach. The use of cuboid voxels is a significant improvement but seemed to be affecting accuracy in reclaiming. Accuracy in reclaiming will not only affect the quantity, but also the quality of the grade as it is estimated proportionally, based on the quantity of the material. To achieve optimal accuracy, the voxel profile will be defined based on the kinematics of the bucket wheel reclaimer. The repetitive process of the coordinate conversion from Cartesian coordinate

to BWR joint space and the calculation of BWR's bucket wheel movement again and again in each cuboid voxel reclaiming may hold back the efficiency of the reclaiming operation. One can argue that the coordinate conversion and the planning of reclaiming path of the BWR's bucket wheel for the whole operation can be carried out before the actual reclaiming begins. However, the process of the reclaiming operation will be complicated for automation as selected voxels are in BWR joint space whilst the remaining stockpile voxels are still in Cartesian coordinate. The use of a single coordinate for both the sickle-shape voxels and the BWR will permit to implement a straight forward automatic reclaiming operation.

Moreover, the dependence on operator's expertise could be reduced by introducing an automatic selection of voxels to reclaim whilst minimizing the reclaimer movement. The consideration of the reclaimer movement in reclaiming voxels will save energy, time and reduce the handling costs, one of the main concerns of the ore producers, as the BWR is one of the giant machine on earth. To achieve the stated aims, the following objectives are listed.

1.4 Objectives of the study

For the purpose of improving in meeting customers' demands, coupled with minimizing handling costs, the following studies are proposed:

- Investigation of the optimal profile of voxels based on the kinematics of the bucket wheel reclaimer
- Voxelization of the stockpile into a sickle-shape voxels based on the BWR's kinematics
- Investigation of the volume model for sickle-shape voxels

- Identification of the cuboid voxels to reclaim in order to meet quality and quantity demand with BWR minimum travelled distance
- Identification of the sickle-shape voxels to reclaim in order to meet quality and quantity demand with BWR minimum joint movements

1.5 Thesis structure

The remaining part of the thesis is structured as follows. Chapter 2 discusses about the methodologies used in this study to achieve the objectives listed in the previous section.

Chapter 3 presents about the investigation of the optimal voxel profile. It starts with the configuration and reclaiming methods of the commonly used bucket wheel reclaimer (BWR). The investigation of the cuboid voxels reclaiming by the BWR regarding the accuracy of the reclaiming is followed. Then, the modeling of the bucket wheel reclaimer's kinematics is conducted. Based on the kinematics model, a sickle-shape voxel is introduced to achieve the optimal accuracy. The study of kinematics model was presented at " The 2011 IEEE International Conference on Robotics and Biomimetics (ROBIO)" held on Phuket Island, Thailand on 7th December, 2011. The extended study of the chapter is published in "*Transaction on Control and Mechanical Systems"*, Vol 2, Issue 2, 2013.

The voxelization of the stockpile into sickle-shape voxels based on the kinematics of the BWR is discussed in Chapter 4. The whole stockpile in Cartesian coordinate is transformed into sickle-shape voxels associated with the BWR joint parameters. The part of the study was presented at the "2013 IEEE 8th Conference on Industrial Electronics and Applications (ICIEA)" held in Melbourne, Australia on June 19, 2013. Moreover, the voxelization study is submitted to the "International Journal of Mining Science and Technology" and it is in the review process.

Chapter 5 presents the investigation of the volume model for the sickle-shape voxel.

The general volume model of the sickle-shape voxel is derived in Spherical coordinate and triple integration is solved numerically. A case study is also conduced to verify the approach. The study was presented at the "11th International Conference on Bulk Materials Storage, Handling and Transportation (ICBMH)" held at the University of Newcastle, Australia on 2nd of July, 2013.

The study of optimization in minimum travelled distance of the BWR in reclaiming cuboid voxels is presented in Chapter 6. The automatic identification of the cuboid voxels based on the minimum movement of the BWR to meet the desired quantity and quality grade is conducted with three case studies. The study was presented at " The 11th International Conference on Control, Automation, Robotics and Vision (ICARCV 2010) held in Singapore on 7 December, 2010. The exteneded study is published in the *International Journal of Minerals Processing*, Volume 98, Issues 1–2, January 2011.

Chapter 7 presents the study on optimization of BWR joint movements in reclaiming sickle-shape voxels. The minimum movement of the BWR joints is considered in the objective function of the optimization problem as sickle-shape voxels are associated with BWR joint parameters. The journal paper based on this chapter was submitted to the "International Journal of Mining, Reclamation and Environment" and currently it is under review process.

The thesis concludes in Chapter 8 with the recommended future works. Discussions and contributions of the studies are also presented.

CHAPTER 2: METHODOLOGIES

In literature, the voxel based approach was used with cubic voxels in a single study without considering the reclaiming pattern of the BWR [15]. The disagreement between the voxel profile and the reclaiming profile of the BWR will have a significant effect on the accuracy of the reclaimed volume and aggregated chemical composition. The investigation is carried out in Section 3.1 about the accuracy of reclaiming cubic voxels by the BWR. In this study, the optimal voxel profile will be defined based on the reclaiming profile of the BWR to achieve the best possible accuracy in reclaiming. In order to derive the reclaiming profile of a BWR, the study of the kinematics model of the BWR is firstly conducted. Based on the reclaiming profile of a BWR, the optimal voxel profile associated with BWR joint parameters can be defined.

Then, the stockpile is divided into sickle-shape voxels associated with the BWR joint parameters. In order to do that, firstly stockpile is scanned, modeled and contours are extracted for specific heights. The scanning, modeling of the stockpile and extracting of the stockpile contours is not covered in this study and are assumed to be available. The extracted contours are modeled for the voxelization process. The study of inverse kinematics is required for the transformation from the stockpile in Cartesian coordinates into voxels associated with the BWR joint parameters. Unlike cubic voxels, the volumes of sickle-shape voxels, which are defined based on the BWR's kinematics, are neither fixed nor identical. The volume of each voxel is different based on the geometric shape of the stockpile and the BWR kinematics at that spot. The investigation about the volume calculation of the sickle-shape voxel is crucial to provide quantity and quality information in reclaiming. The available knowledge of quantity and quality will assist in selecting voxels to fulfill the desired specifications of demand. From the available stockpile voxels, optimization algorithm is essential to select the reclaiming voxels, based on the defined objective function whilst maintaining the required constraints. The binary integer

programming algorithm is used in solving the optimization problem based on the requirement of the problem. The motivations of using binary integer programming is discussed in Section 2.6.

2.1 Bucket wheel reclaimer (BWR)

In mining industries, mechanical machines are essential for bulk material handling operations. One of them, above ground reclaimers are commonly used and offered in many styles to handle bulk material. They can be classified by their arrangement, structure and device. The above ground reclaimer can be divided into three types depends on its structure. In boom type, boom is supported at one-end of the structure whereas in portal and bridge types, both ends are supported. According to their working mode, above ground reclaimers also can be classified into two types: continuous and cyclic machines. The grab bucket, dragline and shovel are the type of cyclic reclaiming machines which reclaim a finite load with a series of motions. In the late 19^{th} and early 20^{th} centuries, the world's largest land based machines was built based on the bucket wheel technology from waterborne ladder dredgers concept to deal with the large increase in transportation of bulk material [26][27]. Since then, bucket wheel system was used in stacking, reclaiming and shipping bulk materials at ports and mine sites, excavating and waste disposed in mines, and handling ore at plants [27]. Bucket wheel reclaimers are one of the continuous reclaiming machines which reclaim material continuously [14]. Bucket wheel stackers and reclaimers have played major role in handling large tonnages of bulk materials in the large Stockyards [26]. Bucket wheel Stackers/Reclaimers are so popular in the mining industry that it is just commonly known as Stacker/Reclaimer [14]. In this study, as a result, the BWR is used for the purpose of reclaiming bulk material such as iron ore from stockpiles in Stockyard. The BWR is available in many types depends on the configuration and structure of the

mechanisms. From all, the rail supported and boom mounted BWR is focused in this study.

Some of BWRs are designed for dual purposes: stacking and reclaiming. Those are called bucket wheel stacker/reclaimer. A typical BWR is approximately *25m* high, *50m* in length and 13,000 tons in weight. A rotation wheel with buckets is attached at the end of a *45m* boom to scoop material [28]. The conveyor belt is fixed in the middle section of the boom to carry materials fallen from buckets [29]. A BWR manufactured by KRUPP is shown in Figure 2.1 [30].

Figure 2.1: Bucket wheel reclaimer from ThyssenKrupp Robins

2.2 The study of BWR's kinematics

Kinematics is the study of motion which includes position, velocity and acceleration without considering the forces that cause it [31]. However, this study will focus only on the position and orientation of the BWR kinematics. The whole body moves along the rail to reach the desired position. The long boom move luffing motion represents up and down movement and a slewing motion for reclaiming in a circular motion. The rotating bucket wheel is attached at the end of the boom to scoop material with the attached buckets from a stockpile.

In summary, the BWR is able to move in 4 motions, consisting of the rotation of the bucket wheel. Based on the number of motions the BWR possesses, it is treated as a 4 DOF robotic manipulator for the purposes of deriving a kinematics model. The Schematic diagram of the BWR is shown in Figure 2.2 [32]. As a first step, coordinate frames are needed to be assigned to the BWR skeleton using modified Danevit-Hartennberg (D-H) notation [31]. Among the links of the BWR, the bucket wheel is the actual link which is in contact with the material in reclaiming. For that reason, the tip of the buckets of the BWR bucket wheel is chosen as the desired position point to derive the kinematics equation. The kinematics model of the BWR will be drived in Chapter 3 after assigning coordinate frames to the BWR skeleton using modified Danevit-Hartennberg (D-H) notation. A detailed kinematic diagram of a 4-DOF BWR is shown in Figure 3.5 and 3.6.

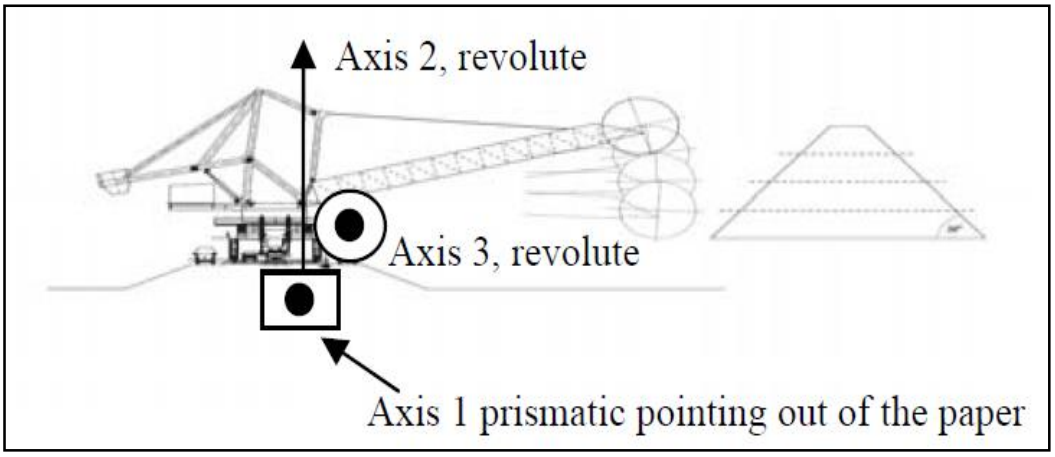

Figure 2.2: Schematic diagram of BWR and stockpile

2.3 The study of inverse kinematics of the BWR

Inverse kinematics refers to the calculating of joint displacements needed to move the end-effector to a desired position and orientation [31]. It means the conversion of points in working space from Cartesian coordinate to Joint parameters is carried out by inverse kinematics. Similarly, in sickle-shape voxelization, the stockpile in Cartesian coordinates is transformed into sickle-shape voxels associated with the BWR joint parameters. In order

to do that, it is necessary to study the inverse kinematics of the BWR. However, the kinematics model of the BWR is required to be derived first in solving inverse kinematics. As the BWR is treated as a 4 DOF robotic manipulator, there are four joint variables to be determined with three available equations. The consideration of bucket wheel rotation in counting DOF happens to generate redundancy in kinematics model. There are numerical methods to solve the inverse kinematics of the redundant robot manipulators. However, the analytical approach is preferred for this study as the closed form solution produces an exact solution instead of an approximate solution. In order to be able to solve a closed form solution for inverse kinematics, the number of variables to be determined needs to be equal to the number of constraint conditions. The investigation is carried out to determine the bucket wheel angle so that the analytical approach can be used to solve the inverse kinematics. A portion of the bucket wheel is in contact with the stockpile when reclaiming. The availability of the bucket wheel contact region will provide the bucket wheel angle to reduce the DOF. The investigation on inverse kinematics is presented in Chapter 3.

2.4 Modelling of stockpile contours

Inverse kinematics is used to transform data from Cartesian coordinate to the BWR joints space. In order to do the coordinate transformation, the boundaries points of the stockpile benches are necessary to be accessible. So the extraction of the contours from stockpile model for all benches is crucial for voxelization process. A stockpile is normally stacked in material handling yards and scanned to obtain the stockpile model. Scanning of a small-scale stockpile in the laboratory using a laser scanner was conducted by Lu et al. to study the stockpile model [33]. The stockpile is 740mm in length, 123mm in width and 140mm in height. The stockpile is sliced into three layers and boundaries are extracted to

define the contours of the stockpile. The 3-D stockpile model with extracted boundaries is shown in Figure 2.3.

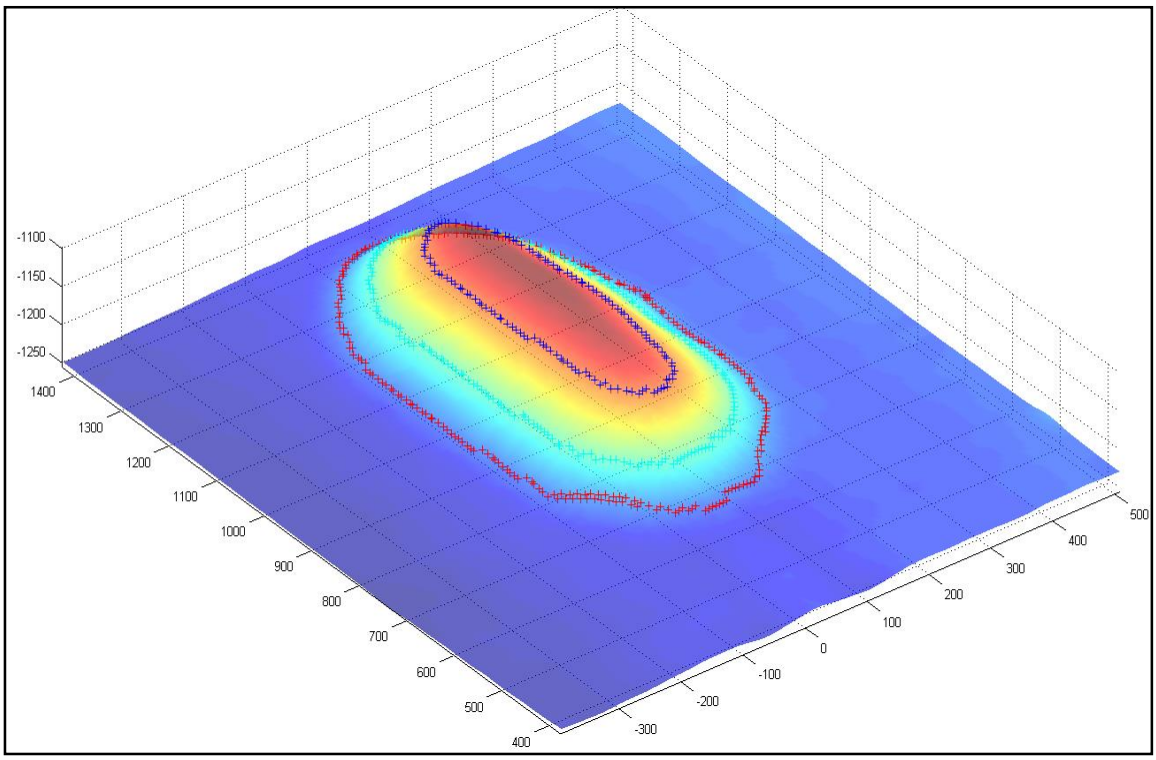

Figure 2.3: Scanned 3-D model of stockpile with boundary contours

The resulted boundary data points are used to define the stockpile contour using curve fitting. The purpose of curve fitting is to find a mathematical equation that describes a set of data which has minimal influence of random noise [34]. The polynomial least square method in finding the coefficients of polynomial equations that are a "best fit" to a set of (x, y) data is used. The boundary curves are fitted as ellipses, as shown in Figure 2.4. In that, 'o' marked curves represent extracted boundary curves and '- -' marked curves represent fitted curves. It can be seen that the fitted curves closely fit with the extracted curves. So, the fitted contours of all layers can be described in the form of the ellipse as:

$$\frac{(z-h)^2}{a^2} - \frac{(x-k)^2}{b^2} = 1 \qquad (2.1)$$

Where,

a = the radius along the z-axis

b = the radius along the x-axis

h, k = the (z, x) coordinates of the ellipse's centre

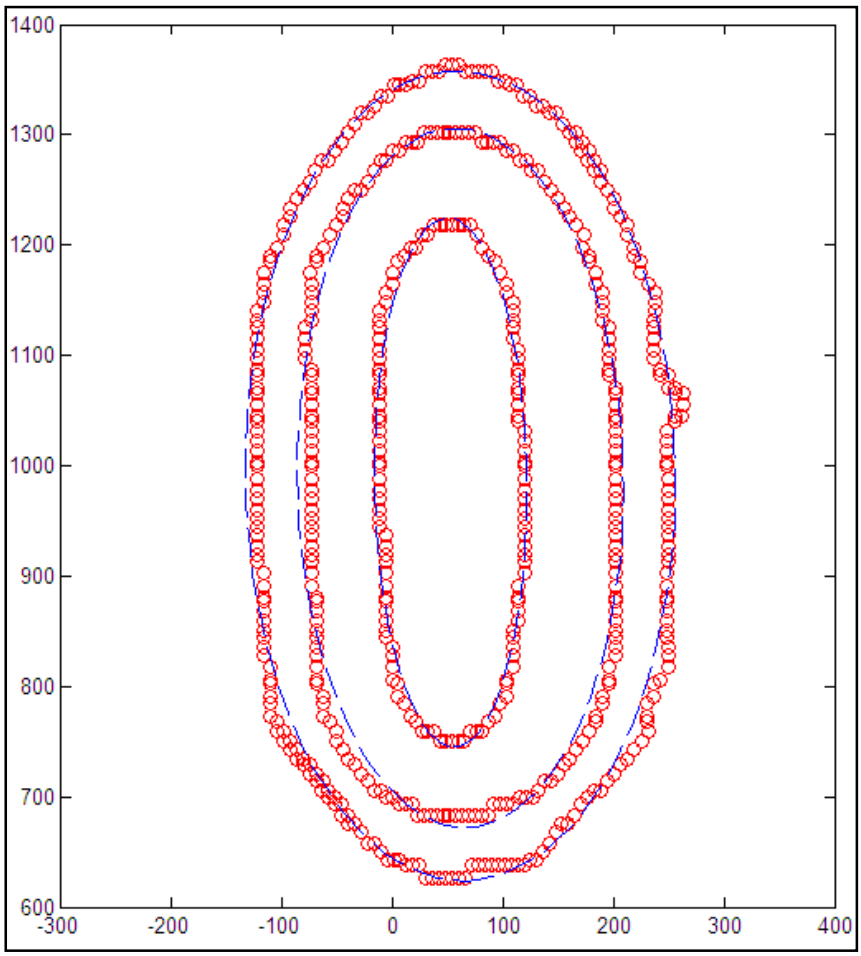

Figure 2.4: Extracted boundary curves and fitted curves

2.5 Triple integration in Spherical coordinates

Triple integration is normally used to calculate the volume of a solid. As the boundary of the voxel is curved in nature, the volume calculation is carried out in a spherical coordinate system. Numerical integration is employed to calculate the volume of the voxel. In spherical coordinates, the volume of the region can be calculated as [35]:

$$V = \int_{\theta_1}^{\theta_2} \int_{\emptyset_1}^{\emptyset_2} \int_{\rho_1}^{\rho_2} \rho^2 sin\emptyset \; d\rho \, d\emptyset \, d\theta \tag{2.2}$$

The definition of the corresponding parameters of Equation (2.2) is illustrated in Figure 2.5 [35].

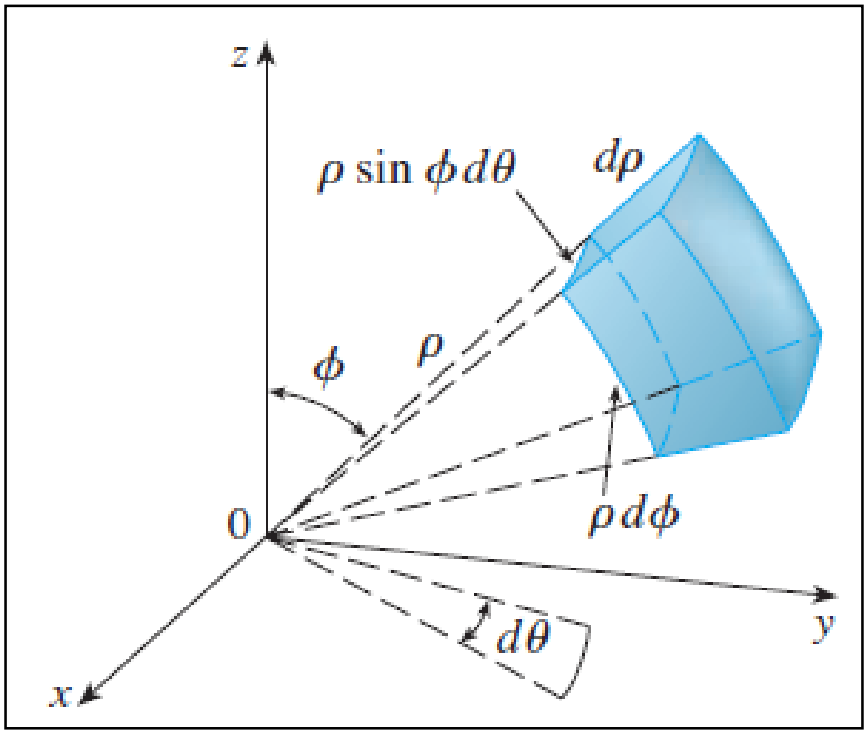

Figure 2.5: Volume element in spherical coordinates

The boundary of the solid is defined by three parameters: $\rho, \emptyset \; and \; \theta$ in spherical coordinates. In relating to the sickle-shape voxel, the boundary parameters of the voxel are required to be defined in calculating the volume. The involvement of the three BWR joint parameters in the voxel volume model compose non-linearity in integrand function. Due to this, a numerical method is required to solve the integration instead of an analytical approach. A Matlab function called “Integral3” is used to solve the numerical integration. “Integral3” employs a better approach between 'tiled' and 'iterated' in solving integration numerically. The 'tiled' method is based on a Quadrature approach of dividing the region into quadrants and approximating the integral over each quadrant by a 2-D quadrature rule.

If the error condition on a rectangle is not met, the rectangle is divided into quadrants and so forth. The 'iterated' method performs the integration as iterated one-dimensional integrals. The strengths of both approaches are used in “Integral3” to obtain better accuracy in integration.

2.6 Optimization using Binary integer programming

Contrary to the manual selection of cubic voxels by the operator to reclaim as in the literature, voxels will be selected automatically using an optimization algorithm. As with any optimization approach, the objective function and constraints are required to be defined to feed into the optimization algorithm. The minimum movement of the BWR is considered in defining the objective function to minimize energy consumption, which leads to a reduction in handling costs. The minimization of the travelled distance is considered for selecting cubic voxels as they are associated with Cartesian coordinates. Conversely, the joint movement minimization is considered for selecting sickle-shape voxels as they are associated with BWR joint parameters. The desired quantity and quality grade are regarded as constraints along with other reclaim order limitations. The details of the defining objective function and constraints will be discussed in Chapters 6 and 7.

Based on the requirements of the study, the appropriate optimization method in literature is reviewed. Though the optimisation in reclaiming has not been reported in literature, there are several studies found in which optimisation is applied in open pit mining operation mainly for scheduling. Open-pit mining is an excavation of ore blocks at the surface of the ground. During the mining process, a deeper and deeper pit is dug until the mining operation terminates [36]. The orebody is usually divided into small mining units called blocks in open pit mining. In general, the ore body block model contains between 50,000 to 500,000 blocks, which must be scheduled over a period of 15-25 years. The

objective of the scheduling procedure is to find the block extraction sequence for the maximum possible net present value whilst maintaining a number of constraints [37]. Many types of mathematical formulations have been considered for the mining scheduling problem since 1965 [38]. There are linear programming (LP), mixed integer programming (MIP), pure integer programming (IP) and dynamic programming (DP).

Last decade, pure integer programming and mixed integer programming became popular as the computation capacity of the solver to handle high volume of variables has increased. On the other hand, available voxels in the database are restricted to only two states which are either selected or not selected in reclaiming. So, the reclaiming states of the voxels is similar to the states of the variables in binary integer programming approach. Binary integer programming is a form of integer programming in which decision variables are required to be either “0” or “1”. Although it seems overly restrictive, there are many problems that can easily be modeled using binary decision variables.

For instance, Gholamnejad developed a binary integer programming model for a short-term production scheduling problem in open pit mines [39]. The approach incorporated all blocks on the same bench to be accessed by the mining equipment, which was not achieved previously by other models. Another study using binary integer programming was conducted by Moosavi et al. [40] for optimal extraction sequence modeling for open pit mining operation. Moreover, Akhtavar et al. carried out optimization of the transition from open-pit to underground operation in combined mining using binary integer programming [41]. Researchers who conducted binary integer programming pointed out that the approach tends to increase the size of the problem. However, the binary integer programming permits to introduce geometric constraints and allows to acess all the available blocks to extract.

All available voxels in stockpile are required to access in reclaiming to meet the

desired specifications, which can be realized by using the binary integer programming. Moreover, the binary integer programming suits the voxels reclaiming as the whole voxel is reclaimed instead of portion reclaiming in cubic voxel approach. The optimization model, along with the objective function, is written in the Mosel programming language. Moreover, the problem is executed using Xpress-Optimizer to select voxels to reclaim. Mosel language is the modeling language and a programming language available in the FICO® Xpress Optimization Suite [42]. Xpress-Mosel programming language is the property of Dash Associates 1984-2001.

2.7 Summary of the chapter

This chapter discusses about the background study of the BWR and methodologies required to use in this study. Firstly, the historical background of the BWR was presented as the study is focused on the commonly used boom type BWR for reclaiming purpose. BWR is the largest continuous reclaiming machine which plays a major role in mining handling operations since 19^{th} centuries. Subsequently, the definitions of the kinematics and inverse kinematics study were explained. It is stated the kinematics model of the BWR will be derived as a 4 DOF robotic manipulator using modified Danevit-Hartennberg (D-H) notation. Then, the approach for solving the inverse kinematics was presented.

After discussing about the studies about the BWR, the discussion continues for the study of stockpile as stockpile will be divided into voxels based on the kinematics of the BWR. The study was started with the modelling of stockpile contour. The scanned stockpile is layered and layers are modelled. The knowledge of voxel quantity is required to cater the demand quantity. fro that, the approach for calculating volume of the sickle-shape voxel is discussed. The background information of triple integration in spherical coordinate was

presented. The last section presented about the Binary integer programming to solve the optimisation problem.

CHAPTER 3: INVESTIGATION OF THE OPTIMAL VOXEL PROFILE

The expectation of steel producers has increased over the years to receive iron ore in tighter required quantity and specified quality tolerance range. The voxel-based approach was introduced to improve in meeting customers' request specifications in terms of quantity and quality grade. However, there has not been any study yet to investigate the optimal profile of the voxel except using cuboid shape. This chapter starts with the study on the compatibility of the cuboid voxel, which was used in the previous study, in reclaiming with the BWR. The investigation is presented in Section 3.1. The derivation of the full kinematics model of the BWR including the bucket wheel, which is treated as a 4 DOF robotic manipulator, is discussed in Section 3.2. Based on the kinematic model of the BWR, the cutting trajectory is simulated in Section 3.3. Lastly the optimal profile of the voxel, which is named as sickle-shape voxel, is introduced in Section 3.4 before concluding the chapter in Section 3.5.

3.1 Investigation of the compatibility of cuboid voxels with the BWR reclaiming

In a cuboid voxel approach of literature study, it is appealing that the specification of the demand can be fulfilled in combining certain voxels before reclaiming physically. However, it is concerned that whether the actual reclaimed volume is achieved as promised in a visual reclaiming process. Firstly, the reclaiming patterns of the BWR will be discussed before the investigation for compatibility with cuboid voxels is conducted.

3.1.1 Reclaiming method of the BWR

The BWR reclaims bulk material from stockpiles normally using either bench reclaiming or pilgrim step reclaiming approach [43]. During the bench reclaiming process, all the stockpile layers are completely reclaimed one by one from top to bottom. The whole layer of the stockpile is reclaimed before the boom is luffed down to the next layer. The

bench reclaiming approach is used when the entire layer or stockpile is required to reclaim [43]. In pilgrim step approach, the only portion of the stockpile layer is reclaimed instead of reclaiming whole layer. The pilgrim step approach is used when the material from one end of the stockpile is required to reclaim first or only portions of the particular stockpile is required to reclaim [43].

In both reclaiming approaches, the BWR reclaims material with slewing motion which is a circular rotational motion of the boom. The slewing trajectory of the BWR's boom tip with translation movement as seen from top view is shown in Figure 3.1. In this figure, "AB" curve is the slewing motion path from position "O" and "A'B'" is the slewing motion path after translating distance "d_1" to position "O'".

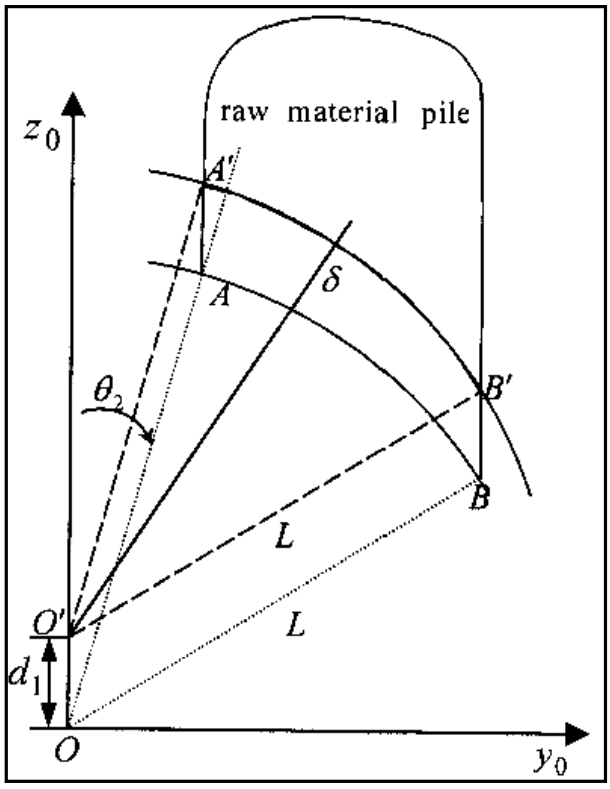

Figure 3.1: Trajectory of a BWR boom tip [44]

Moreover, the luffing motion is used to reclaim lower layer bulk material from stockpiles. Because of the BWR's luffing motion, the remaining shape of stockpile after reclaiming partially is in ladder shape as shown in Figure 3.2 [45].

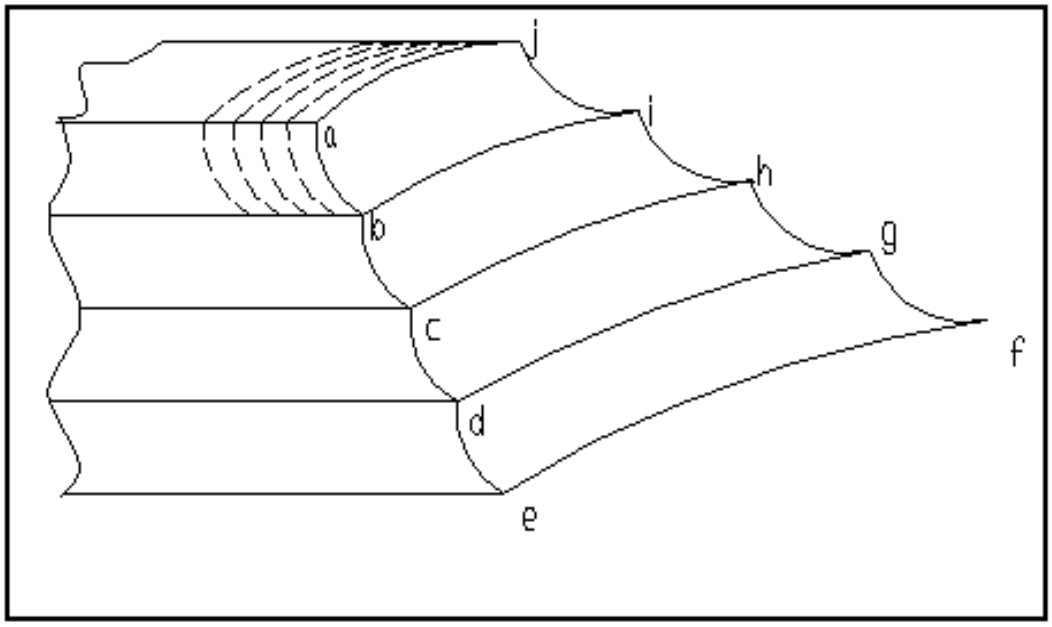

Figure 3.2: Remaining shape of a stockpile after reclaiming partially

3.1.2 Drawbacks of cuboid voxels in reclaiming with the BWR

The investigation is carried out here to compare the reclaiming profile of BWR with cuboid voxels in an actual reclaiming.The reclaiming profile of the BWR in reclaiming cuboid voxel is shown in Figure 3.3. It shows that there is huge disagreement between the reclaiming profile and cuboid voxel which leads to poor estimations in terms of quantity and quality. It will be compensated from other voxels if the whole stockpile or whole bench is reclaimed as in bench reclaiming method. However, certain portions of the stockpile are required to be reclaimed in most of the cases to meet the demand requirement as practiced in pilgrim step method.

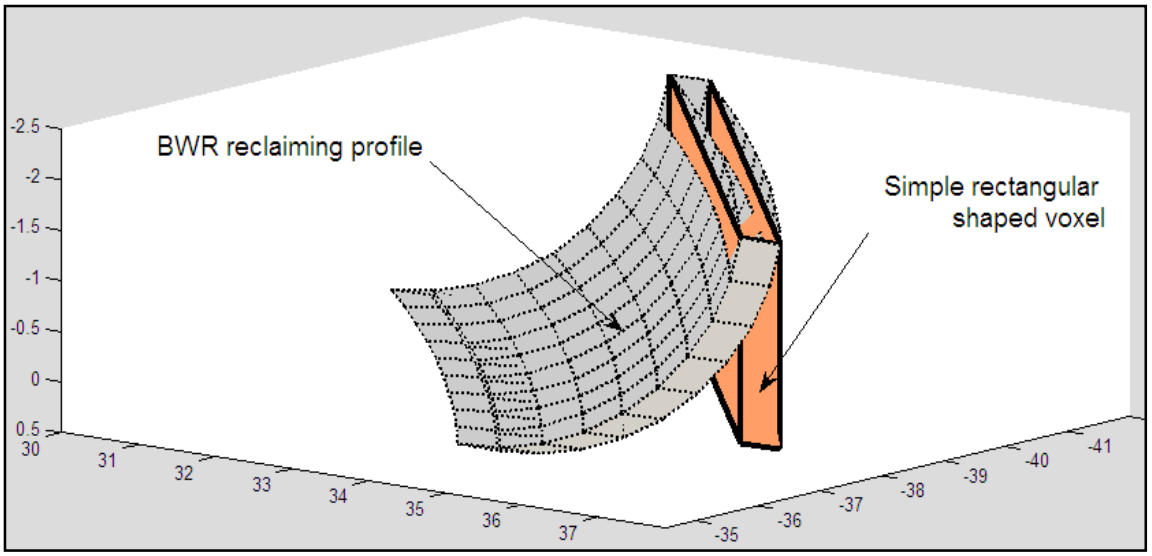

Figure 3.3: BWR reclaiming voxel profile with cuboid voxel

Furthermore, Figure 3.4 shows the disagreement between the BWR reclaiming curve and cuboid voxels from top view. In that figure, stockpile is composed with labelled cuboid voxels available for reclaiming. As an example, voxels No. 1 and 2 are necessary to reclaim to meet the customer demand. So the BWR attempts to reclaim the required voxels 1 and 2 with its reclaiming path as shown in Figure 3.4. However, it can be seen that only the portion of voxels 1 and 2 are able to be reclaimed with a circular reclaiming path. Moreover, the extra portion of the voxel 3 is reclaimed affecting the accuracy of the reclaiming volume. In other words, some unwanted portions of voxels are reclaimed and/or some necessary portions of voxels are left behind. It is observed that the optimal accuracy of reclaiming has not been able to achieve with cuboid voxels for BWR reclaiming. So the concern is mounting that what shapes of the voxels should be most suitable for the BWR reclaiming. The other approach is defining smaller size voxels to improve the accuracy of reclaiming. It is believed that it will increase the accuracy of output to some extent, but there will be some drawbacks attached to it. The stockpile is a large entity and the BWR reclaims high volume at a single movement. The allocation of the smaller size of voxel will make computation very heavy for voxelization and also it is not practical for the huge

reclaiming nature of the operation. It is realized that the best approach of defining the optimal shape of voxel will be a replicate of BWR reclaiming trajectory. The optimal accuracy of reclaiming will be achieved when the BWR reclaims same trajectory with voxel boundary. To study the BWR reclaiming trajectory, the kinematics model of the BWR including bucket wheel is derived in the next section.

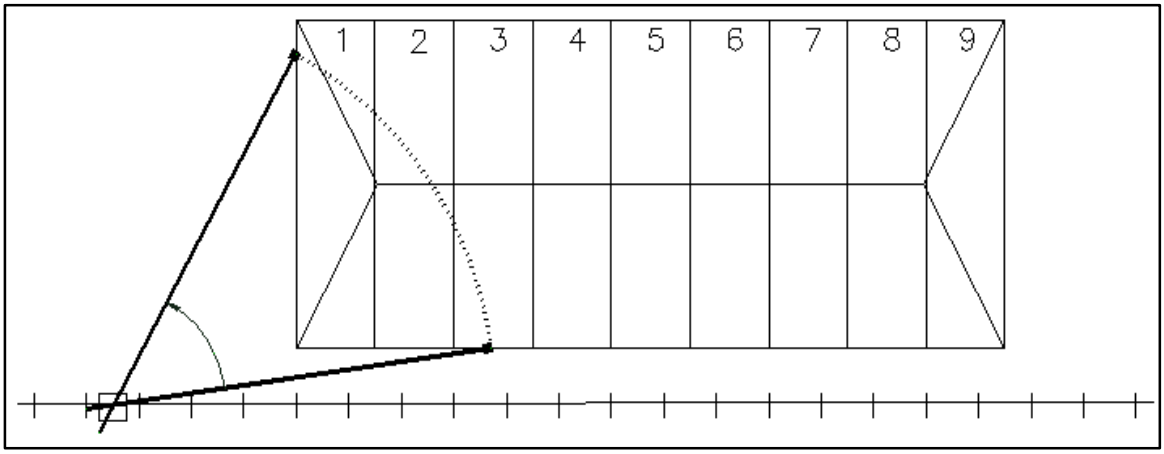

Figure 3.4: Reclaiming curve of BWR and cuboid voxels

3.2 Kinematics model of the BWR

BWR can be classified as a serial manipulator in robotic fields [29] [32] as shown in Figure 3.5. The prismatic joint represents for the translation motion of the main body moving on the rectilinear rail. The slewing motion is rotated about the Axis 2 for reclaiming whereas the luffing motion is rotated on the Axis 3 for accessing lower bench of the stockpile. Lu treated BWR as a 3 DOF robot manipulator considering bucket wheel as an end-effector [32]. However in this study, the BWR will be treated as a 4 DOF manipulator counting bucket wheel as a link.

As stated before, the tip of the buckets on the BWR bucket wheel is chosen as the desired position point to find the kinematics equation. The coordinate frames are assigned to the BWR skeleton as shown in Figure 3.5 using modified Danevit-Hartennberg (D-H) notation [31]. Figure 3.6 shows an enlargement of the bucket wheel from Figure 3.5.

The coordinate frame of the translating joint is attached at the center of the main

body as (x_1, y_1, z_1) with the direction of z_1 in parallel with the rail. The slewing joint is represented by (x_2, y_2, z_2) while z_2 points along the rotational joint axis. The coordinated frame (x_3, y_3, z_3) is assigned for the luffing motion in which the direction of z3 is parallel to the rotational joint axis. The bucket wheel rotation joint is assigned with the coordinate frame (x_b, y_b, z_b).

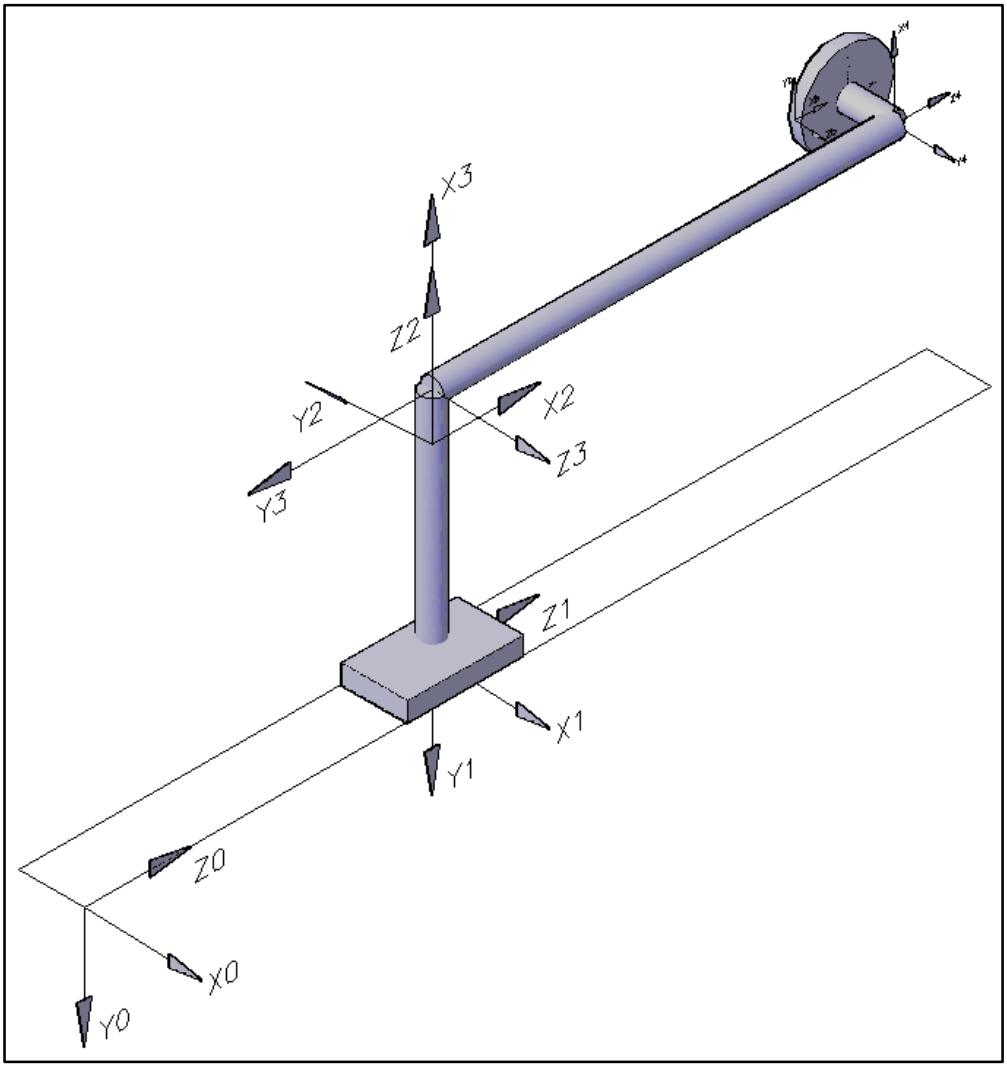

Figure 3.5: BWR skeleton with assigned frames using modified D-H representation

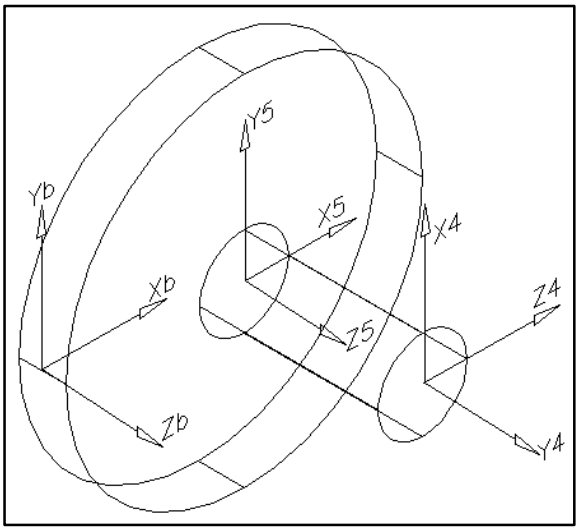

Figure 3.6: Enlargement of bucket wheel with assigned frames

Where,

θ_2 = slewing angle between X2 and X1 measured about Z1.

θ_3 = luffing angle between X3 and X2 measured about Z2.

θ_b= bucket wheel angle between Xb and X5 measured about Z5.

d= translated distance between X1 and X0 measured along Z0.

r = radius of the bucket wheel

L_2, L_3, L_4, L_5, h and k are distances between respected frames and are constant parameters. The value of the constant parameters varies depends on the type and dimension of the BWR. On the other hand, d, θ_2, θ_3 and θ_b are variable parameters representing translating, slewing, luffing and bucket wheel rotation motions.

The transformation matrix for adjacent coordinate frames, *i* and *i-1* using modified D-H representation is given by [31]:

$$ {}^{i-1}_{i}T = \begin{bmatrix} \cos\theta_i & -\sin\theta_i & 0 & a_{i-1} \\ \sin\theta_i\cos\alpha_{i-1} & \cos\theta_i\cos\alpha_{i-1} & -\sin\alpha_{i-1} & -\sin\alpha_{i-1}d_i \\ \sin\theta_i\sin\alpha_{i-1} & \cos\theta_i\sin\alpha_{i-1} & \cos\alpha_{i-1} & \cos\alpha_{i-1}d_i \\ 0 & 0 & 0 & 1 \end{bmatrix} \quad (3.1) $$

The transformation matrix from the bucket wheel frame to the world coordinate is derived by multiplying transformation matrices from Frame 0 to Frame b:

$$ {}^{0}T_{b}={}^{0}T_{1}\,{}^{1}T_{2}\,{}^{2}T_{3}\,{}^{3}T_{4}\,{}^{4}T_{5}\,{}^{5}T_{b}=\begin{bmatrix} m_x & n_x & o_x & x_b \\ m_y & n_y & o_y & y_b \\ m_z & n_z & o_z & z_b \\ 0 & 0 & 0 & 1 \end{bmatrix}=\begin{bmatrix} O & P \\ 0 & 1 \end{bmatrix} \quad (3.2) $$

Where, O represents the orientation part and P represents the position part of the transformation matrix. The orientation information of the bucket tip is:

$$ m_x = -\sin\theta_2 \cos\theta_3 \cos\theta_b + \sin\theta_2 \sin\theta_3 \sin\theta_b $$

$$ m_y = -\sin\theta_3 \cos\theta_b - \cos\theta_3 \sin\theta_b $$

$$ m_z = \cos\theta_2 \cos\theta_3 \cos\theta_b - \cos\theta_2 \sin\theta_3 \sin\theta_b $$

$$ n_x = \sin\theta_2 \cos\theta_3 \sin\theta_b + \sin\theta_2 \sin\theta_3 \cos\theta_b $$

$$ n_y = \sin\theta_3 \sin\theta_b - \cos\theta_3 \cos\theta_b \quad (3.3) $$

$$ n_z = -\cos\theta_2 \cos\theta_3 \sin\theta_b - \cos\theta_2 \sin\theta_3 \cos\theta_b $$

$$ o_x = \cos\theta_2 $$

$$ o_y = 0 $$

$$ o_z = \sin\theta_2 $$

Whereas, the kinematics model of the BWR at the tip of the bucket is:

$$ x_b = -r\sin\theta_2 \cos\theta_3 \cos\theta_b + r\sin\theta_2 \sin\theta_3 \sin\theta_b + h\cos\theta_2 $$
$$ -k\sin\theta_2 \cos\theta_3 - \sin\theta_2 (L_5 \cos\theta_3 + L_4) \quad (3.4) $$

$$ y_b = -r\sin\theta_3 \cos\theta_b - r\cos\theta_3 \sin\theta_b - L_2 - L_3 - k\sin\theta_3 - L_5 \sin\theta_3 \quad (3.5) $$

$$ z_b = r\cos\theta_2 \cos\theta_3 \cos\theta_b - r\cos\theta_2 \sin\theta_3 \sin\theta_b + h\sin\theta_2 $$
$$ +k\cos\theta_2 \cos\theta_3 + L_5 \cos\theta_2 \cos\theta_3 + L_4 \cos\theta_2 + d \quad (3.6) $$

Link dimensions of the commonly used BWRs, L_2=6m, L_3=5m, L_4=5m, L_5=50m, h=0.5m, k=0.5m and r=2.5m, are used in this study for kinematics model. Using the BWR kinematics model, the motion trajectory of the bucket is simulated as shown in Figure 3.7.

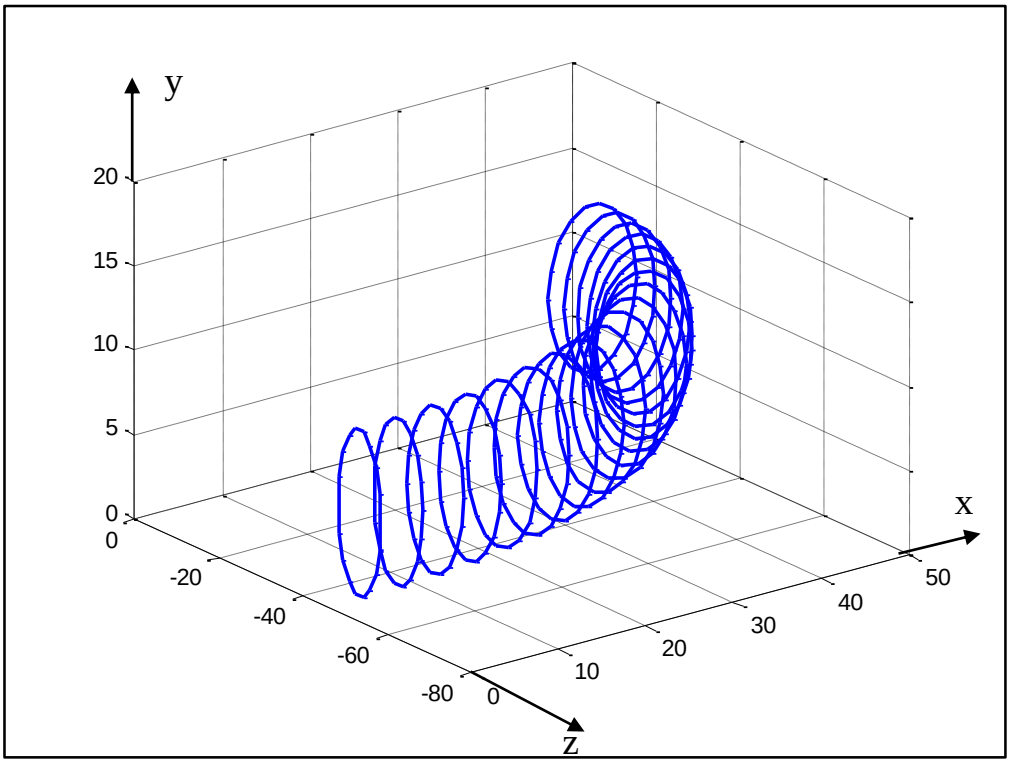

Figure 3.7: Motion trajectory of a bucket wheel

3.3 BWR cutting trajectory

In referring the kinematics equations, the joint parameters involved are translational distance (d), luffing angle (θ_3), slewing angle (θ_2) and bucket wheel angle (θ_b). Among them, the bucket wheel angle, which accounts for contact region between the bucket wheel and stockpile, is investigated here to simulate the cutting trajectory. Schneidersmann indicated that the filling process begins at $\alpha 0 = 0$ degree as shown in Figure 3.8 when the bucket dips into the material [46]. Then at $\alpha 1 = 90$ degree, the filling process of the bucket is completed. Hence, the bucket wheel angle is taken as the range from 0 to 90 degrees for cutting trajectory simulation.

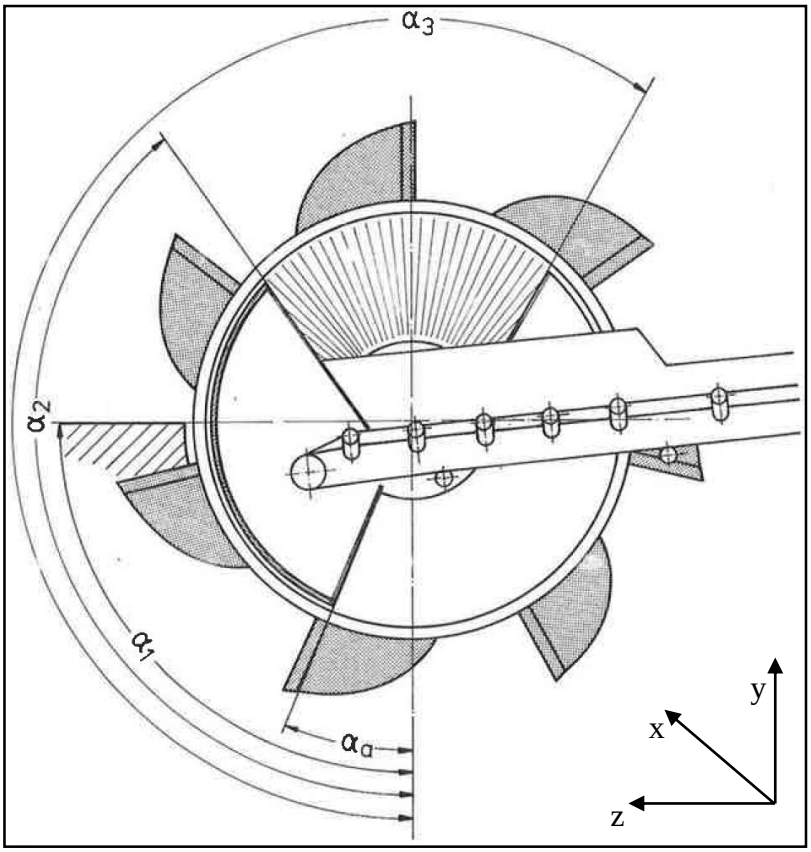

Figure 3.8: Three phases of the bucket wheel cycle

The cutting trajectory of the BWR is modelled as:

$$x_b = -r\sin\theta_2\cos\theta_3\cos(0,\pi/2) + r\ \sin\theta_2\sin\theta_3\sin(0,\pi/2) + h\cos\theta_2$$
$$-k\sin\theta_2\cos\theta_3 - \sin\theta_2\,(L_5\cos\theta_3 + L_4) \quad (3.7)$$

$$y_b = -r\sin\theta_3\cos(0,\pi/2) - r\ \cos\theta_3\sin(0,\pi/2) - L_2 - L_3$$
$$-k\sin\theta_3 - L_5\sin\theta_3 \quad (3.8)$$

$$z_b = r\cos\theta_2\cos\theta_3\cos(0,\pi/2) - r\cos\theta_2\sin\theta_3\sin(0,\pi/2) + h\sin\theta_2$$
$$+k\cos\theta_2\cos\theta_3 + L_5\ \cos\theta_2\cos\theta_3 + L_4\cos\theta_2 + d \quad (3.9)$$

The luffing angle (θ_3) is taken as -20 degree, whereas slewing angle range (θ_2) is taken as (0, 90) degree for simulation. The resulted cutting trajectory is shown in Figure 3.9. In that figure, the dotted curve is the cutting trajectory of the BWR at translation distance d= 0 and the solid curve is the cutting trajectory after translated for d=10m. Moreover, the upper boundary and lower boundary of cutting trajectory has a different

curvature because of the luffing motion involved. In defining the profile of voxel, minimum translated distance of the BWR can be used as the width of the voxel. The boundary of the voxel can be defined using slewing curve of the BWR. The influence of the BWR kinematic in defining the voxel profile will produce non-regular shape contributing difficulty in volume computation.

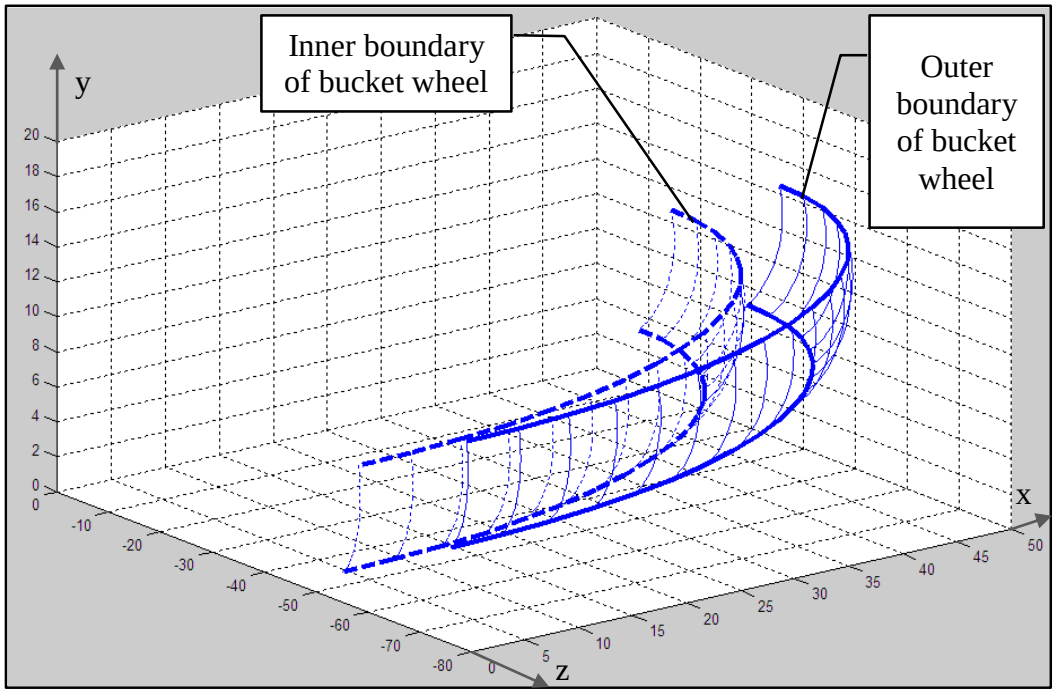

Figure 3.9: Cutting trajectory of BWR for the given parameter

Based on the cutting profile of the BWR, the potential shape of a voxel is shown in Figure 3.10.

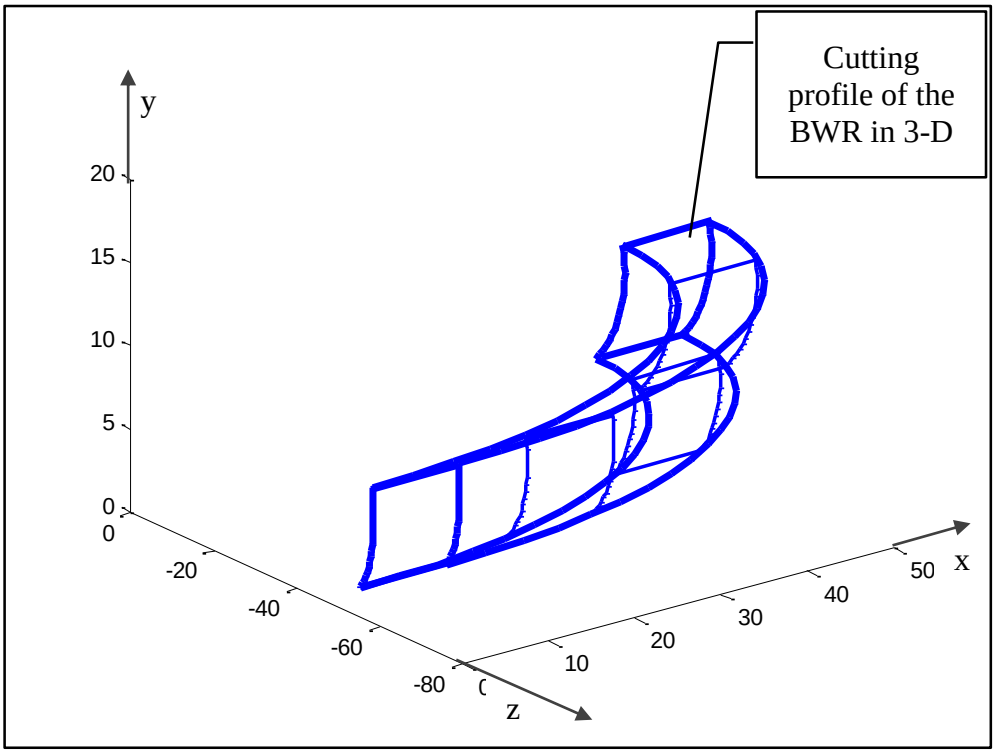

Figure 3.10: Potential voxel profile

3.4 Sickle-shape voxel profile

The kinematics models described by Equations 3.7-3.9 are used to simulate the single cut profile of the slewing to predict the potential voxel profile. For that, d is taken as 11m, θ_3 is taken as 10 degrees and θ_2 range as (30- 40) degree. The resulted voxel shape is shown in Figure 3.11. The shape of the voxel is named as sickle-shape because the shape resembles a sickle form. Given the stockpile model, the whole stockpile can be divided into sickle-shaped voxels associated with BWR joint parameters: translational distance, luffing angle and slewing angle range. Upon voxelization, sickle-shaped voxels and BWR will be in a single coordinate space, assisting to enhance automation for BWR reclaiming. The voxelization process will be conducted in Chapter 4.

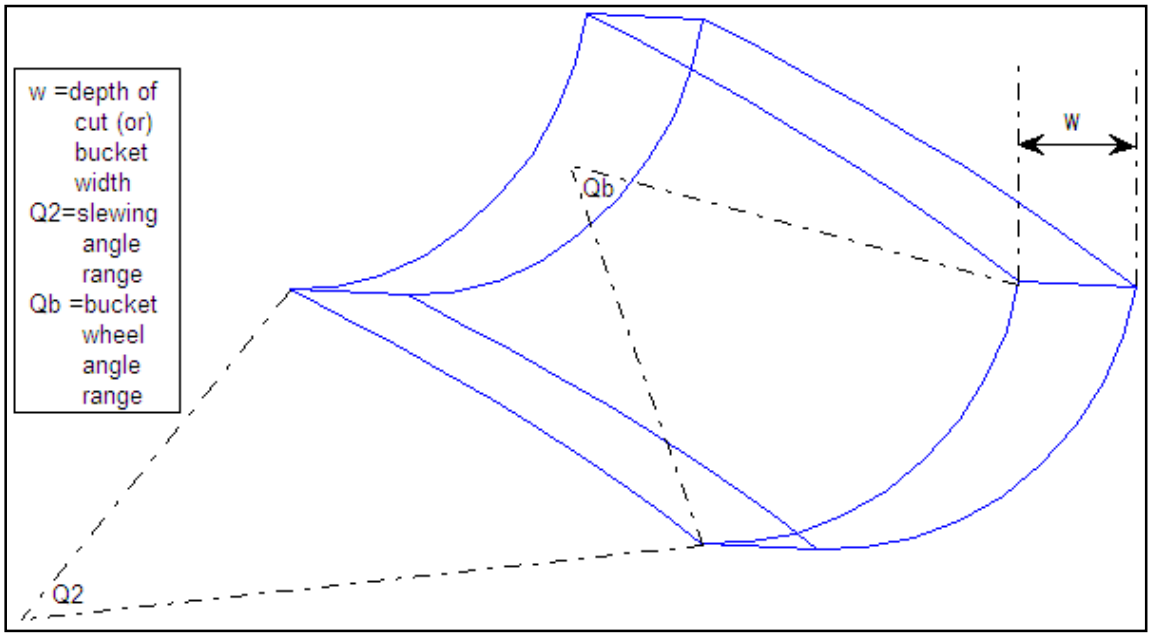

Figure 3.11: Geometry of the single slewing cut using BWR kinematics

3.5 Conclusion

The shortcomings of the cuboid voxels used in the previous study were investigated and demonstrated the disagreement with the BWR reclaiming profile. The accuracy in reclaiming voxels certainly affects meeting the specifications of the demand requested by customers. It had motivated to introduce a new voxel shape based on the kinematics of a BWR for optimal result. The kinematics model of the BWR including bucket wheel was derived treating BWR as a 4 DOF robotic manipulator. The contact region between stockpile and bucket wheel was examined to simulate the cutting trajectory of the BWR for the given parameters. The optimal voxel shape named sickle-shape was firstly introduced based on the kinematics of the BWR. The voxelization process will be carried out in Chapter 4 using the new sickle-shape voxels.

CHAPTER 4: VOXELIZATION OF THE STOCKPILE INTO SICKLE-SHAPE VOXELS

In this chapter, the sickle-shape voxelization process is carried out based on the BWR kinematics presented in Chpater 3. Unlike voxelization with cubic voxels, the reclaimer kinematics is taken into account in voxelization of the stockpile to achieve common coordinate space for both the reclaimer and stockpile voxels. In doing that, the Cartesian coordinate of the stockpile is transformed into sickle-shape voxels associated with BWR joint parameters. The profile of the sickle-shape voxel is shown in Figure 3.11. Stockpile is stacked at a stockyard in Cartesian coordinates, which involves x, y and z coordinates whereas the BWR operates in BWR joint space consisting of translating, luffing and slewing. The conversion of coordinate in voxelization of the stockpile is discussed in Section 4.1. The case study for voxelization of the lab-scaled stockpile is presented in Section 4.2 followed by discussion in Section 4.3. The chapter concluds in Section 4.4.

4.1 Transformation of coordinates in voxelization

In the process of voxelization, the procedure is carried out based on the approach used by the operator manually in reclaiming material from stockpile. The movement of BWR is maneuvered with three joint parameters consisting of translating distance, luffing angle and slewing angle. The reclaiming operation starts with the translated movement to the desired position and then luffed to the required height position. While maintaining the translation distance and luffing angle, the slewing motion is carried out for reclaiming material. So, the reclaiming of any material from the stockpile involves three movement parameters of the BWR. Based on that, a voxel is defined with its associated translation distance, luffing angle and slewing angle range of the BWR. It means that stockpile in Cartesian coordinate space is converted into a combination of sickle-shape voxels in BWR joint parameter space as shown in Figure 4.1. After voxelization, voxels are in BWR joint parameter space possessing translation distance, luffing angle and slewing angle range, so

that BWR can reclaim straight away using known joint parameters. Fully automated reclaiming system can be realized using this approach for bulk material handling operation. The following subsection discusses about the investigation of obtaining translated distance and luffing angle of the voxels in voxelization.

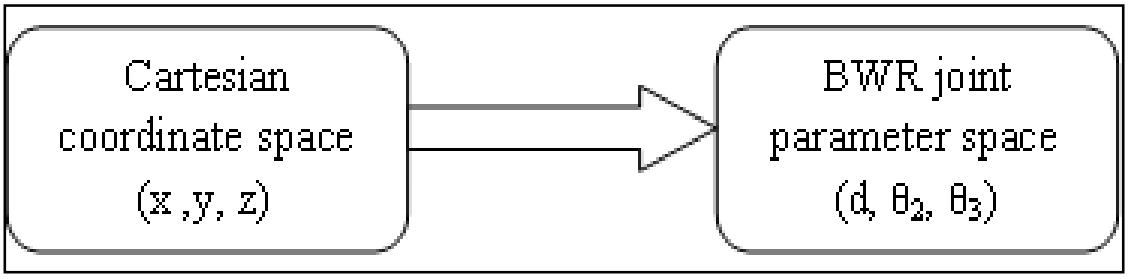

Figure 4.1: Conversion of coordinate space

4.1.1 Translated distance and luffing angle

Based on the reclaiming pattern of the BWR, the initial point on the stockpile boundary is required to determine translated distance and luffing angle. Stockpile contours of three layers are extracted from scanning of the stockpile. In this study, a contour from the small-scaled stockpile which is scanned in the laboratory by Lu et al. [33] is used. The resulted boundary data points are employed to define the stockpile contour using curve fitting. The boundary curves are fitted as ellipses as shown in Figure 4.2. In that, 'o' marked curves represent for extracted boundary curves and '- -' marked curves represents for fitted curves. The fitted contours for three layers in the form of the ellipse are described as:

$$\frac{(z-990mm)^2}{(367mm)^2}-\frac{(x-61mm)^2}{(194mm)^2}=1 \tag{4.4}$$

$$\frac{(z-989mm)^2}{(317mm)^2}-\frac{(x-61mm)^2}{(147mm)^2}=1 \tag{4.5}$$

$$\frac{(z-985mm)^2}{(240mm)^2}-\frac{(x-53mm)^2}{(69mm)^2}=1 \tag{4.6}$$

Where,

367mm & 194mm = the vertical semi-axis and the horizontal semi-axis of the largest ellipse

(990mm, 61mm) = the center of the largest ellipse

317mm & 147mm = the vertical semi-axis and the horizontal semi-axis of the middle ellipse

(989mm, 61mm) = the center of the middle ellipse

240mm & 69mm = the vertical semi-axis and the horizontal semi-axis of the largest ellipse

(985mm, 53mm) = the center of the largest ellipse

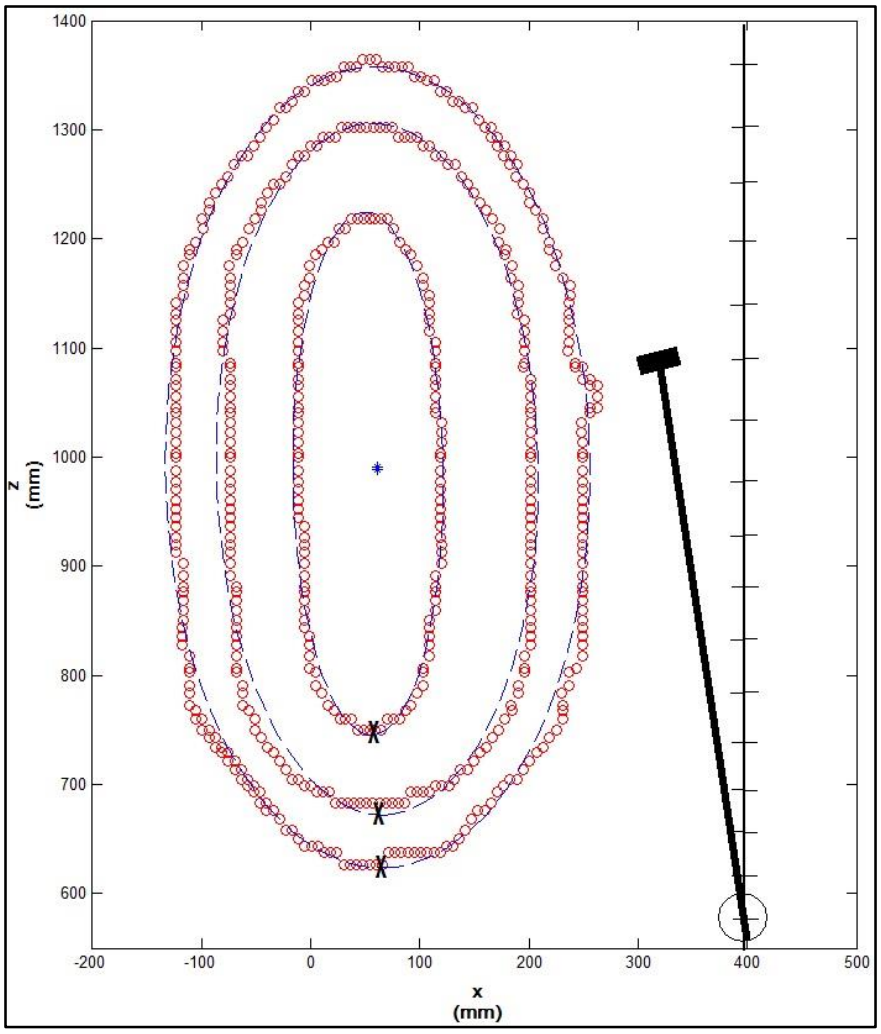

Figure 4.2: Extracted boundary curves and fitted curves

The very end points of the three countours, which are marked as "X" in Figure 4.2, are chosen as the initial point for BWR to reach the stockpile. The kinematics model of the BWR presented in Chapter 3 is used to solve for inverse kinematics. The joint parameters involved are translational distance (d), luffing angle (θ_3), slewing angle (θ_2) and bucket wheel angle (θ_b). The concern in solving the inverse kinematics is that the number of unknown independent parameters related to the available equations. There are four independent unknown parameters (d, θ_3, θ_2, θ_b) involved in the BWR kinematics model which makes impossible to solve analytically. However, Schneidersmann [46] indicated that the filling process begins at α0= 0 degree and completes at α1= 90 degree regarding bucket wheel angle (θ_b). It reduces the BWR kinematics model into 3 DOF and likely achievable to solve analytically. Hence, the kinematics model for the small-scaled BWR can be written with known bucket wheel angle in millimeters as:

$$x_b = -70\sin\theta_2\cos\theta_3\cos(0,\pi/2) + 70\ \sin\theta_2\sin\theta_3\sin(0,\pi/2) + 0.5\cos\theta_2 \\ -0.5\sin\theta_2\cos\theta_3 - \sin\theta_2\,(650\cos\theta_3 + 0.5) \quad (4.7)$$

$$y_b = -70\sin\theta_3\cos(0,\pi/2) - 70\ \cos\theta_3\sin(0,\pi/2) - 280 \\ -0.5\sin\theta_3 - 650\sin\theta_3 \quad (4.8)$$

$$z_b = 70\cos\theta_2\cos\theta_3\cos(0,\pi/2) - 70\cos\theta_2\sin\theta_3\sin(0,\pi/2) + 0.5\sin\theta_2 \\ +0.5\cos\theta_2\cos\theta_3 + 650\ \cos\theta_2\cos\theta_3 + 0.5\cos\theta_2 + d \quad (4.9)$$

Where, (x_b, y_b, z_b) are the very end points of the three countours, which are marked as "X" in Figure 4.2. (0, π/2) refers to the contact region between the bucket wheel and stockpile. For the purpose of deriving inverse kinematics, the kinematics equation can be written for the initial contact point as:

$$x_b = -720.5\sin\theta_2\cos\theta_3 + 0.5\cos\theta_2 - 0.5\sin\theta_2 \quad (4.10)$$

$$y_b = -720.5\sin\theta_3 - 280 \quad (4.11)$$

$$z_b = 720.5\cos\theta_2\cos\theta_3 + 0.5\cos\theta_2 + 0.5\sin\theta_2 + d \quad (4.12)$$

In simplifying Equation 4.11,

$$\sin\theta_3 = -\frac{y_b}{720.5} - \frac{280}{720.5} \tag{4.13}$$

Besides, trigonometric solution for the equations are stated as [47]:

$$\sin\theta = a \quad then, \theta = Atan2\left(a, \pm\sqrt{1-a^2}\right) \tag{4.14}$$

$$a\sin\theta + \mathrm{b}\cos\theta = c \quad then, \ \theta = Atan2(a,b) \pm Atan2\left(\sqrt{a^2+b^2-c^2}, c\right) \tag{4.15}$$

Based on the solution of the trigonometric Equations 4.14, the luffing angle can be calculated as:

$$\theta_3 = Atan2\left(\frac{-y_b-280}{720.5}, \pm\sqrt{1-\left(\frac{-y_b-280}{720.5}\right)^2}\right) \tag{4.16}$$

Equation 4.10 can also be written as:

$$x_b = (-720.5\cos\theta_3 - 0.5)\sin\theta_2 + 0.5\cos\theta_2 \tag{4.17}$$

With known luffing angle (Θ_3), the slewing angle can be calculated by comparing Equation 4.15 and Equation 4.17 as:

$$\theta_2 = Atan2(-720.5\cos\theta_3 - 0.5\,, 0.5) \pm$$

$$Atan2\left(\sqrt{(-720.5\cos\theta_3 - 0.5)^2 + 0.5^2 - {x_b}^2}, x_b\right) \tag{4.18}$$

Using the known luffing and slewing angles, the translation distance can be calculated as:

$$d = z_b - 720.5\cos\theta_2\cos\theta_3 - 0.5\cos\theta_2 - 0.5\sin\theta_2 \tag{4.19}$$

4.1.2 Slewing angle range

As stated before, the slewing operation is carried out while the translation motion and luffing motion is rested. The slewing operation is carried out in a circular motion at the given translated distance and luffing angle. Consequently, the slewing motion of the BWR can be modelled as a circle equation for the given parameters:

$$(z-d)^2+(x-x_s)^2=r^2 \quad (4.20)$$

Where,

d = translation distance of the BWR

x_s = distance of the BWR rail from zero as shown in Figure 4.2

r = radius of the slewing circle can be calculated as in Figure 4.3:

$$r=\sqrt{(x_b-x_s)^2+{y_b}^2+(z_b-d)^2} \quad (4.21)$$

For the given stockpile and BWR, the slewing circles for three layers are modelled in millimeters as:

$$(z-79.5)^2+(x-400)^2=(721.9)^2 \quad (4.22)$$

$$(z-139)^2+(x-400)^2=(728.9)^2 \quad (4.23)$$

$$(z-219.5)^2+(x-400)^2=(701.5)^2 \quad (4.24)$$

Where,

721.9, 728.9 and 701.5 = radius of the slewing circle for the respective layers

In reclaiming, the slewing circle will intersect two times with the stockpile boundary contour. The first point marks when the bucket enters and the other for departing the stockpile as shown in Figure 4.3. Consequently, the intersection points between slewing circle and stockpile boundary contour are determined here. The translation motion is incremented with the voxel width to obtain intersection points between contour and slewing circle for the whole bench. The second dotted slewing circle in Figure 4.3 is shown for incremented translation distance. The intersection points between stockpile boundary contour and slewing circle generates the slewing angle range of the voxels. The slewing angle range is solved using inverse kinematics for the intersection points.

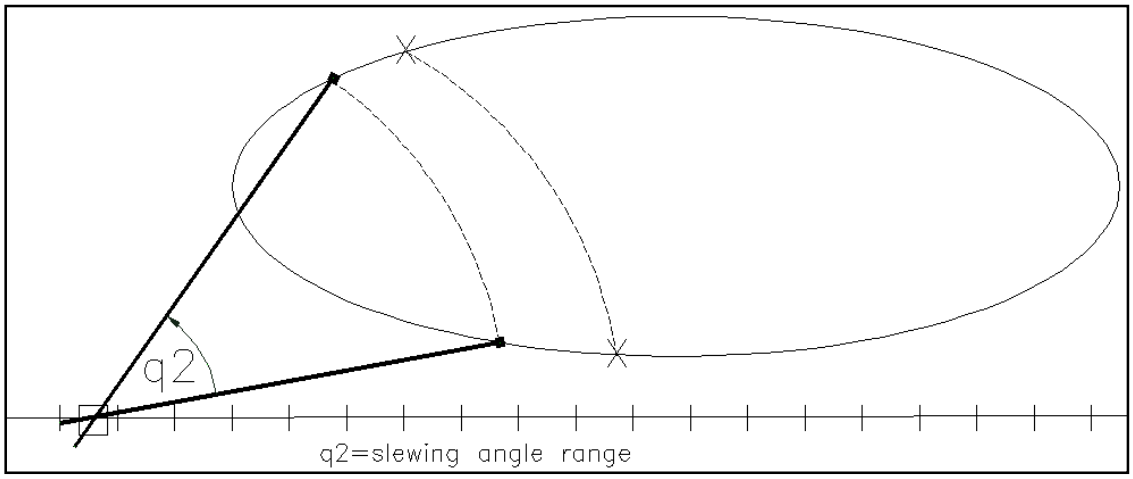

Figure 4.3: Intersection between stockpile contour and BWR slewing circle

4.2 Case Study for voxelization

The small-scaled stockpile is voxelized into sickle-shape voxels associated with BWR joint parameters. The sample of generating voxels associated with BWR joint parameters are shown in Table 4.1. Figure 4.4 shows portion of the stockpile voxelized into sickle-shape voxels to illustrate the location of voxels in the stockpile.

Table 4.1: Sample of sickle-shape voxels in BWR joint parameters space

Voxels index	Translation distance(mm)	Luffing angle (°)	Slewing angle range (°)
111	79.5	-18.6	26.9 – 41.1
112	99.5	-18.6	25.8 – 43.0
121	139	-14.14	20.2 – 33.7
122	159	-14.14	19.4 – 35.1
131	219.5	-9.46	29.4 – 32.4
132	239.5	-9.46	27.9 – 34.1

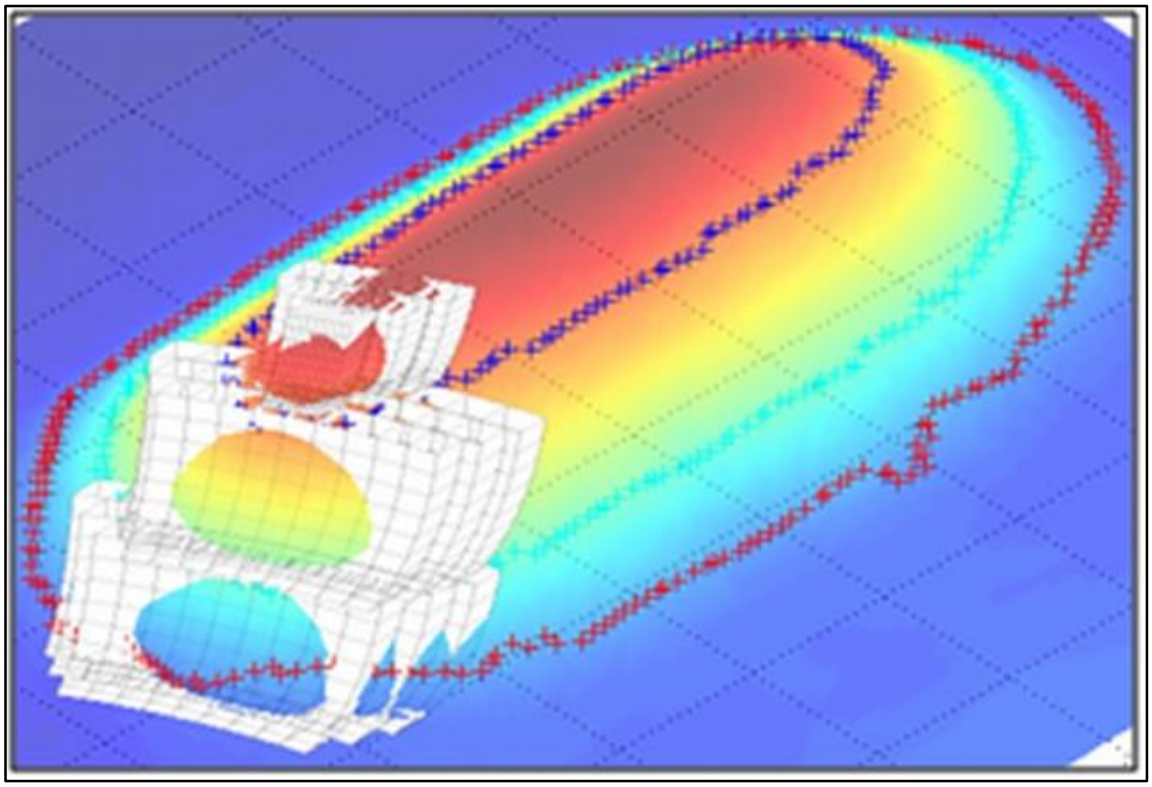

Figure 4.4: Portion of voxels in a small-scaled stockpile

Besides, the resulted sickle-shape voxels of the whole stockpile is shown in Figure 4.5 with highlighted colours. Moreover, sickle-shape voxels in sideview form is shown in Figure 4.6. In that, successive voxels are highlighted with different colours to visualize sickle-shape forms. The entire single slewing motion is taken for the single voxel in this study based on the practical reclaiming pattern of the BWR. The resolution of voxels can be increased by dividing multiple voxels in a single slewing motion. However, the computation cost will be more expensive and it disagrees with the reclaiming practice of the BWR.

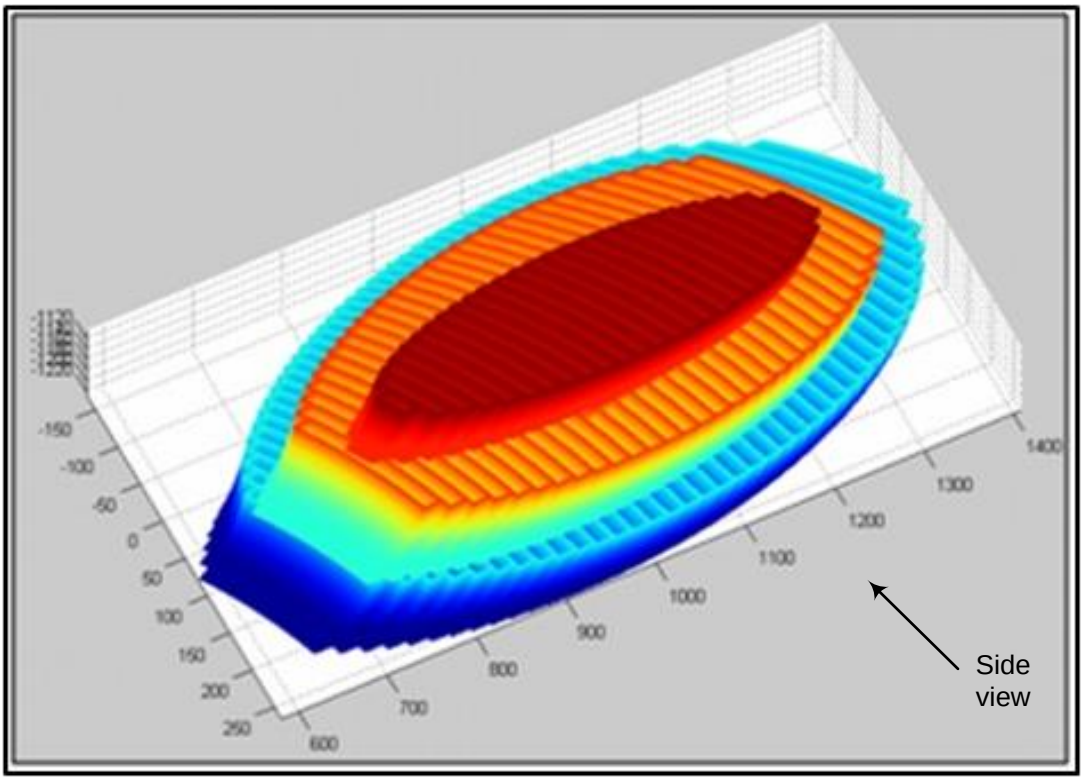

Figure 4.5: Small-scaled stockpile in sickle-shape voxels form in millimeter

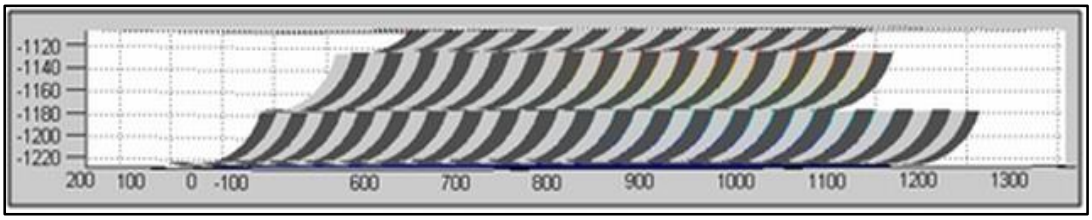

Figure 4.6: Small-scaled stockpile from side view in sickle-shape voxels form in millimeter

4.3 Discussion

In the mining industry, stockpiles are mostly reclaimed using a pilgrim method in which certain portion of the benches is reclaimed instead of reclaiming a whole layer. Then, the reclaimed material from multiple stockpiles are combined and loaded onto ships to meet a particular demand. The sickle-shape voxel approach is perfectly suitable for the pilgrim method as only the required voxels from stockpiles can be reclaimed with a optimal accuracy. The enhanced accuracy in reclaiming required voxels is important in voxel based approach as each voxel possess specific quantity and quality distribution. The capability of

reclaiming required voxels with minimum error will eventually improve meeting an overall demand in terms of quantity and quality.

Conventionally a single overestimated slew range is fixed in reclaiming the whole bench to ensure all material is reclaimed. As a result, some slewing motion reclaims nothing except air. However, the availability of slewing range in this approach for each voxel of the whole bench allows to slew only the required movement saving redundant slewing movements. This approach is flexible to implement with different types of BWR as configuration of the voxel is defined based on the parameters of the BWR. Besides, the virtual voxelization of the stockpile permits repetitive process of voxelization in case of using another BWR or additional material is stacked onto a partially claimed stockpile. The definition of voxels in BWR joint parameters allows straightforward reclaiming process for BWR instead of accessing stockpile in Cartesian coordinate.

4.4 Conclusion

The voxel based approach was practiced in reclaiming ore takes advantage of assay availability, to improve in meeting demand specification. The sickle-shape voxel defined based on BWR kinematics is introduced to improve accuracy in reclaiming. The voxelization process of the small scaled stockpile was carried out to demonstrate sickle-shape voxels and the associated voxelization. Stockpile in Cartesian coordinate was transformed into a combination of sickle-shape voxels associated with BWR joint parameters. The most significance of this approach is that the consideration of BWR's kinematics in voxelization, which will help in implementing a fully automatic reclaiming system with much improved accuracy in reclaiming the desired quantity and quality of bulk solid materials. The increase of automation in reclaiming will increase production rate.

CHAPTER 5: INVESTIGATION OF THE VOLUME MODEL FOR SICKLE-SHAPE VOXEL

In voxel based approach, a particular group of voxels is reclaimed based on their quantity and quality to meet the required demand specification. Thus, the knowledge of volume for all voxels in stockpiles are essential to decide which voxels should be reclaimed to meet the requirement. However, the investigation on volume calculation of the voxels has not been covered in the previous study as cubic voxels are treated as virtual unit volume grids. In this study, the sickle-shape voxel is defined based on the BWR's kinematics. So, the configuration of the BWR's kinematics and geometric shape of the stockpile affect the volume of the voxels. Because of that, the study on volume calculation of the sickle-shape voxel is critical in implementing the newly introduced voxel profile. In this chapter, the general volume model of the sickle-shape voxel will be drived to compute the volume.

The methods for volume computing of varying shapes can be categorised into three main groups [48]. In first approach, the overall volume is subdivided into a series of shapes which can be represented by mathematical formulae such as prisms, prismoids, wedges and pyramids. A rectangular or triangular network of spot heights is defined and a volume is determined by the summation of elemental volumes within the grid in the second approach. A third approach is the most common general method to calculate the volume of the shapes. It uses numerical integration formulae, mostly the end-area formula and the prismoidal formula, to find the volume of the cross-sectional areas. The geometric shape of the sickle-shape voxel as shown in Figure 3.11 is best suited to use the third approach as the model of the voxel profile is accessible for integration. Besides, the sickle-shape voxel is difficult to subdivide into shapes, which can be easily represented by mathematical formulae.

The BWR is maneuvered by four motions to reclaim the material from stockpile. The translation motion is firstly carried out along the rail to reach the desired position. Then, the luffing motion is carried out before slewing motion is carried out. The bucket wheel is rotated to scoop the material whilst slewing is in motion. The motion of the BWR is adapted to Spherical coordinate as the similarity between two movements are noted. The

derivation of the volume model of the sickle-shape voxel is discussed in Section 5.1. The verification of the model is presented with a case study in Section 5.2. The chapter states discussion in Section 5.3 before concludes in Section 5.4.

5.1 Volume of the sickle-shape voxel

In spherical coordinates, the volume of the region can be calculated using [35]:

$$V = \int_{\theta_1}^{\theta_2} \int_{\emptyset_1}^{\emptyset_2} \int_{\rho_1}^{\rho_2} \rho^2 sin\emptyset \; d\rho \, d\emptyset \, d\theta \tag{5.1}$$

The definition of the corresponding parameters of Equation (5.1) is illustrated in Figure 2.5 [35].

In the sickle-shape voxel, ρ is the distance from the base of the BWR to the surface of the voxel as shown in Figure 5.1 and it is defined as:

$$\rho = \sqrt{x^2 + y^2 + (z - d)^2} \tag{5.2}$$

Consequently, the lower limit is the inner surface of the voxel and the upper limit is the outer surface of the voxel as follows:

$$\rho_1 = \sqrt{x_1^2 + y_1^2 + (z_1 - d)^2} \tag{5.3}$$

$$\rho_2 = \sqrt{x_2^2 + y_2^2 + (z_2 - d)^2} \tag{5.4}$$

Where,

$$x_1 = -r_1 \sin\theta_2 \cos\theta_3 \cos\theta_b + r_1 \sin\theta_2 \sin\theta_3 \sin\theta_b + 0.5\cos\theta_2 - 0.5\sin\theta_2 \cos\theta_3 - \sin\theta_2 (650\cos\theta_3 + 0.5) \tag{5.5}$$

$$y_1 = -r_1 \sin\theta_3 \cos\theta_b - r_1 \cos\theta_3 \sin\theta_b - 280 - 0.5\sin\theta_3 - 650\sin\theta_3 \tag{5.6}$$

$$z_1 = r_1 \cos\theta_2 \cos\theta_3 \cos\theta_b - r_1 \cos\theta_2 \sin\theta_3 \sin\theta_b + 0.5\sin\theta_2 + 0.5\cos\theta_2 \cos\theta_3 + 650\cos\theta_2 \cos\theta_3 + 0.5\cos\theta_2 + d \tag{5.7}$$

And

$$x_2 = -r_2 \sin\theta_2 \cos\theta_3 \cos\theta_b + r_2 \sin\theta_2 \sin\theta_3 \sin\theta_b + 0.5\cos\theta_2 - 0.5\sin\theta_2 \cos\theta_3 - \sin\theta_2 (650\cos\theta_3 + 0.5) \quad (5.8)$$

$$y_2 = -r_2 \sin\theta_3 \cos\theta_b - r_2 \cos\theta_3 \sin\theta_b - 280 - 0.5\sin\theta_3 - 650\sin\theta_3 \quad (5.9)$$

$$z_2 = r_2 \cos\theta_2 \cos\theta_3 \cos\theta_b - r_2 \cos\theta_2 \sin\theta_3 \sin\theta_b + 0.5\sin\theta_2 + 0.5\cos\theta_2 \cos\theta_3 + 650\cos\theta_2 \cos\theta_3 + 0.5\cos\theta_2 + d \quad (5.10)$$

In Equations (5.5-5.10), r_1 is the inner radius of the bucket wheel, which is defined here as 70mm and r_2 is the outer radius of the bucket wheel which is defined here as 90mm. In fact, the width of the cut or bucket width shown in Figure 5.1 is the difference between the outer radius and the inner radius of the bucket wheel. As this study is based on spherical coordinates, ∅ is unknown and it is defined as the angle between the lower and the upper boundary of the cut as shown in Figure 5.1. However, the bucket wheel angle θ_b is known for the cut. ρ is not a constant radius throughout arc C but it is a function of θ_b at a given BWR joint parameters. In view of the bucket wheel, the arc length C of the bucket wheel is defined as [35]:

$$C = \mathrm{r}\,\theta_b \quad (5.11)$$

On the other hand, C also represents the arc length for the curve associated with ρ within angle ∅. As the arc C represents only a relatively very small portion of the large curve ρ, the arc of the large curve can be assumed as:

$$C = \rho\emptyset \quad (5.12)$$

By simplifying Equations 5.11& 5.12, ∅ is defined as:

$$\emptyset = \frac{r\,\theta_b}{\rho} \quad (5.13)$$

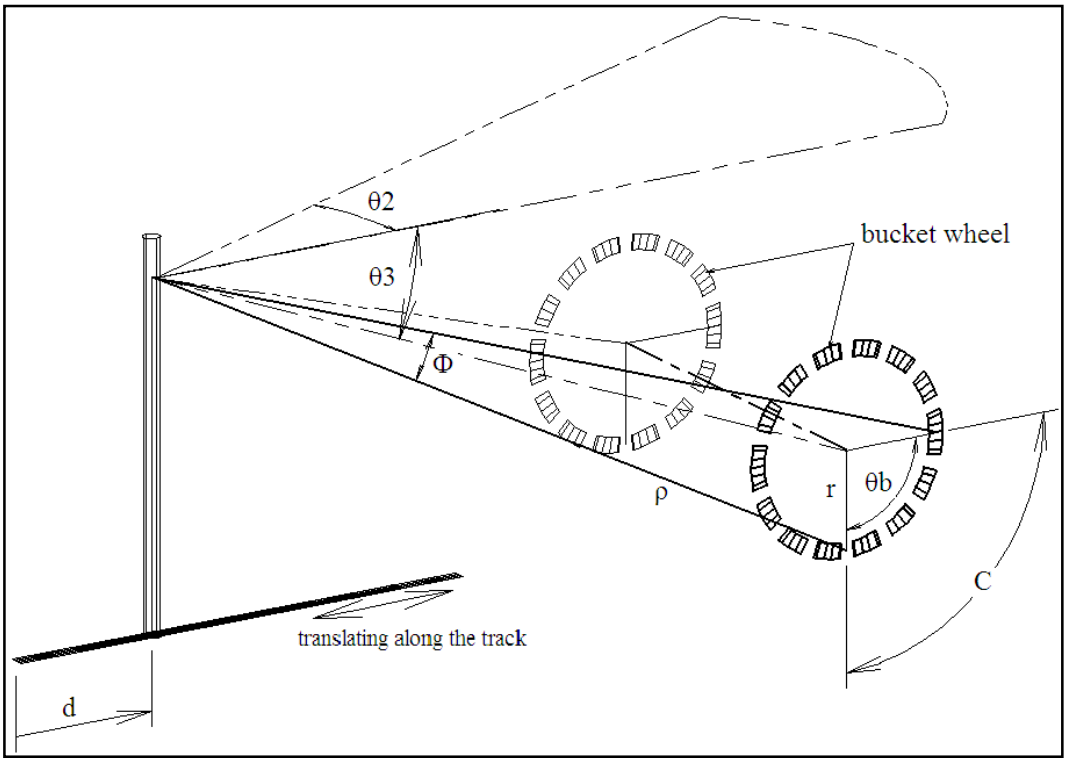

Figure 5.1: Illustration of BWR joint parameters

Lastly, θ in spherical coordinates is identical to the slewing angle range θ_2 of the voxel as shown in Figure 5.1, which defined the left and right boundary of the voxel. In substituting the relevant parameters to the general volume formula, the volume of the sickle-shape voxel can be defined as:

$$V_v = \int_{\theta_{2,1}}^{\theta_{2,2}} \int_{\theta_{b,1}}^{\theta_{b,2}} \int_{\rho_1}^{\rho_2} \rho^2 \sin\left(\frac{r\theta_b}{\rho}\right)\, d\rho\, d\theta_b\, d\theta_2 \qquad (5.14)$$

Where, $\theta_{2,1}$, $\theta_{2,2}$, $\theta_{b,1}$ and $\theta_{b,2}$ are boundary angles of the voxel.

As the BWR joint parameters are available for sickle-shape voxels, Equation 5.14 can be used to determine the volume of the voxels. The non-linearity in integrand function enforced to solve using a numerical method. A triple integral is solved in Matlab using "Integral3" function.

5.2 Verification of the proposed volume model

Sickle-shape voxels produced from voxelization in Chapter 4 is used to calculate the volume in the following section. The triple integration of the volume model is solved numerically to find the volume of each sickle-shape voxel of the stockpile. To verify the model, the sum of the voxels' volume in the stockpile will be compared with the volume of the whole stockpile.

5.2.1 Case Study

A small-scaled stockpile prepared in the laboratory will be used to conduct the case study. Materials used in preparing stockpile are red scoria, blue basalt, brown quartzite and washed beach sand. The dimension of the stockpile is measured as L=350mm, H=140mm, d=400mm, r = 200mm. The prepared stockpile is scanned and modeled as a 3-D stockpile by Lu et al. [33]. The stockpile is divided into three layers and voxelized into sickle-shape voxels associated with the BWR joint parameters using the approach from Chapter 4 as shown in Figure 4.4. The details of voxelization was discussed in Chapter 4. Sickle-shape voxels produced in Chapter 4 will be used here to conduct the case study. To demonstrate the process, the calculation of volume for a single voxel will be discussed here for the given BWR joint parameters. The boundary values of the sickle-shape voxel is listed in Table 5.1.

Table 5.1: Volume of voxels

BWR parameters	Value
$\theta_{2,1}$	0.4703 rad
$\theta_{2,2}$	0.7185 rad
$\theta_{b,1}$	0
$\theta_{b,2}$	-1.5708 rad
θ_3	-0.3255 rad
r_1	70 mm
r_2	90 mm

For the given BWR joint parameters, the volume of a sickle-shape voxel can be calculated using Equation 5.14. Since the analytical solution is unfeasible, the numerical integration method is applied to solve the triple integration of Equation 5.14. The volume of a single sickle-shape voxel is resulted as 75589 mm^3. Similarly, the volumes of voxels on same layer are calculated and added together. The resulted voxels' volumes for each layer in three layers are listed in Table 5.2.

Table 5.2: Volume of voxels

Voxels	Sum of Voxels' Volume (mm^3)
1^{st} bench voxels	8.4545×10^6
2^{nd} bench voxels	6.0262×10^6
3^{rd} bench voxels	1.4514×10^6
Total	1.5932×10^7

In order to compare with the sum of the voxels' volume, the whole stockpile volume is calculated by dividing it into the middle and end sections as shown in Figure 5.2 based on the method proposed by Burch [49].

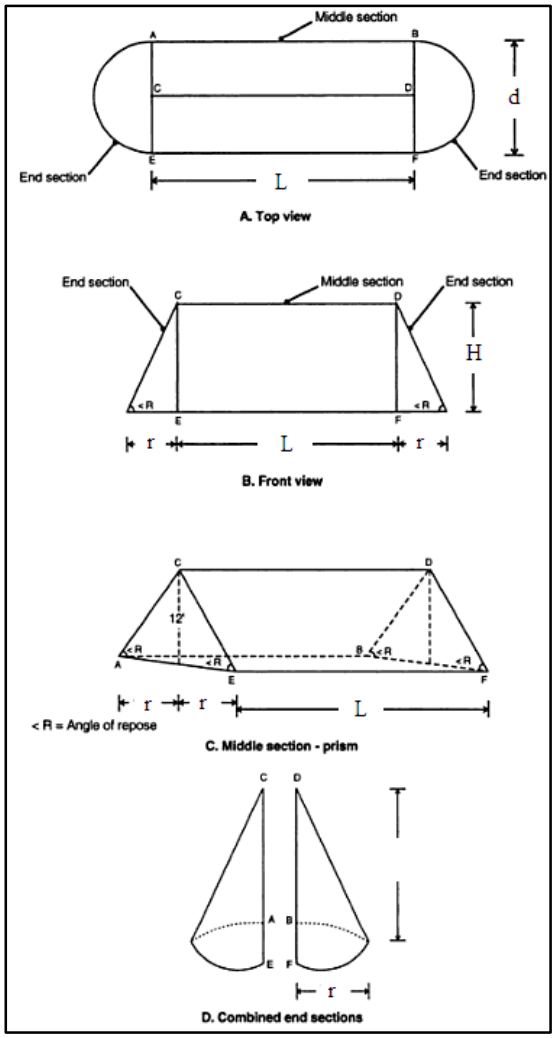

Figure 5.2: Stockpile model and its division form

Firstly, the volume of the middle section is calculated as [49]:

$$V_m = \frac{1}{2}dHL \tag{5.15}$$

Where,

d = Base width of the stockpile

H= Height of the stockpile

L = Length of the stockpile

Then, the end sections of the stockpile resemble half of the the cone which of the

volume can be calculated as [49]:

$$V_c = \frac{1}{2}\left(\frac{1}{3}\pi {r_c}^2\right) H \quad (5.16)$$

Where,

r_c = radius of the cone.

The volume of the middle section and end sections of the stockpile are listed in Table 5.3.

Table 5.3: whole stockpile volume

Stockpile Sections	**Volume (mm^3)**
Middle section	$9.8x10^6$
End section	$2.9322x10^6$
End section	$2.9322x10^6$
Whole stockpile	$1.5664x10^7$

The error of the proposed volume model can be calculated as:

$$error = \frac{|\boldsymbol{Total\ volume\ of\ voxels - volume\ of\ \text{whole}\ stockpile}|}{|\boldsymbol{volume\ of\ \text{whole}\ stockpile}\ |} = \mathbf{1.7}\% \quad (5.17)$$

5.3 Discussion

The error resulted from comparing the sum of all the voxels' volume with the whole stockpile volume is 1.7%. There are limitations in the verification of this volume comparison. In calculating the whole stockpile volume, the stockpile geometry is represented by a simple triangular middle section and end cone sections. Robinson and Ross stated, that this simple representation of the stockpile model is inadequate, as the proportions of the middle and end sections are changed based on the height of the stockpile [50]. Moreover, the more accurate model of the stockpile proposed by Robinson and Ross involves higher-order differential equations and the implementation of it is beyond the

scope of this study. In this study, the separation of the end sections from the middle section is carried out manually which may also contribute errors in computing the volume of the whole stockpile. The main limitation in conducting this case study is the size of the stockpile available. Due to limitations in accessing an actual full-scale stockpile, the error resulting from conducting the case study on a lab-scale stockpile is rather sensitive to the small amount of material. However, the actual volume of the stockpile should be big enough to be adequate for the small error resulting from the proposed approach.

5.4 Conclusion

Ore producers need to maintain a quality reputation in supplying ore to steel producers by satisfying the requested quantity and quality in order to maintain the good relationship with the customers. In order to do that, the volume of the reclaimed ores along with their mineral composition is essential to determine before loading onto a ship can commence. In the voxel-based approach, the accessibility of the voxel volume is vital to decide which group of voxels should be reclaimed in meeting the requested specifications. Unlike cubic voxels, the volume of the sickle-shape voxel varies throughout the stockpile as the profile is defined with the BWR kinematics. A general volume model to compute the volume of sickle-shape voxel associated with BWR joint parameters in spherical coordinates was derived in this study. The case study was conducted by computing the volume of voxels produced from lab-scale stockpile and the verification of the approach is carried out. The comparison of the results from the experimental volume determination with the calculated volume using the proposed sickle-shape voxel approach result seem to be acceptable with minimum error. The limitations in the verification process are highlighted and the implementation of this approach in an actual full-scale stockpile will provide the volume information of sickle-shape voxels. Thereby, sickle-shape voxels with accessible volume knowledge in stockyard stockpiles will be ready for selection of voxels

to reclaim in order to meet the required quantities.

CHAPTER 6: OPTIMISATION OF THE MINIMUM TRAVELLED DISTANCE OF THE BWR'S BUCKET WHEEL IN RECLAIMING CUBOID VOXELS

As it is discussed in literature, Simine^{CIS} [15] adept a manual selection of cubic voxels by the operator to reclaim in order to fulfil the desired quantity and grade specifications. The selection is simply performed for the purpose of meeting the requested quantity and quality without considering the reclaiming movement of the reclaimer. In this chapter, the study of automatic identification of the cuboid voxels is conducted to meet the demand specifications, whilst considering the minimum travelled distance of the BWR's bucket wheel. Cuboid voxels with quantity and quality grade information are assumed to be available to carry out the study presented in this chapter. The objective function of the optimisation problem is defined in Section 6.1 based on the travelled distance of the BWR's bucket wheel. In selecting the voxels, constraints are introduced in Section 6.2. In which, the resulted ore is ensured to fall within the required quantity and quality grade ranges. Moreover, the constraint for reclaiming order is introduced such as voxels located inside the stockpiles and lower layer cannot be accessed until outside and upper layer voxels are reclaimed. Case studies are conducted for three demand cases in Section 6.3 using binary integer programming. Furthermore, more complicated constraints are introduced in Section 6.4 to replicate the actual reclaiming operation. Further two demand cases are conducted in Section 6.4.1 using voxels from SPSim software. The chapter presents discussion in Section 6.5 before concludes in Section 6.6.

6.1 Objective function of the optimisation problem

The Euclidean distance function of voxel positions referenced with the updated reclaimer positions is defined as the objective function of the optimisation problem in this study. The aim of using this objective function is that, the overall travelled distance of the reclaimer in reclaiming voxels can be minimised, leading to a reduction in energy consumption. Moreover, the stockpiled time of stockpiles is treated as a weighting factor in the defined objective function in order to maintain the sequence of stacking and

reclaiming. The weighting factor can also be tuned to reclaim any particular stockpile first. So, The objective function is defined as:

$$\sum_{v \in voxels} -weightfactor_v \times distance_v \times reclaim_v \quad (6.1)$$

Where,

$weightfactor_v$ = weighting factor of voxels based on stockpiled time,

$reclaim_v$ = Optimisation of reclaiming voxels (binary value 1 for selected and 0 for unselected) and

$distance_v$ = Euclidean distance function between voxels positions, and the current reclaimer positions is defined as

$$distance_v = \sum_{v \in voxels} \sqrt{(x_v - x_r)^2 + (y_v - y_r)^2 + (z_v - z_r)^2} \quad (6.2)$$

where,

x_v, y_v, z_v = voxels position coordinates and

x_r, y_r, z_r = current BWR position coordinates.

In the objective function, the minus sign is inserted for minimisation of the weighting factor to reclaim long standing stockpiles first. The normalized weighting factor is introduced based on the stockpiled time of voxels as follows:

$$weightfactor_v = \sum_{v \in voxels} \frac{stockpiling\ time_v}{total\ stockpiling\ time\ for\ all\ voxels} \quad (6.3)$$

6.2 Constraints of the optimisation problem

As a quality constraint, the desired minimum and maximum mineral content percentages are introduced as constraints into the system. The mineral content percentages in the total amount of demand ore are given by the ratio:

$$\frac{\sum_{v \in voxels} P_{vc} \times reclaim_v}{Treclaim} \quad (6.4)$$

Where,

P_{vc} = mineral percentage of voxels and

Treclaim = Total number of reclaiming voxels.

Adding the lower bound $PMIN_c$ and upper bound $PMAX_c$ into Equation 6.4 to express the constraint on the minimum grade of mineral percentage results the following relation:

$$PMIN_c \leq \frac{\sum_{v \in voxels} P_{vc} \times reclaim_v}{Treclaim} \leq PMAX_c \quad (6.5)$$

Consequently, the following linear minimum and maximum constraint for mineral percentages are attained by multiplying with Treclaim to both sides of the nonlinear Equation 6.5:

$$\forall c \in COMP: \sum_{v \in voxels} P_{vc} \times reclaim_v \geq PMIN_c \times Treclaim \quad (6.6)$$

$$\forall c \in COMP: \sum_{v \in voxels} P_{vc} \times reclaim_v \leq PMAX_c \times Treclaim \quad (6.7)$$

Furthermore, the constraint Equation 6.8 guarantees that the reclaiming amount of ore satisfies the demand amount with acceptable tolerance:

$$DEM - Tolerance \leq TOT \leq DEM + Tolerance \quad (6.8)$$

The last constraint is introduced for the reclaiming of voxels in the correct order. Based on the observation, it is not possible to access lower layer voxels until upper layer voxels are reclaimed, the constraint is set for prioritising the reclaiming of upper layer voxels first:

$$\sum_{a \in upper\ layer\ voxels} reclaim_a \geq \sum_{b \in lower\ layer\ voxels} reclaim_b \quad (6.9)$$

6.3 Case studies

The steps for solving the optimisation problem to conduct case studies is presented in a pseudo code form as follows:

! Declare variables

! Enter Demand quantity and required mineral composition (Min-Max) in percentage

! Load voxel data file in excel form

! Define the Euclidean distance function of the voxel position related to the BWR current position

! Calculate weight factor based on stockpiled time
! Assign acceptable quantity tolerance
! Define constraint for the required minimum and maximum mineral composition
! Define constraints for desired quantity with acceptable tolerance
! Define objective function based on Euclidean function and weight factor
! Define constraints for reclaiming order (from higher bench to lower bench)
! Minimise the objective function
! Output selected voxels with total quantity and quality grade
! End of the program

Two stockpiles named Stockpile A and Stockpile B with certain quality grade distributions are set up for the case study. The configuration of the stockyard is shown in Figure 6.1. In this study, stockpiles are not treated as a single volume with certain averaged quality. Rather, both stockpiles are divided into voxels which are represented by symbols such as, for example A11 and B22. In terms of the voxel identification numbers, the first character represents the stockpile name, the second number represents the layer of the stockpile and the remaining digits represent the voxel index number. The model of how voxels are divided in stockpile A and labelled is shown in Figure 6.2 for illustration purpose. In this case, Stockpile A and Stockpile B are divided each into *30* voxels with *3* layers. Each layer comprises of *10* voxels.

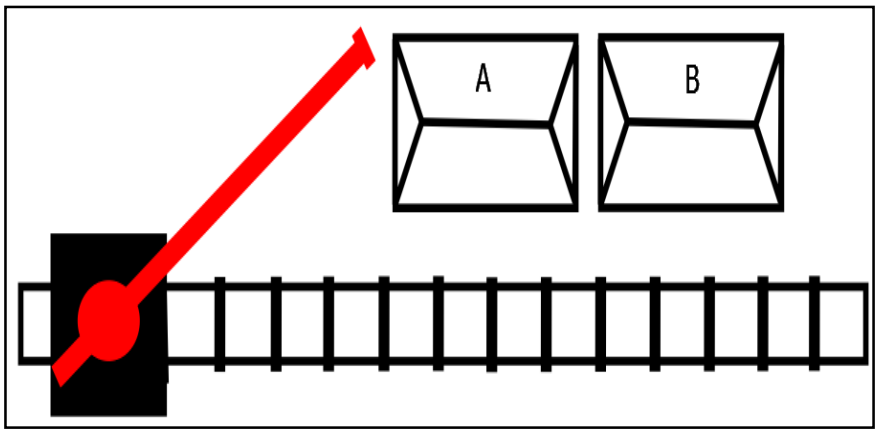

Figure 6.1: Stockyard configuration

The positions, volumes and mineral percentages of all voxels are stored in the stockpile database. The density of iron ore is taken as *2100kg/m*^{3} in these case studies. Volume of voxels are not identical in size as seen in Figure 6.2 and specified as *4000m*^{3} for ground layer voxels, *3000m*^{3} for middle layer voxels and *2000m*^{3} for top layer voxels. The volumes of voxels in the stockpile database are converted into weights in tonnes since the demand amount of iron ore will be requested in tonnes. The stockpiled time for stockpile A voxels are assumed as *5* days, whereas *10* days for stockpile B voxels.

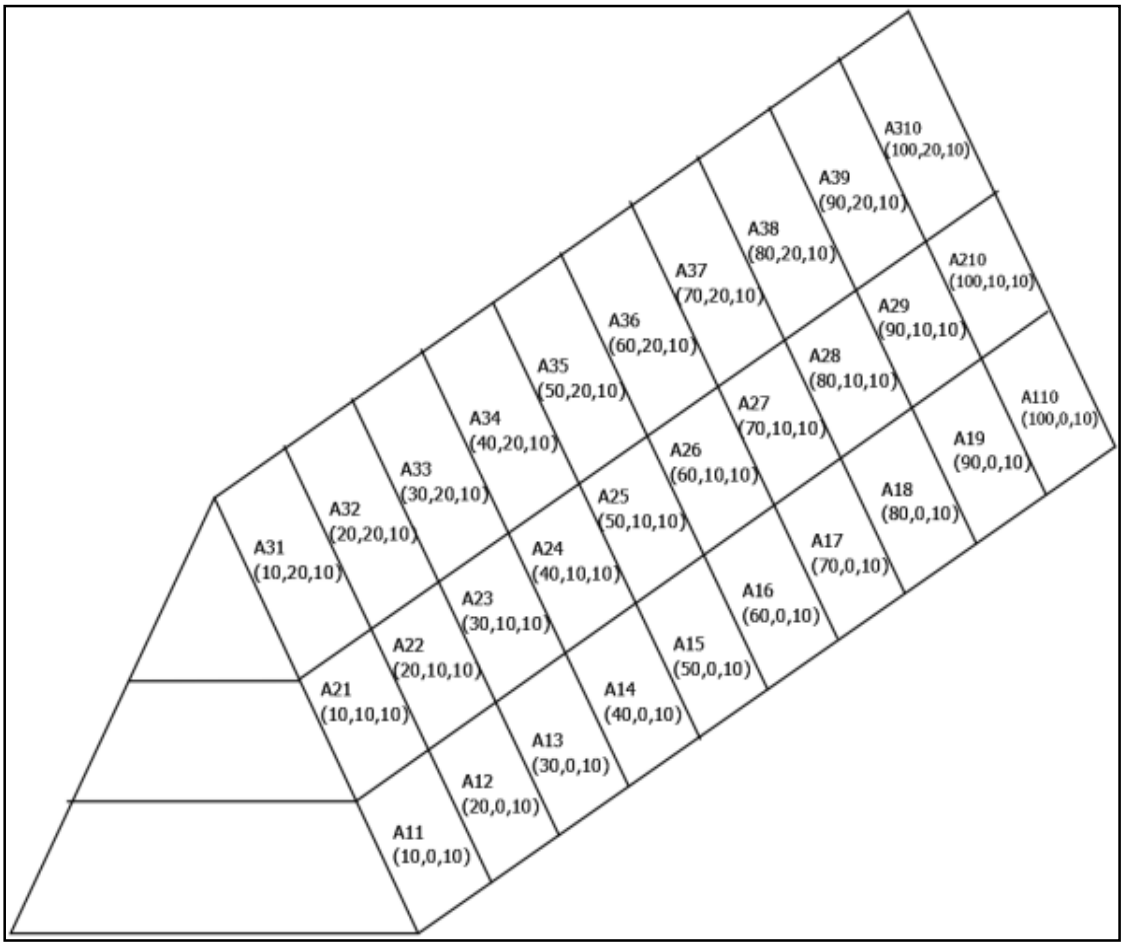

Figure 6.2: Schematic diagram of voxels labelling with position coordinates

There are mainly five iron ore types despite having broad distribution of iron in nature. The percentages of iron contained in five iron ore types are listed in Table 6.1 [51].

Table 6.1: Iron ore minerals and iron percentage

Mineral	**Composition**	**Iron (Approximate %)**
Magnetite	Fe_3O_4	72
Hematite	Fe_2O_3	70
Goethite	$Fe_2O_3.H_2O$	62
Limonite	Mixture of Hydrated iron oxides	50 - 60
Siderite	$FeCO_3$	48

However in reality, the iron percentages mentioned above are rarely attained because of the existence of the impurities such as Silica, Alumina, Sulphur and Phosphorous. In Australia, there are mainly two ore types found. The hematite ore is produced in Middleback Ranges, South Australia and Mount Whaleback, Western Australia. The second type, limonite ore is found at Marillana Creek, Western Australia. Although the presence of impurities can reduce the composition of iron in iron ore, a certain amount of impurities could contribute in producing better products [51]. As an example, the proportion of Silica should exceed that of Alumina for easy fluxing in the furnace and the proportion of both Silica and Alumina should be maintained within a certain limit for a manageable slag. Furthermore, most iron-ore contracts have very strict specification limits placed on the steelmakers'most concerning impurities, Phosphorus and Sulphur.

In stockyard, reclaiming works operate one demand after another according to the number of customer demands and available stockpiles. Consequently, the reclaiming work may start from the stockpile which is partially being reclaimed before. To replicate the actual reclaiming work, three customer demand cases with specific mineral composition are conducted consecutively from the available stockpile voxels in this study. The desired mineral minimum and maximum composition of iron ore for all three cases are listed in

Table 6.2 [52].

Table 6.2: Hematite medium fines grades specifications

Minerals and Size	**Minimum (%)**	**Maximum (%)**
Fe	62	65
SiO_2	0	4
Al_2O_3	0	4.5
P	0	0.1
$Na_2O + K_2O$	0	0.15
Size (>10mm)	0	2

6.3.1 First demand case

The optimisation problem is modelled in the Mosel program and optimised using Express-MP Optimisation suite [42]. In the first case, *48300 tonnes* of iron ore with *1 tonne* tolerance is demanded with the mineral composition listed in Table 6.2. The selected voxels to reclaim are highlighted in Figure 6.3 and the total mineral composition of selected voxels with total ore quantity is stated in Table 6.3.

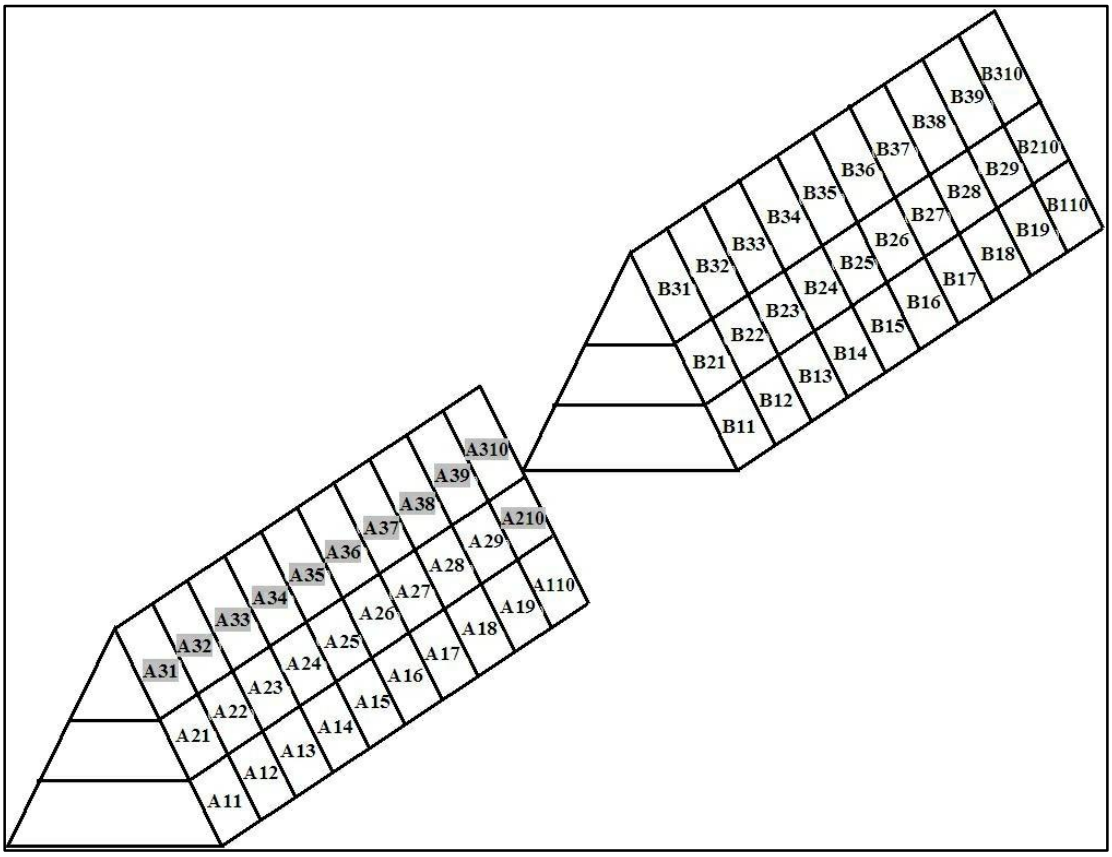

Figure 6.3: Selected optimal voxels for 1st demand case

Table 6.3: Result for 1st demand case

1st demand (48300 tonnes)	Total weight of selected reclaiming voxels	48300 tonnes					
	Selected optimal voxels	A210, A31, A32, A33, A34, A35, A36, A37, A38, A39, A310					
	Total mineral percentages (%)	Fe	SiO_2	Al_2O_3	P	Na_2O+K_2O	>10mm size
		62	3.41	3.77	0.07	0.11	0.95

6.3.2 Second demand case

In this case, the selected voxels for the first demand case are not included in the stockpile database as they are considered to being reclaimed and are represented with no label voxels. Consequently, the available stockpile voxels in this demand case are all labelled voxels of stockpile A and stockpile B. Whilst constraining to the mineral

composition stated in Table 6.2, iron ore quantity is requested for *54600 tonnes* with *1 tonne tolerance*. The selected voxels are highlighted in Figure 6.4 and the total mineral composition of selected voxels with total ore quantity is listed in Table 6.4.

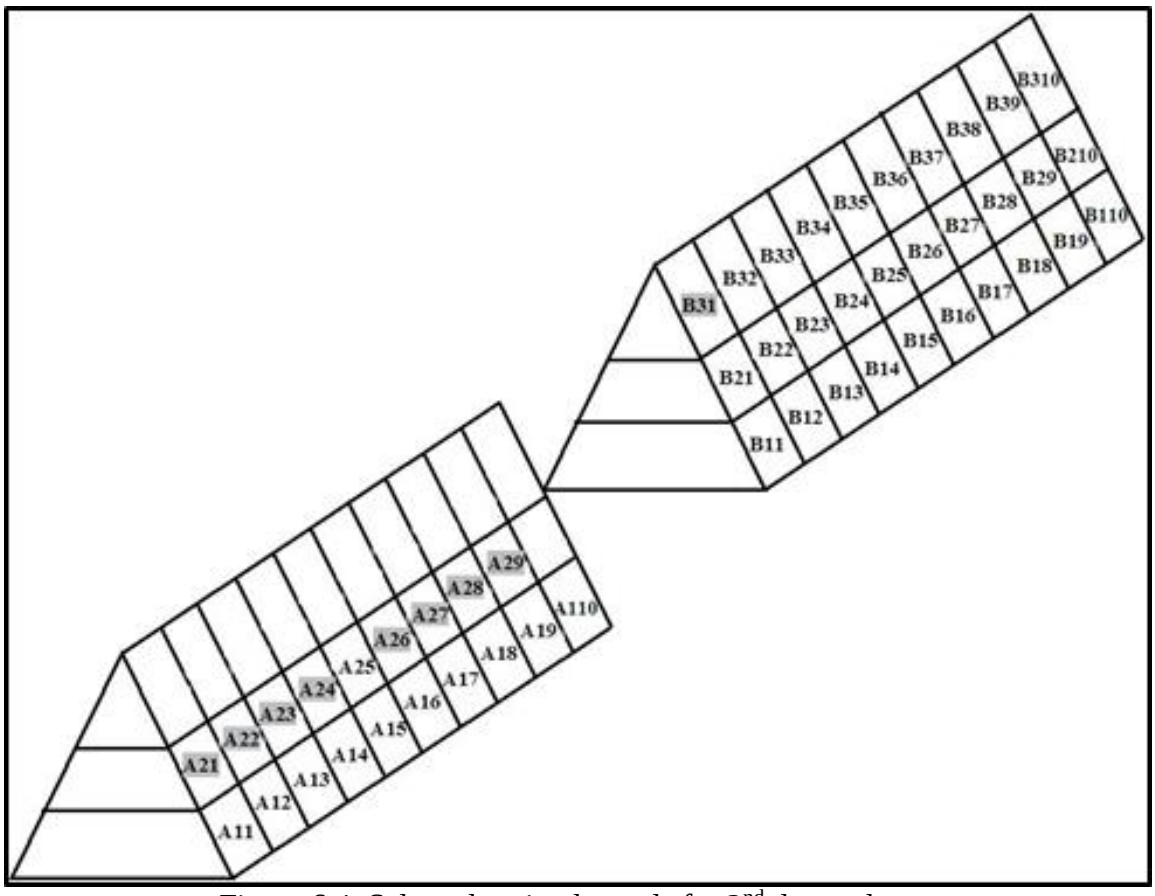

Figure 6.4: Selected optimal voxels for 2nd demand case

Table 6.4: Result for 2nd demand case

2nd demand (54600 tonnes)	Total weight of selected reclaiming voxels	54600 tonnes					
	Selected optimal voxels	A21, A22, A23, A24, A26, A27, A28, A29, B31					
	Total mineral percentages (%)	Fe	SiO_2	Al_2O_3	P	Na_2O+K_2O	>10mm size
		62.2	2.94	2.67	0.06	0.09	1.78

6.3.3 Third demand case

As stated in the second demand case, the stockpile voxels selected for the previous case are regarded as being reclaimed and extracted from the available stockpile database in this case. The amount of iron ore requested by the customer is *56700 tonnes* with *1 tonne* tolerance whilst retaining mineral composition of Table 6.2. Figure 6.5 shows the highlighted selected voxels and Table 6.5 listed the total mineral composition of selected voxels with total iron ore quantity to be reclaimed.

Table 6.5: Result for 3rd demand case

3rd demand (56700 tonnes)	Total weight of selected reclaiming voxels	56700 tonnes					
	Selected optimal voxels	A11, A16, A17, A18, A19, A110, A25					
	Total mineral percentages (%)	Fe	SiO_2	Al_2O_3	P	Na_2O+K_2O	>10mm size
		62.1	3.43	3.79	0.08	0.12	1.6

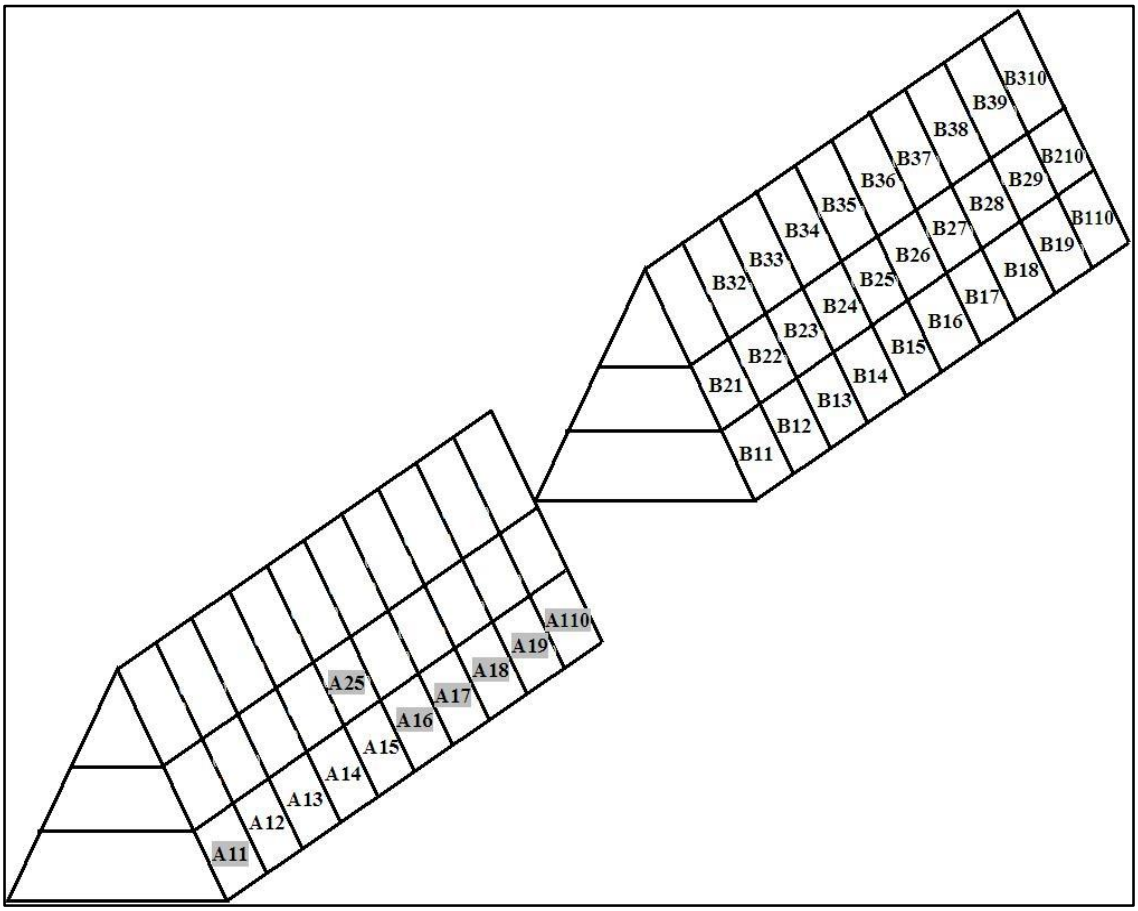

Figure 6.5: Selected optimal voxels for 3rd demand case

As a reference to the stockyard configuration in Figure 6.1, stockpile A stands near to the BWR which makes stockpile A voxels having a shorter distance to the BWR's starting position than stockpile B voxels. After first voxel selection, the successive travelled distance of the reclaiming voxels is calculated based on the BWR current position. In all the cases, Stockpile A voxels are selected ahead of stockpile B voxels due to the shorter travelled distance of the BWR. So, it is verified that the selection of stockpile voxels does comply with the defined objective distance function to achieve the BWR minimum movement whilst meeting quantity and quality constraints. Moreover, the selected voxels agrees with the order of reclaiming constraints introduced in Section 6.2 by giving priority to higher layer voxels.

6.4 Constraints enhancements for optimisation problem

However, the selected voxels are not in sequence form spreading throughout stockpile in previous case studies. The BWR is a very large and continuous type reclaiming machine which reclaims material continuously in forward direction. So, the scattering selected voxels throughout stockpile makes almost impossible for BWR to reclaim. To reflect the actual reclaim practice, additional constraints will be added for forward continuous reclaiming in this section. The top end voxels are prioritised to select first and the subsequent voxels are constrained to select continuously. Furthermore, more constraints are introduced into the optimisation problem to prevent stockpile from collapsing when reclaiming.

As voxels are assigned with a particular index consists of x, z and y position information, The constraint for continuous reclaiming is defined in the optimisation problem as:

$$\sum_{voxel_{x,z,y}} reclaim_{x,z,y} \geq \sum_{voxel_{x,z+1,y}} reclaim_{x,z+1,y} \quad (6.10)$$

Morever, the constraint to prevent from collapsing of the stockpile as introduced as:

$$\sum_{voxel_{x,z+1,y+1}} reclaim_{x,z+1,y+1} \geq \sum_{voxel_{x,z,y}} reclaim_{x,z,y} \quad (6.11)$$

Where,

x = slewing movement coordinate

z = translation movement coordinate

y = luffing movement coordinate

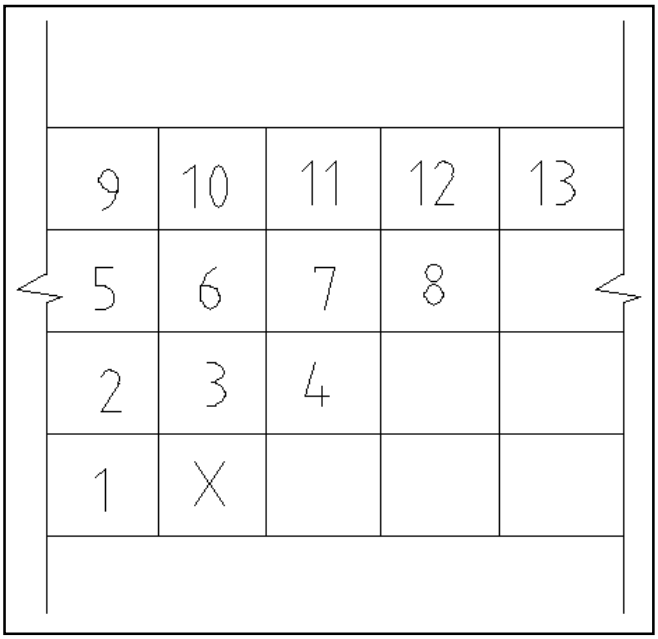

Figure 6.6: One possible distribution of stockpile voxels from side view

Alternately, one example is presented here how a particular voxel is selected with the introduction of constraints the optimisation problem. Figure 6.6 illustrates the cross section of voxels inside a stockpile with certain voxel labels. Figure 6.7 shows the constraint hierarchy graph of selecting voxel (X) from the stockpile of Figure 6.6. Arrowhead indicates the higher hierarchy, which means that it can be only selected after preceding lower hierarchy voxels are selected.

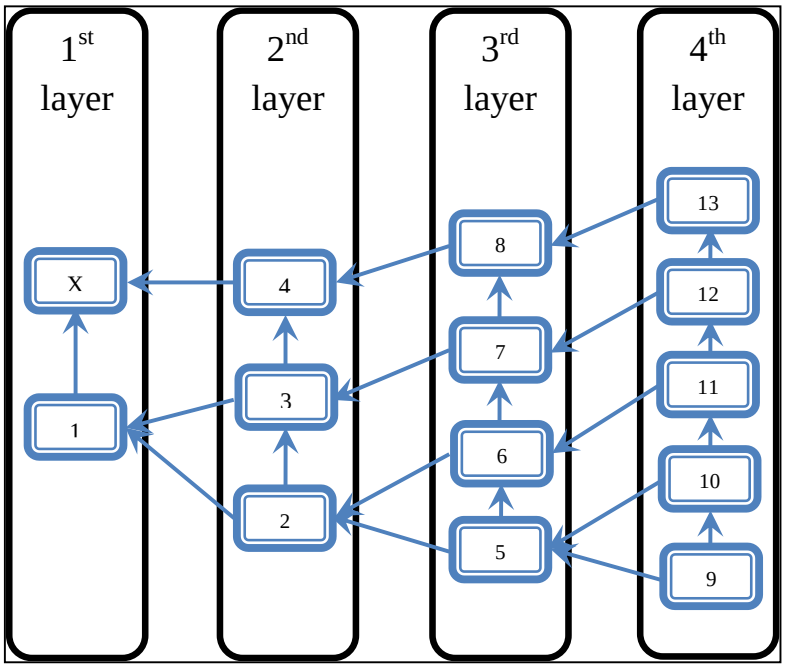

Figure 6.7: Constraint hierarchy graph of stockpile voxel (X)

6.4.1 Case studies

The steps for solving the optimisation problem to conduct case studies is presented in a pseudo code form as follows:

! Declare variables
! Enter Demand quantity and required mineral composition (Min-Max) in percentage
! Load voxel data file in excel form
! Define the Euclidean distance function of the voxel position related to the BWR current position
! Calculate weight factor based on stockpiled time
! Assign acceptable quantity tolerance
! Define constraint for the required minimum and maximum mineral composition
! Define constraints for desired quantity with acceptable tolerance
! Define objective function based on Euclidean function and weight factor
! Define constraints for reclaiming order (from higher bench to lower bench)
! Define constraints for continuous reclaiming
! Define constraints for preventing from collapsing in reclaiming
! Minimise the objective function

! Output selected voxels with total quantity and quality grade

! End of the program

Material is stacked onto four stockpiles and voxalized in SPSim software written by Lu and Xu [53]. The stockyard with four stockpiles marked as A, B, C and D is shown in Figure 6.8 and the voxalized form is shown in Figure 6.9. The starting position of the BWR is marked with a circle in Figure 6.8. The voxels produced from voxelization of stockpile A and B are used for Demand 1 study and voxels from that of stockpile C and D are used for Demand 2 study. The resulted voxels with quantity and quality grade information are stored in the separate spreadsheet database. The material composition of each voxel is calculated using common knowledge material composition of iron types stated in Table 6.6.

The objective function defined in Section 6.1 is used to identify the reclaiming voxels to meet the requested quantity and quality specifications. The density of iron ore is taken as $2100kg/m^3$. Two demand cases are conducted in the following sections.

Table 6.6: Typical mineral composition of common iron ore types

Ore types	**Fe (%)**	**SiO_2 (%)**	**Al_2O_3 (%)**	**P (%)**	**Na_2O+K_2O (%)**	**Size (>10mm) (%)**
Magnetite	72	2	3	0.05	0.07	1
Hematite	70	3	4	0.06	0.08	1.5
Goethite	62	4	4	0.09	0.13	2
Limonite1	50	5	5.5	0.1	0.15	2.5
Limonite2	60	4	4.5	0.8	0.14	3
Siderite	48	5	5	1.1	0.16	2

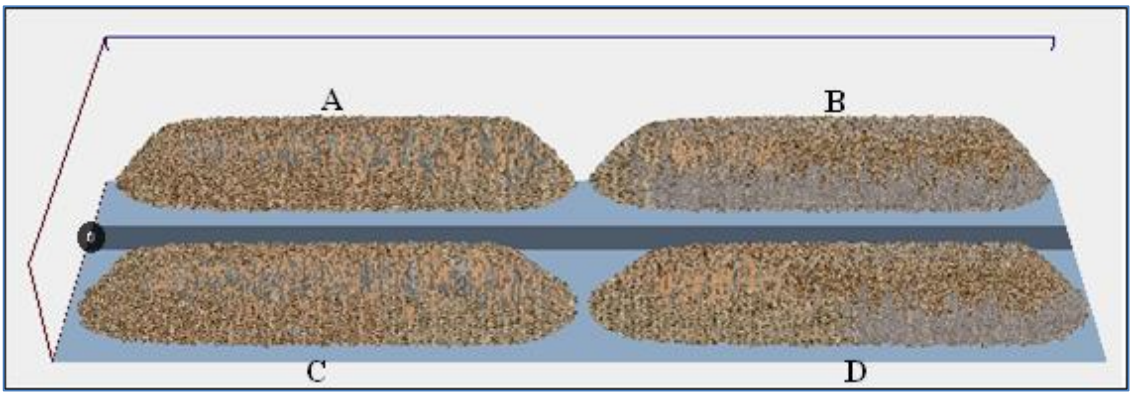

Figure 6.8: Stockyard configuration with four stockpiles from SPSim

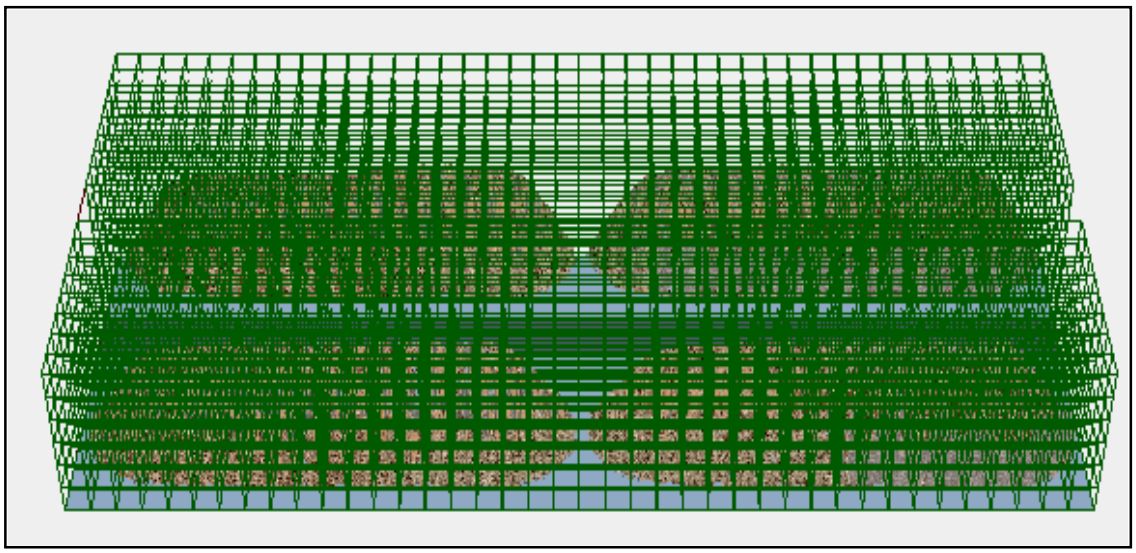

Figure 6.9: Stockyard with voxalized stockpile form

6.4.1.1 Demand 1

The optimisation problem is modelled in the Mosel program and optimised using Express-MP Optimisation suite. Voxels of stockpile A and B are used for the study. The 4200 *tonnes* of iron ore with *1 tonne* tolerance is requested with the mineral composition listed in Table 6.7. From optimisation, the total quantity of selected voxels is resulted as 4200 tonnes. The mineral composition of selected voxels is also stated in Table 6.7.

Table 6.7: Requested and resulted mineral composition

Minerals	**Fe**	**SiO_2**	**Al_2O_3**	**P**	**Na_2O+K_2O**	**Size (>10mm)**
Minimum requested (%)	50	2	3	0	0	1.5
Maximum requested (%)	55	5	5.5	5	0.16	3
Resulted minerals (%)	51.8	4.7	5.02	4.7	0.15	2.3

6.4.1.2 Demand 2

In this case, it is requested for 8010 *tonnes* of iron ore with *1 tonne* tolerance. The mineral composition requested is listed in Table 6.8. Voxels of stockpile C and D are used for the study. From optimisation, the total quantity of selected voxels is resulted as 8009.4 tonnes. The overall mineral composition of selected voxels is also stated in Table 6.8.

Table 6.8: Requested and resulted mineral composition

Minerals	**Fe**	**SiO_2**	**Al_2O_3**	**P**	**Na_2O+K_2O**	**Size(>10mm)**
Minimum requested (%)	55	2	3	0	0	1.5
Maximum requested (%)	60	5	5.5	5	0.15	3
Resulted minerals (%)	55.5	4.4	4.9	4.4	0.14	2.5

The selected voxels are not able to illustrate in the figure as the size of the stockpile voxels is small. With reference to the demand specifications of iron ore, it can be observed that the selected iron ore quantity and mineral percentages lies within the specifications of the desired demand. The upper layer voxels are selected ahead of lower layer voxels meeting the constraint introduced in Equation (6.9) to agree with the common reclaiming practice of the BWR.

6.5 Discussion

The minimum travelled distance of the BWR's bucket wheel to reclaim cuboid voxels in Cartesian coordinate is targeted meeting desired quantity and quality specifications in this chapter. To achieve that, the distance function between the voxel's position and the current BWR position is defined in the objective function. Based on the result of conducted case studies, it is found out that voxels close to the BWR starting position is selected ahead of other voxels fulfilling the objective of the study. Moreover, longer stockpiled-time stockpile is also selected ahead of other stockpiles due to weight factor, which is defined based on stockpiled time, introduced in the objective function. Moreover, the weight factor can be tuned based on the need of the particular stockpile to be reclaimed before other stockpiles if the need arises.

Case studies in Section 6.3 demonstrated that the overall quantity and quality of selected voxels falls within the range of desired specifications. The selection of lower layer voxels after or with that of higher layers voxels agrees with the layer constraint defined in Section 6.2. However, the continuous reclaiming practice of the BWR and the danger of stockpile collapsing in reclaiming have not been taken into account. The aforementioned

factors are introduced as constraints in Section 6.4 to conduct the case studies in Section 6.4.1.

6.6 Conclusion

In literature, the manual selection of the voxels by the operator from available stockpiles is practiced to meet the required quantity and grade specification without considering the movement of the reclaimer. In this chapter, an automatic selection of the voxels to reclaim based on the minimum travelled distance of the reclaimer to meet the demand quantity and quality specification was presented. The optimisation algorithm based on binary integer programming was introduced to select reclaiming voxels. In optimisation, the Euclidean distance function is defined in the objective function along with stockpiled time. The requested quantity and quality grade are considered as constraints to make sure the demand specifications are met. Moreover, the common practices used in reclaiming are defined as constraints in the optimisation problem. The cutback in the movement of heavy machine, BWR, will definitely reduce the handling cost whilst improving in meeting customer demand specifications. So, the use of this approach will assist in improving ore producers' objectives as handling cost and quality reputation are main concerns of ore producers.

CHAPTER 7: OPTIMISATION OF MINIMUM BWR JOINT MOVEMENTS IN RECLAIMING SICKLE-SHAPE VOXELS

As stated before, the BWR requires a massive amount of energy to carry out the reclaiming operation as being one of the biggest machines on earth. So, even the slightest reduction in the movement of the BWR could potentially save a significant amount of energy leading to lower handling cost. In Chapter 6, the optimisation focuses on the travelled distance of the BWR's bucket wheel in Cartesian coordinates for reclaiming cuboid voxels. The presence of cuboid voxels in Cartesian coordinate makes suitable to use the Euclidean distance function in minimizing the travelled distance of the BWR. However, the minimum travelled distance may not guarantee the minimum energy consumption as the movement of an individual joint is not taken into account in the objective function. The energy consumptions of certain joints are higher than other joints based on the load required to bear. For instance, translation motion involves the movement of the whole BWR, which makes translating joint consumes more energy than luffing and slewing joints, which involve the movement of the boom alone. So, the minimum travelled distance does not guarantee the minimum movement of the particular BWR joints.

In this chapter, the minimum movement of the BWR joints is considered in an optimisation problem to minimise the energy consumption of the BWR. Besides, the association of sickle-shape voxels with BWR joint parameters makes easier to use this approach. Additionally, the movement of the high energy consumption joints is more focused than that of low energy consumption joints to achieve the minimum energy consumption in reclaiming. The voxelization approach introduced in Chapter 4 will be used to produce sickle-shape voxels from stockpiles in the stockyard. In selecting voxels to reclaim, the quantity and quality grade of the voxels are essential to be accessible in order to meet the required specifications. The volume of the sickle-shape voxels will be computed based on the approach introduced in Chapter 5. The quality grades of the sickle-shape voxels are estimated based on the approach presented by Robinson [19] in Section 7.1. The average mineral composition of the sickle-shape voxels are taken from the grades of the

reclaimed benches. The resulted voxels, which are associated with the BWR joint parameters, volume information and grade percentages, are stored in the voxels' database. The optimisation study is carried out in Section 7.2. The case study is carried out in Section 7.3 for a stockyard which has six stacked stockpiles. Section 7.4 presents discussion and the chapter is concluded in Section 7.5.

7.1 Mineral composition of sickle-shape voxels

Due to short term fluctuations in mineral composition of the excavated blocks, different blocks of iron ore are stacked onto single stockpile layer by layer to reduce grade variation. This is called a blending operation. As a result, many layers are stacked onto a single stockpile, as shown in Figure 7.1. Theoretically, bed-blending assumes that each reclaimed bench includes equal amounts of materials from all layers of the stacked material. However, in reality, due to the geometric shape of the stockpile, reclaimed benches do not include equal amounts from stacked layers of the stockpile [19]. As a result, Robinson presented an approach in which the grade of the reclaimed benches is calculated from the stacked layers of the stockpile based on its geometry [19]. In his approach, the mineral composition of each reclaimed bench is estimated based on the proportion of the stacked layers included in the reclaimed bench.

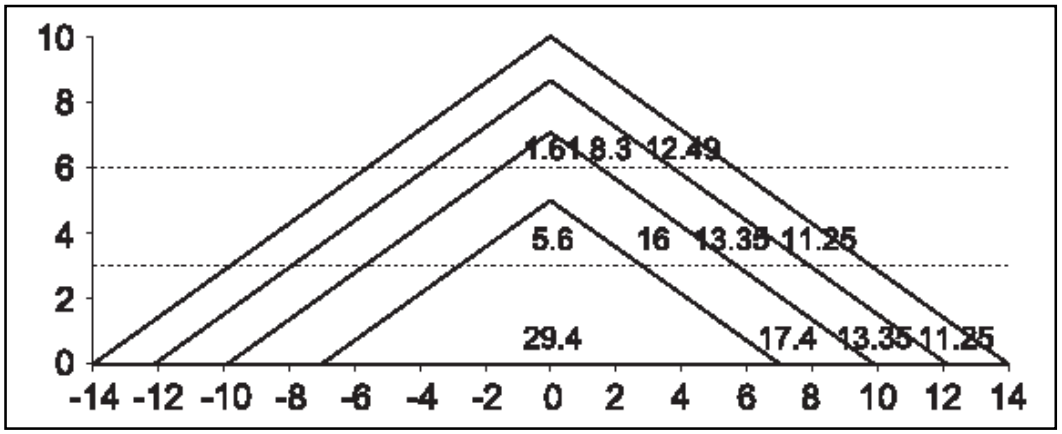

Figure 7.1: Cross section view of stacked layers and reclaimed benches [19]

In the sickle-shape voxel approach, all stacked layers are not uniformly distributed inside a voxel due to the geometrical diversity between the layers and the voxel shape. It is even possible that some layers might not be included in a voxel at all. Ideally, the volume of each layer in the voxel is required to know the exact amount of each material layer included in order to estimate the mineral composition; however, this is not feasible to carry out due to the high number of stacked layers involved inside a voxel, as shown in Figure 7.2. The dotted lines may represent the stacked layers included in a single voxel. So the layers inscribed in the voxels are very thin, which makes it very difficult to calculate the volumes. On the other hand, the thinner layers involved in a voxel will produce a negligible error if the average mineral composition is assigned to all voxels in the same bench. Based on that, voxels in the same bench are assigned with an average mineral composition in this study.

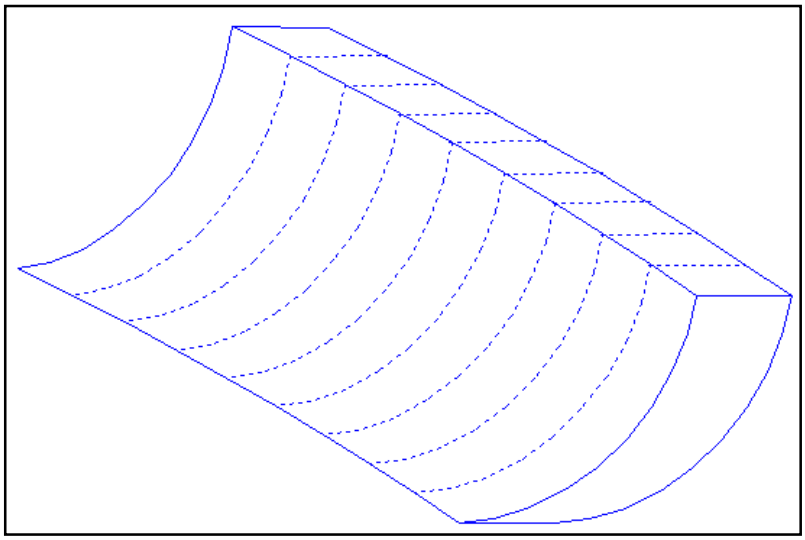

Figure 7.2: Layers inscribed inside the sickle-shape voxel

7.2 Optimisation of BWR joint movements in selecting sickle-shape voxels

Steel producers specify a target grade range while buying ore from ore producers, along with a quantity amount. In order to meet the demand specifications, certain groups of stockpile voxels from the stockyard are required to reclaim. The minimum movement of the BWR joints is considered in selecting sickle-shape voxels to reclaim. In addition, a high energy consumption joint is prioritized for minimum movements by assigning it more weight than low consumption joints. This approach is well suited for the sickle-shape voxels, as the locations of the voxels are associated with BWR joint parameters instead of Cartesian coordinates. The objective function of the optimisation problem to minimise the movement of the BWR joints is defined as:

$$objective\ function: \sum_{v \in voxels} joint\ movement_v \times reclaim_v \quad (7.1)$$

Where,

joint movement$_v$ = Joint movement of the BWR associated with sickle-shape voxels

reclaim$_v$ = Optimisation of reclaiming voxels (binary value 1 for selected and 0 for unselected voxels)

Sickle-shape voxels are associated with BWR joint parameters involving translating

distance, luffing angle and slewing range. In order to minimise the movement of BWR joints, the translating distance and luffing angle of the voxel in reference to the current BWR's translating and luffing angle are considered in the objective function. Moreover, the slewing angle range is included in the objective function to minimise the slewing movement. As mentioned before, weight factors are introduced for individual joint movements to give priority to high energy consumption joints. Although weight factors can be tuned, it is recommended to give more weight to translating joint as it requires more power to move the whole BWR unit. However, the equal value of the weighting factors will give smoother continuous trajectory. Then, the joint movements of the BWR associated with sickle-shape voxels are defined as:

$$joint\ movement_v = \sum_{v \in voxels} \sqrt{w_d (d_v - d_r)^2 + w_3 \left(\theta_{3,v} - \theta_{3,r}\right)^2 + w_2 \left(\theta_{2,2} - \theta_{2,1}\right)^2} \qquad (7.2)$$

where,

d_v, $\theta_{3,v}$ = translating distance and luffing angle of the voxel

d_r, $\theta_{3,r}$ = current translating distance and luffing angle of the BWR

($\theta_{2,2}$- $\theta_{2,1}$) = slewing angle range of the voxel

w_d, w_3, w_2= weight factors for joints and the sum of all weight factors are limited to:

$$w_d + w_3 + w_2 = 1 \qquad (7.3)$$

As a quality grade constraint, the desired minimum and maximum grades are introduced as constraints into the problem. The quality grade in the total amount of demanded ore is given by the ratio:

$$\frac{\sum_{v \in voxels} P_g \times reclaim_v}{Treclaim} \qquad (7.4)$$

Where,

P_g = mineral grade of voxels and

Treclaim = Total number of reclaiming voxels.

Adding the lower bound $PMIN_g$ and upper bound $PMAX_g$ into Equation 7.4 to

express the constraint on the minimum grade percentage results in the following relation:

$$PMIN_g \leq \frac{\sum_{v \in voxels} P_g \times reclaim_v}{Treclaim} \leq PMAX_g \quad (7.5)$$

Consequently, the following linear minimum and the maximum constraints for grade percentages are attained by multiplying with Treclaim to both sides of the nonlinear Equation 7.5.

$$\forall g \in GRADE: \sum_{v \in voxels} P_g \times reclaim_v \geq PMIN_g \times Treclaim \quad (7.6)$$

$$\forall g \in GRADE: \sum_{v \in voxels} P_g \times reclaim_v \leq PMAX_g \times Treclaim \quad (7.7)$$

Furthermore, the constraint Equation 7.8 guarantees that the reclaiming amount of ore satisfies the demand amount with acceptable tolerance

$$DEM - Tolerance \leq TOT \leq DEM + Tolerance \quad (7.8)$$

The constraints , Equation 7.9 & 7.10, are introduced for the reclaiming of voxels in the correct sequence. It is obvious that upper layer voxels are required to be reclaimed before immediate lower layer voxels can be accessed; the constraint, Equation 7.9 is set for prioritizing the reclaiming of upper layer voxels first. Moreover, the need to access voxels continuously from the end is ensured in the constraint, Equation 7.10.

$$\sum_{a \in upper\ layer\ voxels} reclaim_a \geq \sum_{b \in lower\ layer\ voxels} reclaim_b \quad (7.9)$$

$$\sum_{c \in closest\ voxels\ to\ BWR} reclaim_c \geq \sum_{d \in faraway\ voxels} reclaim_d \quad (7.10)$$

The case study is conducted for the automatic selection of sickle-shape voxels using the proposed algorithm. Firstly, six stockpiles are voxelized into sickle-shape voxels based on the approach presented in Chapter 4. Then, the volumes for all the sickle-shape voxels are calculated using the volume model proposed in Chapter 5. Details of the voxelization and volume calculation are not discussed here as they have been presented in previous chapters. Mainly, the estimation of mineral composition and automatic selection of voxels are discussed in details in the case study.

7.3 Case study

The steps for solving the optimisation problem to conduct case studies is presented in a pseudo code form as follows:

! Declare variables
! Load voxel data file in xecel form
! Estimate mineral composition of the sickle-shape voxel
! Enter Demand quantity and required mineral composition (Min-Max) in percentage
! Assign weight factors for individual joints (total is 1)
! Define the joint displacement function of the voxel's parameters related to the BWR current position
! Assign acceptable quantity tolerance
! Define constraint for the required minimum and maximum mineral composition
! Define constraint for desired quantity with acceptable tolerance
! Define objective function based on the BWR joint displacement function with joint weight factors
! Define constraint for the reclaiming order (from higher bench to lower bench)
! Define constraints for continuous reclaiming
! Minimise the objective function
! Output selected voxels with total quantity and quality grade
! End of the program

A small-scaled stockpile prepared in the laboratory is used for the case study. The length, height and width of the stockpile are measured as 350mm, 140mm and 400mm which can be scaled up to match with real life scenarios. Another two stockpiles on the left side and three stockpiles on the right side of the BWR rail are emulated to set up the reclaiming operation of the stockyard as shown in Figure 7.3. The process starts with the voxelization of the stockpile into sickle-shape voxels after stacking is completed. Volumes of sickle-shape voxels are calculated and parameters associated with voxels along with volumes are stored in the stockpile database. Sample form of voxel information stored in the database is listed in Table 7.1.

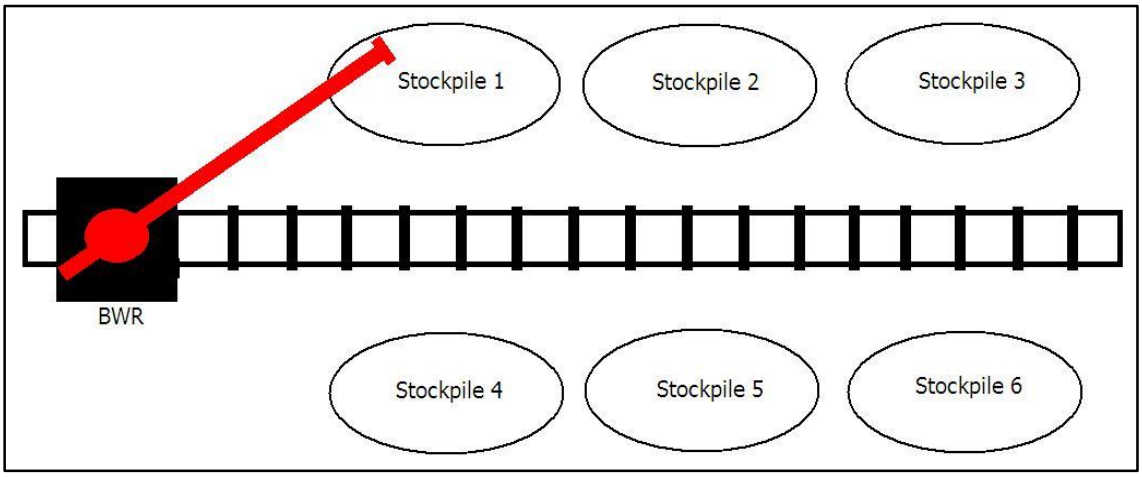

Figure 7.3: Stockyard configuration with six stockpiles

Once quantitative information associated with the voxels is stored, the grade quality information for the voxels is required to be accessible in order to select which voxels should be reclaimed. Stockpiles being stacked with four layers as shown in Figure 7.4, in which layers 1, 2, 3, and 4 represent the stacked layers and Bench 1, 2, and 3 represent the reclaimed benches. The cross-sectional areas of the stacked layers inscribed in benches through the chevron-stacked Stockpile 1are illustrated as well in Figure 7.4. The proportions of the stacked layers are attained by dividing with the total volume and listed in Table 7.1. The grades are calculated based on the volume proportions included in the reclaimed benches, based on the method presented by Robinson [19]. The approach was discussed in Section 7.1.

Table 7.1: Cross sectional areas and proportions of layers in Stockpile 1

Benches	**Cross sectional area of layers comprised in bench (mm^3)**	**Proportion of the layers comprised in bench**
3	Layer 1: 2500 Layer 2: 1660 Layer 3: 322 Layer 4: 0	Layer 1: 0.557 Layer 2: 0.3703 Layer 3: 0.0718 Layer 4: 0
2	Layer 1: 2250 Layer 2: 2670 Layer 3: 3199 Layer 4: 1120	Layer 1: 0.2435 Layer 2: 0.2890 Layer 3: 0.3462 Layer 4: 0.1212
1	Layer 1: 2250 Layer 2: 2670 Layer 3: 3479 Layer 4: 5880	Layer 1: 0.1576 Layer 2: 0.1870 Layer 3: 0.2436 Layer 4: 0.4118

For instance, the iron ore grades of the stacked layers in Stockpile 1 are 13, 15, 14 and 17 as it is graded ore in the maining industry. The calculation is carried out by multiplying grades with the respected proportion to obtain the average grade for the bench. As a result, the grades of the Bench 3, 2 and 1 of the Stockpile 1 would be 13.83, 14.41 and 15.26. All stockpiles associated with stacked layers are graded and the resulted reclaimed bench grades are listed in Table 7.3. Then the average grades of the voxels are assigned for the whole reclaimed bench.

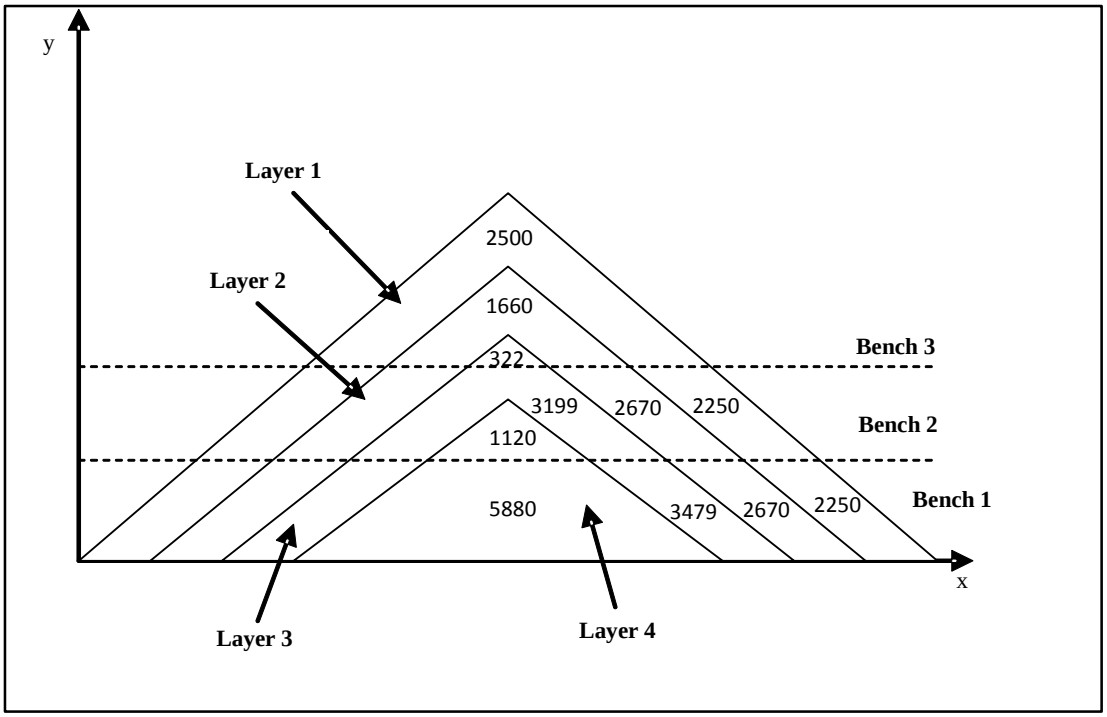

Figure 7.4: Cross-section through a chevron-stacked stockpile

Table 7.2: Sample of voxels information stored in stockpile database

Voxels index	**Translated distance**	**Luffing angle (°)**	**Slewing angle range (°)**	**Volume (mm^3)**	**Grade (%)**
1	79.5	-18.6	26.9 – 41.1	75589.4	15.26
2	99.5	-18.6	25.8 – 43.0	93651.4	15.26
40	139	-14.14	20.2 – 33.7	87230.3	14.41
41	159	-14.14	19.4 – 35.1	104146.8	14.41
70	219.5	-9.46	29.4 – 32.4	12097.3	13.83
71	239.5	-9.46	27.9 – 34.1	25554.4	13.83

Table 7.3: Grade for stacked layers and reclaimed benches

Stockpiles	**Stacked layers**	**Grade**	**Reclaimed benches**	**Grade**
Stockpile 1	Layer 1	13	Bench 3	13.83
	Layer 2	15	Bench 2	14.41
	Layer 3	14	Bench 1	15.26
	Layer 4	17		
Stockpile 2	Layer 1	15	Bench 3	14.77
	Layer 2	14	Bench 2	15.16
	Layer 3	17	Bench 1	14.48
	Layer 4	13		
Stockpile 3	Layer 1	14	Bench 3	15.04
	Layer 2	17	Bench 2	14.64
	Layer 3	13	Bench 1	14.73
	Layer 4	15		
Stockpile 4	Layer 1	17	Bench 3	15.38
	Layer 2	13	Bench 2	14.79
	Layer 3	15	Bench 1	14.53
	Layer 4	14		
Stockpile 5	Layer 1	15	Bench 3	14.19
	Layer 2	13	Bench 2	14.32
	Layer 3	14	Bench 1	15.21
	Layer 4	17		
Stockpile 6	Layer 1	13	Bench 3	13.51
	Layer 2	14	Bench 2	14.47
	Layer 3	15	Bench 1	15.32
	Layer 4	17		

Translated distances of voxels listed in the Table 7.2 are calculated based on the BWR starting position. However, during the voxels selection process, the BWR's bucket wheel position will be updated to current voxel position for the subsequent voxel selection. From the available voxels in the database, the optimisation algorithm is applied to identify voxels for reclaiming. The simulation is carried out using the Xpress MP Optimisation

package. The case study is simulated for three continuous demand cases. Weight factors are assigned as $w_d = 0.6$, $w_3 = 0.2$ and $w_2 = 0.2$. The voxel database is updated for each demand case, considering selected voxels are reclaimed before another demand case is carried out. The volume tolerance for quantity is taken as 100 mm^3 for all cases**.** The demand specification and resulted quantity and grade are listed in Table 7.4. The selected voxels are marked in side-view of the stockpiles in Figure 7.5. In that Figure, the selected voxels for case study 1 are marked with 1 followed by 2 for case study 2 and 3 for case study 3.

Table 7.4: Result of demand cases

1st demand in Volume ($1.2x10^6$ mm^3) Target Grade: 14.5-14.6%	Total volume of selected reclaiming voxels	$1.2\ x10^6$ mm^3
	Resulted Grade	14.53 %
2nd demand in Volume ($63\ x10^4$ mm^3) Target Grade: 15-15.1%	Total volume of selected reclaiming voxels	$62.93\ x10^4 mm^3$
	Resulted Grade	15.1 %
3rd demand in Volume ($7.5\ x10^5$ mm^3) Target Grade: 14-14.1%	Total volume of selected reclaiming voxels	$7.495\ x10^5 mm^3$
	Resulted Grade	14.1 %

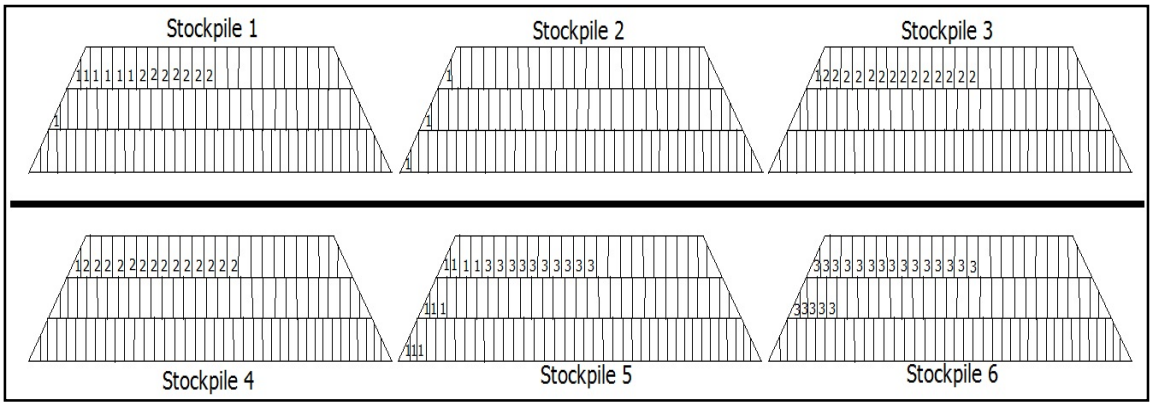

Figure 7.5: Selected voxels for case 1, 2 and 3

7.4 Discussion

The resulted quantity and quality grade fall within the desired quantity and quality range in all demand cases as stated in Table 7.4. Moreover, the sequence of voxels to be accessible in reclaiming satisfied the constraints defined in the algorithm. The consideration of joint movements in the objective function is better suited than travelled distance as the joints are the fundamental mechanisms to carry out any movement.

The movement of high energy consumption joints is more focused by assigning more weight factor in the objective function than low consumption joints. Besides, the energy consumption of joints can evaluate directly and accurately if it is required for the optimisation. In the objective function of Equation 7.2, weight factors can be adjusted for each individual joint to give more attention to higher energy consumption joints. In three joints, the highest energy consumption joint is considered to be the translation joint as the movement involves the whole BWR. For that, the translation joint was assigned more weight than other two joints to achieve the smallest movement in translation motion in the case study. So, the minimum movement of joints, especially the high energy consumption joints in reclaiming will result in lower energy consumption leading to lower handling costs.

7.5 Conclusion

The minimum movement of the BWR joints is taken into account in the objective function of the optimisation problem. Moreover, the weight factors of the joints in the objective function can be adjusted to focus on high energy consumption joints to move less than low energy joints. The association of sickle-shape voxels with the BWR joint parameters makes the approach easier to implement a straightforward automatic reclaiming. The automatic identification of the voxels to reclaim will minimise the need of the human experiences and trial-and-errors. The approach will improve the ability to meet demand specifications more accurately, which leads to an efficient use of iron ore reserves. Moreover, the reduction of handling costs will increase the ability to compete in the global market in terms of price.

CHAPTER 8: DISCUSSIONS AND CONCLUSIONS

This chapter mainly presents discussions and conclusions of the study along with potential future studies. In the discussion section, the contributions of the study are highlighted. In addition, the results of the case studies conducted for the newly introduced approaches are discussed with the inclusion of limitations encountered in the study. The contributions of the study are summarized in Section 8.2. Then, the achievements of the study based on the objectives of the study are highlighted in the conclusions section. Finally, the possible future studies are presented in Section 8.4.

8.1 Discussions

The results and constraints of all the studies conducted here are summarised in this section before presenting conclusion of the study. As it was pointed out in the introduction of Chapter 1, the material handling process is in need of operating automatically with full knowledge of the material in order to meet the current industry demands. Along with the successful introduction of Robotics technology in mining operations over the past ten years [10], this study also used Robotics technology in designing automatic reclaiming system by treating the BWR as a robotic manipulator.

Bulk material is generally stored as stockpiles at the port for the purpose of buffering between processes and reducing grade variation among stockpiles [19]. Then, they are reclaimed by the BWR and loaded onto ships to export overseas. The reclaiming phase plays a vital role in supplying the ore as close as possible to the requested specifications to maintain a quality reputation as it is the final stage of material handling operations. However, stacking stage with blending operation is given more attention than reclaiming stage in order to reduce the grade variation before reclaiming automation was introduced in last decade. Furthermore, the blending operation is carried out using the forecast assay as the process of attaining accurate assay takes few hours. On the contrary, reclaiming phase is more focused in this study as the accurate assay is available at this stage

to carry out the reduction of grade variation operation. So, it can be claimed that the availability of the accurate assay at the reclaiming stage will even cut down the need of blending as voxels from multiple stockpiles can be reclaimed in order to meet demand specifications.

Though a number of studies have focused on blending approach at the stacking stage, a single study has been found in literature which focuses on the reclaiming stage. In that study, Simine [15] introduced a voxel based approach in which stockpile is considered as a combination of volume elements contrary to the single volume approach. The details of the Simine study can be found in Section 1.2. As it was discussed in Section 3.1, the limitation of the Simine study is that the use of cubic shaped voxels without taking into accounts the reclaiming pattern of the BWR. Moreover, there has not been a single study in literature which investigates the optimal shape of voxel based on the reclaiming pattern of a BWR.

Before studying the optimal shape of voxel, the cuboid voxel which was used in a literature study was investigated for the reclaiming accuracy in reclaiming with the BWR in Section 3.1.2. In that investigation, the graphical illustration of the cuboid voxels reclaiming shows the discrepancy between the cuboid voxels and the reclaiming profile of the BWR. Consequently, the constraint in reclaiming cuboid voxels accurately by the BWR will make challenging for the supply ore to fall within the range of demand specifications. Alternatively, the sickle-shape voxel was firstly introduced based on the kinematics of a BWR in this study to obtain optimal accuracy. The use of sickle-shape voxels will improve the reclaiming accuracy as it resembles the reclaiming profile of the BWR. The comparison of the sum of sickle-shape voxels' volume with the whole stockpile volume, presented in Chapter 5 study, proves positive results can be obtained with negligible margins of 1.7 % error.

Using the newly introduced sickle-shape voxel, the study on voxelization is carried

out in Chapter 4. Virtual voxelization approach of the stockpile allows the repetitive process of voxelization to take place even if new BWR is introduced or additional material is stacked onto a partially reclaimed stockpile. Continuous scanning of the stockpile and repeated voxelization can update the voxel database whenever the geometry of the stockpile is changed. In voxelization, the whole slew range is defined as a single voxel in this study based on the commonly used reclaiming practice in the industry. It is possible that even the whole slew range can be divided into small voxels in order to acquire a greater accuracy in quantity and quality. However, the approach is contrary to the practice of the industry as slewing motion is generally carried out as a single movement across the stockpile to reclaim all material within the slewing range. Moreover, the BWR has to retract the slewing motion to its initial position before another slewing starts if the slewing motion is disrupted in the middle of the stockpile to prevent possible collision of the boom with the stockpile. That extra movement of the BWR will increase the operating cost. Based on the reasons stated, the definition of the whole slew range as a single voxel seems appropriate and practical.

The BWR reclaims material by performing its joint movements which includes translation, luffing, slewing and bucket wheel rotation. It means BWR operates in its own BWR joint space whereas cuboid voxels are defined in Cartesian coordinates. The implementation of reclaiming automation using cuboid voxels involves the repetitive process as the conversion of coordinate is required each time the reclaiming process is conducting. Moreover, the accuracy of reclaiming will be compromised as the reclaiming pattern which forms the circular profile is not agreed with the Cartesian coordinate system. In sickle-shape voxel approach, the coordinate conversion is done at the stage of voxelization of the stockpile. Sickle-shape voxels are stored in BWR joint parameters space so that there is no requirement for the coordinate conversion and the reclaiming path planning at each reclaiming process. The straight forward approach will enable to introduce fully automatic reclaiming operation in meeting industry demands.

An automatic selection of voxels based on the more accurate assay of the stockpile improve in meeting the demand quantity and quality when placing the demanded quantity and quality as parts of the constraints without relying on the experiences of operators, nor trial-and-error. The case studies presented in Chapters 6 and 7 verified that the sum or the group of selected voxels lies within the desired quantity and quality grade specifications. Moreover, the movement of the huge machine, BWR is minimized both in the joint space for sickle-shape voxels and Cartesian space for cuboid voxels in reclaiming to reduce the handling cost. The use of virtual voxelization and simulated selection of voxels will display the resulted specification of the reclaimed ore in terms of quantity and quality, even before it is physically reclaimed. The proposed approach can be implemented with different types of BWR, as the voxel profile is defined based on the parameters of the actual BWR's kinematics to be used. Furthermore, the approach is applicable to any stockpiles of any size as the stockpiles' contours can be extracted from scanned stacked stockpiles waiting to be reclaimed. The elimination of reliance on human operator's knowledge and experience in selecting reclaiming material from stockpiles will make easier to implement full automatic system. Overall, the study assists in improving the three main objectives of the ore producers mentioned by Everett [7], which includes to produce maximum output tonnage, to minimize material handling costs and to deliver quality grade targets with a minimum tolerance. Moreover, the treatment of the BWR as a robotic manipulator enables the transformation of the existing manual reclaiming operation to an automatic operation without replacing the existing reclaimer with new machine.

One may argue that the voxel approach is not required to carry out the reclaiming operation in meeting demand specifications. The reason can be given that that the required BWR joint movements can be obtained based on the kinematics of the BWR with the knowledge of the stockpile model without voxelization of the stockpiles. However, the implementation of automatic selection of stockpiles portions from multiple stockpiles

without operator's involvement and expertise will be a challenging task. In voxel approach, the automatic selection of optimal voxels is a simple straightforward procedure without the need of operator. Moreover, the voxel approach can be used as a backbone to extend the study for the fully automated material handling operation. For instance, the study on estimation of the material composition of the sickle-shape can be conducted to use for the optimal reclaiming. Moreover, the automated selection of optimal voxels can be carried out for the next demand task without the stockpile scanning again as voxels information are stored in database.

8.2 Contributions to the study

The summary of contributions to the whole study is listed as:

- Highlighted the inaccuracy of using cuboid voxel in reclaiming with the BWR;
- Derived the kinematics model of the BWR including bucket wheel as a 4 DOF robot manipulator;
- First one to introduce sickle-shape voxel based on the kinematics model of BWR;
- The process of voxelization of the stockpile into sickle-shape voxels associated with the BWR joint parameters;
- Defined the volume model of sickle-shape voxels;
- Introduced automatic identification of the cuboid voxels to reclaim based on the minimum travelled distance of BWR's bucket wheel; and
- Introduced automatic identification of the sickle-shape voxels to reclaim based on the BWR joint movements.

8.3 Conclusions

To conclude this thesis, the achievement of each of the objectives will be summarized. Firstly, the giant BWR is treated as a 4 DOF robot manipulator to derive the kinematics model. Based on the kinematics model, optimal voxel shape was introduced; a sickle-shaped voxel which resembles the shape of a sickle. The introduction of sickle-shaped voxel covers the first objective of the study, which is listed as an investigation of the optimal voxel profile. Besides, it is one of the contributions of the study as the investigation of the optimal voxel shape has not been investigated yet. In literature, cubic-shaped voxel was only used without considering the reclaiming pattern of reclaimer.

The second objective is the voxelization of stockpile into a proposed sickle-shaped voxels based on the BWR's kinematics. In order to achieve this, the whole stockpile was divided into sickle-shape voxels, in which the stockpile in Cartesian coordinates is converted into voxels associated with the BWR joint parameters. The resulted sickle-shape voxels associated with the BWR joint parameters are stored in the database in order to select voxels for reclaiming. The advantage of the sickle-shape voxels is that the ability to reclaim directly by the BWR, without the computational expenses to convert coordinates. As the implementation of reclaiming automation in cuboid voxels requires coordinate conversations as they are in different coordinate systems. It may contribute to the reasons that only manual selection of voxels is used in literature instead of automated selection of voxels. The benefit of using sickle-shape voxel goes far beyond the coordinate conversion. The agreement between the reclaiming profile of the BWR and sickle-shape voxel will improve the reclaiming accuracy which will lead to improvements in meeting demand quality and quantity specifications. The investigation carried out in this study proved that the reclaiming profile of the BWR clearly contradicts with and superior than cuboid voxels.

As the configuration and profile of the sickle-shape is defined based on the kinematics of BWR, the volumes of voxels are not unique. For that, the volume model of

sickle-shaped voxel was derived in spherical coordinates to calculate every individual voxel volume so that it will provide information about the reclaimed material. The spherical coordinate used for sickle-shaped voxels are associated with the BWR joint parameters, which are similar to spherical coordinate space. The case study carried out verifies the volume model, by comparing the sum of the voxels' volume with the whole stockpile volume.

There are two studies carried out for identification of the voxels to meet the quantity and quality demand specifications. The first study was carried out for cuboid voxels optimizing the BWR minimum travelled distance. The case study was carried out for the three demand cases and the results all lie within the required specifications. The second study was carried out for sickle-shaped voxels in minimizing BWR joint movements. The joint movement is employed in this study as the sickle-shaped voxels are associated with BWR joint parameters. The minimization of the joint movements of the BWR significantly reduces energy consumption as it is one of the biggest machines on earth.

8.4 Future works

There are a number of works can be extended from the current studies. Firstly, this study can be integrated with the scanning and mineral distribution, to develop a voxel-based material handling system. Moreover, real-time material handling system can be achieved by scanning the stockpile each time stockpile geometry is changed. Based on the reformed stockpile, the voxelization process can be carried out recurrently.

In the automatic selection of voxels, there is a limitation on using a single BWR and multiple stockpiles in this study. The current study can be extended for reclaiming multiple stockpiles with multiple BWRs in future studies. The study on trajectory planning of BWR involving obstacles avoidance mainly avoiding from other reclaimers/stackers and stockpiles to reclaim automatically is included in future works.

The minerals distribution study of the stockpile in Chapter 7 is limited to stockpiles, which are stacked using the chevron stacking method. The study can be extended to stockpiles, which are stacked using other stacking methods such as cone shell and windrow methods. The optimisation algorithm can be enhanced based on the requirements and constraints encountered in different stockyards with another types of reclaimers. The optimisation can be extended using hybrid approach to combine the minimum travelled distance with the minimum joint movement for the better result.

REFERENCES

[1] Minerals council of Australia, "2011-2012 Pre-budget Submission," Minerals council of Australia, 2011.

[2] B. Pink, "Year Book Australia," no. 92. pp. 1–904, 2012.

[3] A. J. B. Muwanguzi, A. V Karasev, J. K. Byaruhanga, xf, P. nsson, xe, and G. r, "Characterization of Chemical Composition and Microstructure of Natural Iron Ore from Muko Deposits," *Int. Sch. Res. Not.*, vol. 2012, p. 9, 2012.

[4] D. J. Jorgen, "U.S Geological Survey, Mineral Commodities Summary," 2013.

[5] J. E. Everett, "Simulation to reduce variability in iron ore stockpiles," *Math. Comput. Simul.*, vol. 43, no. 3–6, pp. 563–568, 1997.

[6] J. E. Everett, "Iron Ore Handling Procedures Enhance Export Quality," *Interfaces (Providence).*, vol. 26, no. 6, pp. 82–94, 1996.

[7] J. E. Everett, "Computer aids for production systems management in iron ore mining," *Int. J. Prod. Econ.*, vol. 110, no. 1–2, pp. 213–223, 2007.

[8] A. W. Roberts and O. J. Scott, "Bulk Materials Handling in the Mining Industry," *Madencilik KongresiXIII*. Turkey, 1993.

[9] B. S. Fisher, S. Schnittger, and Bae. P. Ltd, "Autonomous and Remote Operation Technologies in the Mining Industry: Benefits and Costs," BAEconomics Pty Ltd, Canberra, Australia, 2012.

[10] D. Lynas and T. Horberry, "Human factor issues with automated mining equipment," *Ergon. Open Journal*, vol. 4, no. S2-M3, pp. 74–80, 2011.

[11] J.-V. Douglas, "The future of Robotics: Robotic Wonders," *Mining & Technology Australia*, no. 1, Mining Media International, Australia, pp. 20–22, 2010.

[12] T.-F. Lu, "Bucket wheel reclaimer modeling as a robotic Arm," *IEEE International Conference on Robotics and Biomimetics (ROBIO 2009)*. Guilin, China, 2009.

[13] ABB Group, “S/SR Reclaiming/stacking methods,” 2012. [Online]. Available: http://www.abb.com/industries/db0003db002806/e29095140f8c008fc12573b1002d9a69.aspx?tabKey=6.

[14] A. T. Yu and D. Mahr, “Chapter 31: Above Ground Handling and Storage,” in *Materials handling handbook*, Second., R. A. Kulwiec, Ed. United States of America: John Wiley & Sons,Inc, 1985, pp. 1216–1245.

[15] K.-H. Gerlach, “Achieving the Right Quality Mix,” *Siemens’ Customer Magazine Metals & Mining*, vol. 2, pp. 20–22, 2009.

[16] M. Binkowski and B. J. McCarragher, “A Queueing Model for the Design and Analysis of a Mining Stockyard,” *Discret. Event Dyn. Syst.*, vol. 9, no. 1, pp. 75–98, 1999.

[17] J. E. Everett, “Iron ore production scheduling to improve product quality,” *Eur. J. Oper. Res.*, vol. 129, no. 2, pp. 355–361, 2001.

[18] ThyssenKrupp Fordertechnik, “Open Pit Mining, Mineral Processing, Materials Handling program,” A company of ThyssenKrupp Technologies, Essen, 2001.

[19] G. K. Robinson, “How much would a blending stockpile reduce variation?,” *Chemom. Intell. Lab. Syst.*, vol. 74, no. 1, pp. 121–133, 2004.

[20] F. F. Pavloudakis and Z. Agioutantis, “Simulation of Bulk Solids Blending in Longitudinal Stockpiles,” vol. 17, no. 2, pp. 98–112, 2003.

[21] Z. Cheng, Z. Zhang, and P. Zhang, “Research on Blending Optimized Algorithm of WSICO Industrial Port Based on Logistics Equilibrium,” in *Business and Information Management, 2008. ISBIM ’08. International Seminar on*, 2008, vol. 1, pp. 151–153.

[22] J. E. Everett, T. Howard, and M. Kamperman, “The development of an MIS for iron ore mining operations,” in *Proceedings of the Informing Science 2001 Conference*, 2001, pp. 337–345.

[23] S. Zhao, T.-F. Lu, B. Koch, and A. Hurdsman, “Dynamic modelling of 3D stockpile for life-cycle management through sparse range point clouds,” *Int. J. Miner. Process.*, vol. 125, pp. 61–77, 2013.

[24] S. Zhao, T.-F. Lu, B. Koch, and A. Hurdsman, “3D stockpile modelling and quality calculation for continuous stockpile management,” *Int. J. Miner. Process.*, vol. 140, pp. 32–42, 2015.

[25] S. Zhao, T.-F. Lu, B. Koch, and A. Hurdsman, “Automatic quality estimation in blending using a 3D stockpile management model,” *Adv. Eng. Informatics*, vol. 29, no. 3, pp. 680–695, 2015.

[26] J. Brisco, “Design, Application and Operation of Bucket Wheel Reclaimers and Stackers,” in *National Conference on Bulk Materials Handling* , 1996, pp. 181–185.

[27] K. Casteel, “Big wheels keep on turning,” *WOMP-The official mining newsletter in association with Engineering and Mining journal* , vol. 4, pp. 1–9, 2008.

[28] C. Choi, K. Lee, K. Shin, K. S. Hong, and H. Ahn, “Automatic landing method of a reclaimer on the stockpile,” *IEEE Trans. Syst. Man Cybern. C Appl. Rev.*, vol. 29, no. 1, pp. 308–314, 1999.

[29] K.-S. Hong and C. Choi, “Task-oriented approaches to the inverse kinematics problem for a reclaimer excavating and transporting raw material,” *Adv. Robot.*, vol. 14, no. 3, pp. 185–204, 2000.

[30] ThyssenKrupp Engineering (Australia), “BHP Billiton-Bucket wheel reclaimer.” ThyssenKrupp Engineering (Australia), Stirling W.A.

[31] J. J. Craig, *Introduction to Robotics, Mecahnics and Control*, Second. Addison-Wesley Publishing Company, 1989.

[32] T.-F. Lu, “Preparation for turning a bucket wheel reclaimer into a robotic arm,” *IEEE International Conference on Robotics and Biomimetics (ROBIO 2008)* . Bangkok, Thailand, pp. 1710–1715, 2009.

[33] T.-F. Lu, S. Zhao, S. Xu, B. Koch, and A. Hurdsman, “A 3DOF system for 3 dimensional stockpile surface scanning using laser,” in *Industrial Electronics and Applications (ICIEA), 2011 6th IEEE Conference on*, 2011, pp. 1–5.

[34] T. C. O’Haver, “Curve fitting A: Linear Least Squares,” *An Introduction to Signal Processing with applications in Chemical Analysis*. pp. 1–92, 2012.

[35] J. Stewart, “Triple Integrals in Spherical Coordinates,” in *Multivariable Calculus*, Seventh., L. Covello, Ed. Belmont, California: Thompson Learning, 2012.

[36] H. Amankwah and T. Larsson, “Mathematical Optimization Models and Methods for Open-Pit Mining,” Linköping University, Sweden, 2011.

[37] M. Menabde, G. Froyland, P. Stone, and G. Yeates, “Mining schedule optimisation for conditionally simulated orebodies,” *Orebody Min. Strateg. mine planning, Spectr. Ser.*, vol. 14, pp. 353–357, 2007.

[38] M. Osanloo, J. Gholamnejad, and B. Karimi, “Long-term open pit mine production planning: a review of models and algorithms,” *Int. J. Mining, Reclam. Environ.*, vol. 22, no. 1, pp. 3–35, 2008.

[39] J. Gholamnejad, “A zero-one integer programming model for open pit mining sequences,” *J. South. African Inst. Min. Metall.*, vol. 108, pp. 759–762, 2008.

[40] E. Moosavi, J. Gholamnejad, M. Ataee-Pour, and E. Khorram, “Optimal extraction sequence modeling for open pit mining operation considering the dynamic cutoff grade,” *Gospodarka Surowcami Mineralnymi*, vol. 30, no. 2. p. 173, 2014.

[41] E. Bakhtavar, K. Shahriar, and A. Mirhassani, “Optimization of the transition from open-pit to underground operation in combined mining using (0-1) integer programming,” *J. South. African Inst. Min. Metall.*, vol. 112, pp. 1059–1064, 2012.

[42] Dash Optimisation, “Xpress-MP Essentials,” Dash Associates, 2002.

[43] ABB Company, “S/SR Reclaiming/stacking methods.” [Online]. Available: http://www.abb.com/industries/db0003db002806/e29095140f8c008fc12573b1002

d9a69.aspx?tabKey=6.

[44] K.-S. Hong and S.-H. Kim, “Robust Time-Delay Control of a Reclaimer,” *KSME Int. J.*, vol. 13, no. 7, pp. 575–583, 1999.

[45] Liyimin, “Bucket wheel stacker reclaimer of transmission capacity ,” in *The second session of the China Association of Science Annual Meeting Satellite Conference of youth, Liaoning Province Second Youth Annual Conference* , 1995.

[46] E. O. Schneidersmann, “Function and Disign of the Bucket Wheel,” in *Stacking, blending, reclaiming of bulk materials*, R. H. Wöhlbier, Ed. Trans Tech Publ., 1977.

[47] S. Kucuk and Z. Bingul, “ Robot Kinematics: Forward and Inverse Kinematics,” in *Industrial Robotics: Theory, Modelling and Control*, S. Cubero, Ed. Croatia : plV pro literatur Verlag Robert Mayer-Scholz , 2006.

[48] D. R. Twigg, “Volume Computations Using Shape Functions,” *Surv. Rev.*, vol. 33, no. 255, pp. 2–16, 1995.

[49] D. Burch, “Calculating the Volume of a Stockpile ,” in *Estimating Excavation*, California: Craftsman Book Company, 1997, pp. 184–186.

[50] G. K. Robinson and K. A. Ross, “Blending in the ends of chevron stockpiles,” *Bulk Solids Handl.*, vol. 11, no. 3, pp. 595–602, 1991.

[51] G. Cash, K. R. Perry, and P. Guj, “Iron Ore in Western Australia.” Department of Minerals and Energy, pp. 1–19, 1995.

[52] P. S. Ranawat, “Iron Ore ,” *Info Portal of Geology with special reference to Rajasthan,India*,2007.[Online].Available: http://www.geologydata.info/mettalic/ironore.htm.

[53] S. Xu and T.-F. Lu, “a Fast Stockpile Simulation Engine and Its Application in Mineral Ore Handling,” vol. 4, no. 2. p. 1250031.